# Grant Agreement Number 608553

# IMAGE
## Integrated Methods for Advanced Geothermal Exploration
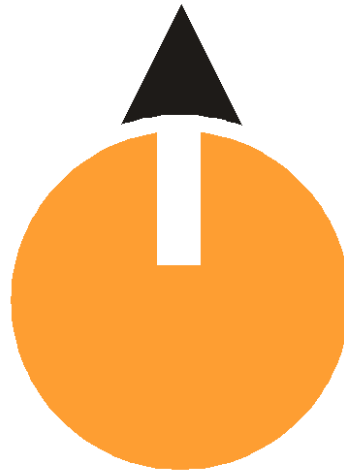
# IMAGE-D7.03:
# FINAL REPORT ON CHEMICAL GEOTHERMOMETERS AND TRACERS

| Contributions by: | B. Sanjuan, F. Gal, R. Millot, Ch. Dezayes (BRGM)<br>H. Jirakova, V. Frydrych (GEOMEDIA)<br>C. Nawratil de Bono, F. Martin (SIG) |
|---|---|
| Responsible WP7-leader: | J. Hopman (TNO) |

# Introduction & summary

In the framework of the IMAGE project, the main objective of the task 7.3 was to develop auxiliary chemical geothermometers and tracer tests adapted to environments of crystalline basements and sedimentary basins in order to consolidate the temperature estimation of the geothermal reservoir from surface exploration and better know the fluid circulation in this type of reservoir, respectively. To begin, two exhausted literature reviews were carried out.

The first one was focussed on the development of potential auxiliary geothermometers, using the chemical composition of deep fluids discharged from crystalline basements or sedimentary basins and collected from wells, in order to better estimate the temperature of the geothermal reservoir in this type of environments. In addition to classical geothermometers (Na-K, Na-K-Ca, K-Mg, silica, etc.), auxiliary geothermometers like Na-Li, Na-Rb, Na-Cs, K-Sr, K-Fe, K-Mn, K-F and K-W were found for dilute deep geothermal waters from more than 60 granite areas, in Europe (Michard, 1990). For saline geothermal waters discharged from sedimentary basins, only the Na-Li and Mg-Li thermometric relationships were found in the literature. From chemical compositions of 20 deep geothermal and oil brines found in the literature, especially from the Rhine Graben and Salton Sea areas, three new relationships Na-Rb, Na-Cs and K-Sr, different from those applied to dilute geothermal waters, were determined in a temperature range of 70-320°C and will be very useful for the exploration of geothermal systems where this type of fluids will be circulating (Sanjuan *et al.*, 2016b). Other less reliable thermometric relationships (K-Fe, K-Mn, K-F) were also found.

The second literature review was associated with the development of tracing tests in environments of crystalline basement and has benefited from the long BRGM experience in the Soultz geothermal site. After a review of the tracers recommended in the literature following the fixed objectives, examples of applications in different crystalline sites were given. The most recent inter-well tracer tests conducted in June 2013 at the Habanero EGS site, central Australia, and in 2014, in the Rittershoffen site, Alsace, near Soultz-sous-Forêts, in granite environments, were also integrated in this review. Unfortunately, after on-site works, no tracer test could be conducted in the PVGT-LT1 borehole, only borehole available in the Litomerice area, Czech Republic, and in the Thônex-1 borehole, near Geneva, in Switzerland, especially because of the very low fluid flow-rate existing in these boreholes. Consequently, we decided to focus our on-site works on the development of auxiliary chemical geothermometers at low-temperatures.

After the literature review, the chemical compositions of deep fluids discharged from existing boreholes drilled up down the crystalline basement, in the Litomerice area, Northwest Bohemia, in Czech Republic, were investigated. Only the fluid chemical compositions from 5 deep boreholes were found and among these boreholes, only one (PVGT-LT1 borehole) could be sampled by GEOMEDIA, in May 2015, and by BRGM, in November 2015. Another fluid sample was collected by BRGM from the Pravridlo thermal spring, at Teplice, near the Litomerice city. The poor concordance between estimated and measured fluid temperatures for these boreholes is probably due to the low values of this parameter, which do not allow reaching a full chemical equilibrium between the fluids and the surroundings rocks. At temperatures ≤ 50°C, only the chalcedony, K-Fe and K-Mn thermometric relationships seem give relatively good estimations of temperatures. At temperatures > 50°C, a significant part of the auxiliary geothermometers determined by Michard (1990) gives concordant temperature values for the dilute geothermal waters collected from the Litomerice PVGT-LT1 borehole (55 ± 20°C) and from the Pravridlo spring (100 ± 25°C), as well as from the Thônex-1 (70 ± 20°C) and Lavey-les-Bains (105 ± 25°C) boreholes, in Switzerland. However, additional chemical and isotope analyses must be performed by BRGM in the Thônex-1 fluid, in the next months, in order to confirm and be sure this fluid is representative of the deep reservoir. Even if the auxiliary geothermometers are very useful tools, they must be always used together and in the framework of a global geochemical data interpretation because if it is not the case, they may induce important errors in the estimations of the reservoir temperatures in geothermal exploration. A scientific paper is envisaged in 2017 within the WP8 framework.

# Table of Content

# 1. Theoretical developments

This chapter is divided in two parts: 1) an exhaustive literature review about the existing geothermometers in environments of crystalline basements and sedimentary basins, and the determination of new auxiliary thermometric relationships for geothermal brines discharged from crystalline basements and sedimentary basins, 2) a literature review about the tracer tests carried in environments of crystalline basements and sedimentary basins.

## 1.1 Geothermometers

### 1.1.1 Description of the geothermometers

One of the major applications of water geochemistry in the exploration of the potential geothermal reservoirs involves estimation of their temperature using chemical and isotopic geothermometers on fluid samples collected either from geothermal wells or thermal springs. Since 1965, several geothermometers such as Na-K, Na-K-Ca, Na-K-Ca-Mg, K-Mg, $SiO_2$, $\delta^{18}O_{H2O-SO4}$ are commonly available in geothermal exploration for all types of geological environments (Lloyd, 1968; Mizutani and Rafter, 1969; White, 1970; Fournier, 1979; Michard, 1979; Fournier and Truesdell, 1973; Fournier and Potter, 1979; Giggenbach, 1988; Nicholson, 1993; Arnorsson, 1983, 2000; Serra and Sanjuan, 2004), but unfortunately, the estimates of reservoir temperatures using these classical tools are not always concordant, especially at low and medium temperature.

The absence of chemical or isotopic equilibrium reactions between water and minerals occurring in the geothermal reservoirs, the mixing of the deep geothermal fluids with surface waters or their cooling and the associated precipitation/dissolution processes during their rising to the surface can be responsible of these discordances. For instance, for dilute thermal waters collected from volcanic or granite areas, the Na-K geothermometer often yields overestimated reservoir temperatures. The Na-K and Na-K-Ca geothermometers cannot be used with seawater and seawater derived fluids not controlled by chemical equilibrium reactions with surrounding rocks.

### 1.1.2 Theoretical development of new geothermometers

#### a) Auxiliary geothermometers for dilute geothermal waters in granite environments

From numerous data obtained in several world geothermal fields located in volcanic and granitic areas (more than 120 fluid samples), Fouillac and Michard (1981) proposed an auxiliary geothermometer for thermal and geothermal waters based on two empirical and statistical thermometric Na-Li relationships which take into account the concentrations of dissolved chloride in the waters (Cl < 0.3 M and Cl ≥ 0.3 M). The thermometric relationship associated with dilute waters (Cl < 0.3 M) between 25 and 320°C is the following one (Na/Li being a molar ratio):

$$t\ (°C) = 1000\ /\ [\log\ (Na/Li) + 0.38] - 273.15 \qquad r^2 = 0.97 \quad (1)$$

From statistical analyses of selected hot springs in more than 60 areas in granites from Europe (Eastern and Western Pyrénées in Spain-France, Corsica in France, Alps in France-Italy, Sardinia in Italy, Vosges in France, Bulgaria, Sweden, Galicia in Spain), Michard (1990) proposed several thermometric relationships constituted of the concentration of dissolved potassium or sodium and of that of different trace elements such as Li, Rb, Cs, Sr, Fe, Mn, Fe and W, for dilute geothermal waters between 25 and 150°C.

Among the latter, a new Na-Li thermometric relationship, close to the previous one, was determined according to the following equation:

$$t\ (°C) = 1040\ /\ [\log\ (Na/Li) + 0.43] - 273.15 \qquad r^2 = 0.91 \qquad (2)$$

Verma and Santoyo (1997) presented a new improved equation for the Na-Li geothermometer, obtained by statistical treatment of the data used by Fouillac and Michard (1981) and application of outlier detection and rejection as well as theory of error propagation. New equations were also developed for estimating errors associated with the use of this new thermometric equation and comparing with the performance of the original equation (Fouillac and Michard, 1981). For temperatures ranging from about 50 to 320°C, their new equation for Na-Li geothermometer showed errors of about 13-34% as compared to 15-39% for the original equation.

The new Na/Li equation obtained by Verma and Santoyo (1997), for a final number of 130 observations, is:

$$t\ (°C) = 1049\ /\ [\log\ (Na/Li) + 0.44] - 273.15 \qquad r^2 = 0.91 \qquad (3)$$

This equation is very close to the previous one (equation 2) obtained by Michard (1990).

The equation 1 proposed by Fouillac and Michard (1981) was validated by numerous new data (Sanjuan and Millot, 2009). By integrating these data with those used to determine the equation 1 (a total of 119 data), another straight line was obtained by Sanjuan *et al.* (2014) with a slightly different equation. This equation is:

$$t\ (°C) = 1074\ /\ [\log\ (Na/Li) + 0.60] - 273.15 \qquad r^2 = 0.98 \qquad (4)$$

However, it remains very close to the previous ones (equations 1, 2 and 3) and confirms their relevance.

Sanjuan *et al.* (2014) determined another Na-Li thermometric relationship for 17 diluted waters from different high-temperature (200-325°C) Icelandic geothermal waters (Krafla, Namafjall, Nesjavellir and Hveragerdi areas) located in a volcanic environment. The corresponding equation:

$$t\ (°C) = 2002\ /\ [\log\ (Na/Li) + 1.322] - 273.15 \qquad r^2 = 0.97 \qquad (5)$$

is very different from the previous ones (equations 1, 2, 3 and 4). This equation was also successfully applied to high-temperature dilute geothermal waters from the East African Rift (Ethiopia, Kenya).

Most of these thermometric relationships give estimations of temperature with an uncertainty close to ± 20°C.

Due to a rather low reactivity of the lithium during the ascent of the geothermal waters up to the surface, the use of these thermometric relationships often give more reliable deep temperature estimates than those of the classical geothermometers.

The significant difference between the first equations (1, 2, 3 and 4) and the equation (5) indicates that, if temperature and mobile ion concentrations are dominant factors to determine the concentration of lithium, regional and geological variations can be also very important.

In addition to these Na-Li thermometric equations, among the other thermometric relationships proposed by Michard (1990) for more than 60 dilute deep geothermal waters discharged from granitic areas located in Europe between 25 and 150°C, we can enumerate the following equations (with molar element ratios):

$$t\ (°C) = 1920\ /\ [\log\ (Na/Rb) + 1.0] - 273.15 \qquad r^2 = 0.86 \qquad (6)$$

$$t\ (°C) = 1400\ /\ [\log\ (Na/Rb) - 0.66] - 273.15 \qquad r^2 = 0.83 \qquad (7)$$

$$t\ (°C) = 1400\ /\ [\log\ (Na/Rb) - 0.27] - 273.15 \qquad r^2 = 0.87 \qquad (8)$$

$$t\ (°C) = 2610\ /\ [\log\ (Na/Cs) + 2.48] - 273.15 \qquad r^2 = 0.86 \qquad (9)$$

$$t\ (°C) = 2450\ /\ [4.44 - \log\ (K^2/Sr)] - 273.15 \qquad r^2 = 0.93 \qquad (10)$$

$$t\ (°C) = 2440\ /\ [5.32 - \log\ (K^2/Fe)] - 273.15 \qquad r^2 = 0.85\ \text{for}\ n = 35 \qquad (11)$$

$$t\ (°C) = 2880\ /\ [7.64 - \log\ (K^2/Mn)] - 273.15 \qquad r^2 = 0.81 \qquad (12)$$

$$t\ (°C) = -2170\ /\ [\log\ (K \times F) + 1.79] - 273.15 \qquad r^2 = 0.69 \qquad (13)$$

$$t\ (°C) = -3330\ /\ [\log\ (K^2 \times W) + 5.94] - 273.15 \qquad r^2 = 0.77 \qquad (14)$$

Some of these thermometric equations, especially for the Mn, F and W elements, can only give very approximate estimations of reservoir temperature. However, as concluded by Michard (1990), all these relationships can be not only considered as auxiliary geothermometers, but can also be used to calculate the total concentration of these trace elements in a fluid in chemical equilibrium with the surrounding rocks, if temperature and the mobile ions concentrations are known. Indeed, it has already been shown that the composition of major species dissolved in this type of fluid can be calculated only from temperature and the sum of the electric charge of mobile ions (Michard and Fouillac, 1980; Arnorsson *et al.*, 1983; Giggenbach, 1984). Estimation of major species is reliable within ± 50%. For some trace elements (Sr, Li, Rb), estimation is within a factor ± 2 and within a factor ± 3 for other cationic elements.

Shortly later, Alaux-Négrel (1991) found relatively poor relationships for the auxiliary geothermometers K-Fe, K-W, K-Mo and K-U determined using alkaline thermal waters in a granitic environment given that the associated mean square correlation coefficients were lower than 0.61. The corresponding equations are (with molar element ratios):

$$t\ (°C) = 1950\ /\ [3.95 - \log\ (K^2/Fe)] - 273.15 \qquad r^2 = 0.59 \qquad (15)$$

$$t\ (°C) = -2870\ /\ [\log\ (K^2 \times W) + 7.22] - 273.15 \qquad r^2 = 0.57 \qquad (16)$$

$$t\ (°C) = -2800\ /\ [\log\ (K^2 \times Mo) + 7.94] - 273.15 \qquad r^2 = 0.61 \qquad (17)$$

$$t\ (°C) = -1140\ /\ [\log\ (K \times U) + 11.12] - 273.15 \qquad r^2 = 0.50 \qquad (18)$$

Alaux-Négrel *et al.* (1993) demonstrated that, for alkaline thermal waters discharged from granitic areas of Southern Europe, most transition metals were limited to very low concentrations probably by sulfide minerals ($CoS$, $MoS_3$, $ZnS$, $Sb_2S_3$…) and uranium was limited in solution by uraninite. All these elements showed very weak variations of concentrations *versus* temperature, between 20 and 120°C.

In parallel to these auxiliary geothermometers, Michard (1990) also proposed new or adapted thermometric relationships integrating some major species for dilute geothermal waters discharged from granite environments between 25 and 150°C. The corresponding equations are (with molar element ratios):

$$t\ (°C) = 1170 / [\log (Na/K) + 1.42] - 273.15 \tag{19}$$

$$t\ (°C) = -880 / [\log (H_4SiO_4 \text{ in mol/l}) + 0.76] - 273.15 \quad r^2 = 0.90 \tag{20}$$

$$t\ (°C) = 3030 / [\log (Ca/K^2) + 3.94] - 273.15 \quad r^2 = 0.94 \tag{21}$$

$$t\ (°C) = 3000 / [\log (Mg/K^2) + 5.84] - 273.15 \quad r^2 = 0.88 \tag{22}$$

It is well known that silica content in thermal waters is controlled by quartz or by chalcedony (Fournier, 1977; Fournier and Potter, 1982). In the basaltic area of Iceland, Arnorsson (1975) showed that quartz was the controlling phase above 170°C, and by chalcedony below 125°C. In the granitic waters of this study (Michard, 1990), the transition temperature was about 100°C. In general, waters with aquifer temperatures lower than 80°C equilibrates with chalcedony, but some low-temperature waters equilibrate with quartz. In the 80-100°C temperature range, silica concentrations are intermediate between quartz and chalcedony solubility. This explains the rather low correlation between $H_4SiO_4$ and deep temperature.

### b) Auxiliary geothermometers for saline geothermal waters from crystalline basements and sedimentary basins

The second empirical and statistical thermometric Na-Li relationship determined by Fouillac and Michard (1981) is associated with the saline geothermal waters (Cl ≥ 0.3 M) discharged from crystalline and volcanic environments between 25 and 320°C. The corresponding equation is (Na/Li being a molar ratio):

$$t\ (°C) = 1195 / [\log (Na/Li) - 0.13] - 273.15 \quad r^2 = 0.98 \tag{23}$$

The new improved equation proposed by Verma and Santoyo (1997), on the basis of a statistical treatment of data given by Fouillac and Michard (1981) and the application of outlier detection and rejection as well as the theory of error propagation, was the following one:

$$t\ (°C) = 1267 / [\log (Na/Li) + 0.07] - 273.15 \tag{24}$$

For temperatures ranging from about 50 to 320°C, this new equation showed errors from 10 to 44%, much lower than 26-106% estimated for the corresponding original equation 23, but remains very close to this last one.

The equation 23 proposed by Fouillac and Michard (1981) was validated by numerous new data (Sanjuan and Millot, 2009). By integrating these data with those used to determine the equation 23 (a total of 61 data), another straight line was obtained by Sanjuan *et al.* (2014) with a slightly different equation. This equation is:

$$t\ (°C) = 1222 / [\log (Na/Li) - 0.03] - 273.15 \quad r^2 = 0.98 \tag{25}$$

However, it remains very close to the previous ones (equations 23 and 24) and confirms their relevance.

From about 88 fluid data obtained in world geothermal and US oil fields, Kharaka *et al.* (1982) and Kharaka and Mariner (1989) proposed another empirical and statistical Na/Li thermometric relationship as well as an auxiliary Mg-Li geothermometer for hot saline fluids discharged from sedimentary basins between 0 and 350°C. The corresponding equations are respectively (with molar element ratios):

$$t \ (°C) = 1590 \ / \ [\log (Na/Li) + 1.299] - 273.15 \qquad r^2 = 0.91 \qquad (26)$$

$$t \ (°C) = 4400 \ / \ [\log (Mg/Li^2) + 7.640] - 273.15 \qquad r^2 = 0.96 \qquad (27)$$

Kharaka and Mariner (1989) found a slightly different equation for the oil field waters only which is the following one:

$$t \ (°C) = 3820 \ / \ [\log (Mg/Li^2) + 5.960] - 273.15 \qquad r^2 = 0.90 \qquad (28)$$

The equation 26 is very different from the equations 23, 24 and 25. However, it was validated by numerous new data (Sanjuan and Millot, 2009). By integrating these data with those used to determine the equation 26 (a total of 141 data), another straight line was obtained by Sanjuan *et al.* (2014) with a slightly different equation. This equation is:

$$t \ (°C) = 1588 \ / \ [\log (Na/Li) + 1.286] - 273.15 \qquad r^2 = 0.98 \qquad (29)$$

However, it remains very close to the equation 26 and confirms its relevance.

The deep geothermal waters collected from the granite basement located in the Rhine Graben (Soultz-sous-Forêts in Alsace, France, and Landau, Insheim, in Germany) agree with the Na/Li and Mg/Li relationships relative to the sedimentary basins. In fact, the chemical and isotopic compositions of these waters suggest that their origin is sedimentary (Triassic Buntsandstein formation) and have reached chemical equilibrium at 220-240°C with these sedimentary rocks rather with granite (Sanjuan *et al.*, 2010).

No other thermometric relationship was found in the literature for this type of fluids and environments. For fluids derived from seawater-basalt interaction processes existing in emerged rifts such as those of Iceland (Reykjanes, Svartsengi, and Seltjarnarnes geothermal fields) and Djibouti (Asal-Ghoubbet and Obock geothermal areas), or in numerous oceanic ridges and rises (Mid-Atlantic and Middle-Valley ridges, East Pacific rise, etc.), Sanjuan *et al.* (2014) proposed the following equation:

$$t \ (°C) = 920 \ / \ [\log (Na/Li) - 1.105] - 273.15 \qquad r^2 = 0.99 \qquad (30)$$

Unfortunately, the performance of the Na/Li geothermometer is poorly known, but the existence of several different relationships (equations 23, 26, 29 and 30) confirms that the Na/Li ratio is not only dependent on temperature and fluid salinity, but also on the nature of the reservoir rocks reacting with the geothermal waters.

Mineralogical considerations, results of thermodynamic calculations as well as literature values, suggest that the Na/Li ratios, for the two new thermometric relationships obtained by Sanjuan *et al.* (2014), are probably controlled by full equilibrium reactions between, at least, albite, K-feldspar, quartz, kaolinite and clay alteration products such as illite and Li-mica. Similar equilibrium reactions involving slightly different mineral assemblages could explain the other three existing Na/Li relationships (Fouillac and Michard, 1981; Kharaka and Mariner, 1989).

## 1.1.3 Determination of appropriate thermometric relationships for saline geothermal waters from crystalline basements and sedimentary basins

Apart the Na/Li and Mg/Li thermometric relationships, no other auxiliary chemical geothermometer was found in the literature for the saline geothermal waters discharged from sedimentary basins or crystalline basements. In order to develop new auxiliary geothermometers applied to this type of fluids, 33 deep saline waters were considered in the literature, especially the deep waters discharged from wells located in oil fields and geothermal areas of the Rhine Graben (Pauwels *et al.*, 1993; Sanjuan *et al.*, 2010, 2016a), in oil fields of the North Sea (Warren and Smalley, 1994; Ziegler *et al.*, 2001) and in the Salton Sea geothermal area (Werner, 1970; Williams and McKibben, 1989). Their deep temperatures range from 70 to 320°C. Their characteristics and chemical compositions are given in table 1.

| Regional area | Local area | Well | Stratigraphic age | Lithology | References | Date | Depth m | Measured T_bottom-well °C | Estimated T_bottom-well °C | 1000/T K⁻¹ |
|---|---|---|---|---|---|---|---|---|---|---|
| Rhine Graben, Germany | Landau | GTLA-1 | Carboniferous | Granite | Sanjuan *et al.* (2015a) | 09/08/2011 (10:11) | 3044 | 160 | 220 | 2.028 |
| Rhine Graben, Germany | Landau | GTLA-1 | Carboniferous | Granite | Sanjuan *et al.* (2015a) | 20/06/2013 (09:40) | 3044 | 160 | 220 | 2.028 |
| Rhine Graben, Germany | Insheim | INSH | Carboniferous | Granite | Sanjuan *et al.* (2015a) | 20/06/2013 (14:00) | 3600 | 165 | 220 | 2.028 |
| Rhine Graben, France | Soultz-sous-Forêts | GPK-2 | Carboniferous | Granite | Sanjuan *et al.* (2015a) | 19/06/13 | 5000 | 200 | 220 | 2.028 |
| Rhine Graben, France | Rittershoffen | GRT-1 | Carboniferous | Granite | Sanjuan *et al.* (2015a) | 10/01/2013 (14:00) | 2580 | 160 | 220 | 2.028 |
| Rhine Graben, France | Cronenbourg | CRON | Triassic (Buntsandstein) | Sedimentary rock | Sanjuan *et al.* (2015a) | 1980 | 2870 | 140 | 220 | 2.028 |
| Rhine Graben, Germany | Bruchsal | GBRU-1 | Triassic - Permian | Sedimentary rock | Sanjuan *et al.* (2015a) | 03/04/12 | 2542 | 120 | 190 | 2.159 |
| Rhine Graben, Germany | Bruchsal | GBRU-1 | Triassic - Permian | Sedimentary rock | Sanjuan *et al.* (2015a) | 1992 | 2542 | 120 | 190 | 2.159 |
| Rhine Graben, Germany | Bühl | BUHL | Triassic (Buntsandstein) | Sedimentary rock | Sanjuan *et al.* (2015a) | 1992 | 2655 | 115 | 115 | 2.576 |
| Rhine Graben, Germany | Bühl | BUHL | Triassic (Buntsandstein) | Sedimentary rock | Sanjuan *et al.* (2015a) | 1992 | 2655 | 115 | 115 | 2.576 |
| Rhine Graben, Germany | Landau oilfield | LA-95 | Oligocene (Chattian) | Sedimentary rock | Sanjuan *et al.* (2015a) | 09/08/2011 (15:35) | 1002 | | 100 | 2.680 |
| Rhine Graben, Germany | Landau oilfield | LA-134 | Oligocene (Chattian-Rupelian) | Sedimentary rock | Sanjuan *et al.* (2015a) | 09/08/2011 (15:45) | 1447 | | 100 | 2.680 |
| Rhine Graben, Germany | Landau oilfield | LA-53 | Oligocene (Rupelian) | Sedimentary rock | Sanjuan *et al.* (2015a) | 09/08/2011 (16:23) | 959 | | 100 | 2.680 |
| Rhine Graben, Germany | Landau oilfield | LA-15 | Oligocene (Chattian) | Sedimentary rock | Sanjuan *et al.* (2015a) | 09/08/2011 (16:54) | 999 | | 100 | 2.680 |
| Rhine Graben, Germany | Landau oilfield | LA-7 | Oligocene (Chattian-Rupelian) | Sedimentary rock | Sanjuan *et al.* (2015a) | 09/08/2011 (17:02) | 1451 | | 100 | 2.680 |
| Rhine Graben, Germany | Landau oilfield | LA-33 | Oligocene (Chattian-Rupelian) | Sedimentary rock | Sanjuan *et al.* (2015a) | 09/08/2011 (17:17) | 1527 | | 100 | 2.680 |
| Rhine Graben, Germany | Landau oilfield | LA-42 | Oligocene (Chattian) | Sedimentary rock | Sanjuan *et al.* (2015a) | 09/08/2011 (17:24) | 1050 | | 100 | 2.680 |
| Rhine Graben, France | Scheibenhart oilfield | NDL-101 | Oligocene (Rupelian) | Sedimentary rock | Sanjuan *et al.* (2015a) | 10/08/2011 (10:00) | 947 | | 70 | 2.914 |
| Rhine Graben, France | Scheibenhart oilfield | NDL-102 | Oligocene (Rupelian) | Sedimentary rock | Sanjuan *et al.* (2015a) | 10/08/2011 (10:53) | 561 | | 70 | 2.914 |
| Rhine Graben, France | Soultz-sous-Forêts | Les Hélions | | | Pauwels *et al.* (1993) | 1992 | | 72 | 220 | 2.028 |
| North Sea, Norway | Clyde oilfield | 30/17b-A01 | Upper Jurassic | Sandstone | Warren and Smalley (1994) | Water Atlas data | 3718 | 146 | 146 | 2.386 |
| North Sea, Norway | Gyda oilfield | N1/03-3A | Upper Jurassic | Sandstone | Warren and Smalley (1994) | Water Atlas data | 4225 | 154 | 154 | 2.341 |
| North Sea, Norway | Oseberg oilfield | C-10 | Middle Jurassic | Sandstone | Ziegler *et al.* (2001) | 25/10/1993 | | 100 | 110 | 2.610 |
| North Sea, Norway | Buchan oilfield | Well? | Devonian | Sandstone | Warren and Smalley (1994) | Water Atlas data | 2926 | 105 | 105 | 2.644 |
| North Sea, Norway | Hyde oilfield | 48/6-25 | Permian | Sandstone | Warren and Smalley (1994) | Water Atlas data | 2600 | 85 | 85 | 2.792 |
| North Sea, Norway | Brage oilfield | N31/43 | Middle Jurassic | Sandstone | Warren and Smalley (1994) | Water Atlas data | 2160 | 71 | 71 | 2.906 |
| North Sea, Norway | Orwell oilfield | 50/26a-2 | Triassic | Sandstone | Warren and Smalley (1994) | Water Atlas data | 1540 | 65 | 65 | 2.957 |
| North Sea, Norway | Thames oilfield | 49/28-9Z | Permian | Sandstone | Warren and Smalley (1994) | Water Atlas data | 2481 | 83 | 83 | 2.808 |
| North Sea, Norway | Ivanhoe oilfield | 15/21a-33 | Upper Jurassic | Sandstone | Warren and Smalley (1994) | Water Atlas data | | 125 | 125 | 2.512 |
| North Sea, Norway | Miller oilfield | 16/8b-3 | Upper Jurassic | Sandstone | Warren and Smalley (1994) | Water Atlas data | 4103 | 120 | 120 | 2.544 |
| North Sea, Norway | Sleipner West oilfield | N15/9-7 | Middle Jurassic | Sandstone | Warren and Smalley (1994) | Water Atlas data | 3672 | 135 | 135 | 2.450 |
| Imperial Valley, California, USA | Salton Sea | Typical analysis | | | Werner (1970) | | | 300 | 300 | 1.745 |
| Imperial Valley, California, USA | Salton Sea | SSSDP | | | Williams and McKibben (1989) | June 1988 | 2000 | 320 | 320 | 1.686 |

| Well | T_measures °C | pH | Eh_nc mV | Na mg/l | K mg/l | Ca mg/l | Mg mg/l | Cl mg/l | SO₄ mg/l | NO₃ mg/l | Alk. meq/l | SiO₂ mg/l | TDS g/l | I.B. % | F mg/l | Br mg/l | Cl/Br mass ratio | B mg/l | Li mg/l | Sr mg/l | Mn µg/l | Fe µg/l | Rb µg/l | Cs µg/l |
|---|---|---|---|---|---|---|---|---|---|---|---|---|---|---|---|---|---|---|---|---|---|---|---|---|
| GTLA-1 | 25.1 | 5.15 | 12 | 28200 | 4000 | 7700 | 76.0 | 64200 | 126 | < 0.5 | 2.89 | 159 | 106 | -3.36 | 3.2 | 219 | 293 | 39.0 | 179 | 430 | 26100 | 21700 | 27600 | 19300 |
| GTLA-1 | 26.3 | 4.96 | 122 | 29600 | 3795 | 7391 | 85.1 | 64500 | 131 | < 0.5 | 2.03 | 158 | 106 | -2.24 | | 198 | 326 | | 182 | | | | | |
| INSH | 46.2 | 5.23 | 104 | 29900 | 3816 | 7254 | 99.4 | 64900 | 131 | < 0.5 | 2.46 | 167 | 107 | -1.70 | < 1 | 185 | 351 | 41.1 | 168 | 456 | 25160 | 25064 | 27200 | 14530 |
| GPK-2 | 37.0 | 4.98 | -199 | 28140 | 3195 | 7225 | 131 | 58559 | 157 | < 0.5 | 2.75 | 201 | 99 | 3.25 | 2.9 | 216 | 271 | 40.8 | 173 | 455 | 16900 | 25500 | 25700 | 14900 |
| GRT-1 | 50.8 | 6.27 | -101 | 28451 | 3789 | 7200 | 138 | 59900 | 220 | < 0.5 | 3.06 | 146 | 101 | 2.75 | < 5 | 251 | 239 | 45.9 | 190 | 498 | 15565 | 48671 | 30159 | 16800 |
| CRON | | 6.70 | | 54000 | 4030 | 4810 | 126 | 62000 | 480 | < 0.5 | 2.2 | 143 | 104 | -0.14 | 5.5 | 361 | 172 | 37.9 | 210 | 405 | | 29000 | 12000 | |
| GBRU-1 | 27.0 | 5.06 | 56 | 35127 | 3113 | 7363 | 301 | 73566 | 267 | < 0.5 | 6.18 | 77 | 121 | -2.56 | < 1 | 203 | 362 | 39.4 | 159 | 391 | 25170 | 42380 | 23388 | 12478 |
| GBRU-1 | | | | 38100 | 2200 | 7740 | 434 | 75200 | 387 | < 0.5 | 7.7 | 42 | 125 | 1.36 | 0.85 | 230 | 327 | 40.0 | 166 | 324 | | 78000 | 19000 | 2200 |
| BUHL | | | | 64000 | 494 | 11600 | 1930 | 120300 | 1586 | | | 201 | 201 | 3.31 | 31.8 | 711 | 169 | 29.0 | 41.0 | 456 | | 41000 | 900 | 600 |
| BUHL | | | | 63900 | 503 | 11700 | 1900 | 120500 | 1525 | | | 201 | 201 | 3.15 | 31.0 | 726 | 166 | 31.1 | 41.2 | 485 | | 36000 | 1000 | 600 |
| LA-95 | 16.9 | 6.78 | | 16100 | 287 | 1580 | 320 | 29900 | 142 | < 0.5 | 4.39 | 45 | 49 | -3.76 | 1.7 | 178 | 168 | 44.0 | 19.0 | 151 | 487 | 3130 | 814 | 205 |
| LA-134 | 25.5 | 6.70 | -78 | 16100 | 193 | 1710 | 246 | 28800 | 1110 | < 0.5 | 7.05 | 30 | 49 | -2.92 | 0.7 | 170 | 169 | 55.0 | 24.5 | 94 | 1090 | 43800 | 393 | 137 |
| LA-53 | 25.7 | 6.97 | -84 | 16400 | 295 | 1740 | 244 | 28200 | 764 | < 0.5 | 5.89 | 47 | 48 | 2.03 | 0.7 | 180 | 157 | 55.0 | 20.2 | 146 | 323 | 3900 | 1200 | 855 |
| LA-15 | 25.8 | 6.62 | -80 | 23000 | 286 | 2970 | 438 | 44000 | 484 | < 0.5 | 4.48 | 21 | 72 | -4.52 | < 0.5 | 263 | 167 | 56.0 | 23.0 | 158 | 972 | 19900 | 458 | 74.6 |
| LA-7 | 25.5 | 5.86 | -43 | 33000 | 481 | 4200 | 450 | 62800 | 233 | < 0.5 | 6.09 | 16 | 102 | -4.76 | 1.0 | 412 | 152 | 85.0 | 20.9 | 308 | 1540 | 11400 | 1480 | 329 |
| LA-33 | 25.7 | 6.51 | -65 | 31300 | 368 | 4400 | 572 | 56700 | 697 | < 0.5 | 6.69 | 30 | 95 | 1.75 | 1.1 | 385 | 147 | 65.0 | 29.4 | 272 | 2190 | 33100 | 532 | 100 |
| LA-42 | 26.2 | 6.50 | -56 | 33000 | 399 | 4600 | 593 | 60500 | 310 | < 0.5 | 5.42 | 47 | 101 | 0.89 | 1.1 | 389 | 156 | 65.0 | 23.9 | 264 | 1560 | 33000 | 838 | 151 |
| NDL-101 | 31.9 | 6.06 | -136 | 48000 | 504 | 6500 | 1180 | 87500 | 462 | < 0.5 | 4.90 | 21 | 145 | 1.79 | 0.7 | 500 | 175 | 3.8 | 39.7 | 36 | 206 | 50300 | 78.9 | 16.1 |
| NDL-102 | 33.9 | 6.85 | -90 | 31100 | 209 | 2330 | 1450 | 55100 | 178 | < 0.5 | 4.85 | 16 | 91 | 2.39 | < 0.5 | 356 | 155 | 23.6 | 17.6 | 614 | 4360 | 4360 | 175 | 10.9 |
| Les Hélions | | 6.20 | | 5200 | 564 | 1500 | 111 | 11300 | 675 | | 5.09 | 37 | 20 | -2.42 | 3.9 | 47.3 | 239 | 37.4 | 29.6 | 67.8 | | 4250 | | |
| 30/17b-A01 | | 6.00 | | 62750 | 3750 | 9650 | 870 | 122000 | 335 | | 2.46 | | 200 | -1.62 | | | | | | 680 | | 50000 | | |
| N1/03-3A | | 5.63 | | 59250 | 3830 | 36810 | 3190 | 171000 | | | 1.20 | 34 | 276 | -0.26 | | | | | | 956 | | 467000 | | |
| C-10 | | 6.05 | | 16500 | 304 | 770 | 117 | 23000 | 5 | | | 29 | 41 | 17.85 | | 115 | 200 | | 7.8 | 146 | | 2000 | | |
| Well? | | 5.80 | | 56700 | 1525 | 16075 | 1250 | 121600 | 220 | | 3.28 | | 199 | -0.10 | | | | | | 938 | | 100000 | | |
| 48/6-25 | | 5.20 | | 72100 | 1425 | 19900 | 2540 | 146000 | 420 | | | 30 | 244 | 6.60 | | 40.6 | 37.8 | | | 855 | | 290000 | | |
| N31/43 | | 5.69 | | 16330 | 438 | 2056 | 321 | 29991 | 58 | | 13.20 | | 50 | -0.44 | | | | | | 280 | | | | |
| 50/26a-2 | | 5.59 | | 59130 | 550 | 8300 | 500 | 107710 | 845 | | 1.21 | 6 | 177 | -0.25 | | 40.0 | 8.2 | | | 275 | | 43000 | | |
| 49/28-9Z | | 5.59 | | 73430 | 1660 | 15510 | 4980 | 156905 | 520 | | 0.69 | | 254 | -0.02 | | | | | | 570 | | 130000 | | |
| 15/21a-33 | | 6.35 | | 32960 | 560 | 5850 | 840 | 64300 | 12 | | 4.92 | 8 | 105 | 0.24 | | 47.0 | | | | 565 | | 51000 | | |
| 16/8b-3 | | 7.66 | | 27080 | 1340 | 735 | 105 | 43660 | 5 | | 41.31 | | 76 | -0.44 | | | | | | 180 | | 175000 | | |
| N15/9-7 | | 6.36 | | 45701 | 2080 | 5226 | 1495 | 87810 | | | 6.70 | | 143 | -2.13 | | | | | | 315 | | | | |
| Typical analysis | | | | 51000 | 25000 | 40000 | 730 | 185000 | 56 | 35 | | > 110 | 307 | -0.61 | 18 | 146 | 1267 | 520 | 300 | 750 | 2000000 | 3200000 | 169000 | 20000 |
| SSSDP | | 5.30 | | 53700 | 17100 | 26300 | 43 | 152000 | 123 | | | > 840 | 252 | -0.74 | | 111 | 1369 | 380 | 215 | 410 | 1470000 | 1620000 | | 23000 |

*Table 1 - Characteristics and chemical compositions of saline waters discharged from wells located in oil fields and geothermal areas of the Rhine Graben, in oil fields of the North Sea and in the Salton Sea geothermal area.*

If the concentrations of dissolved strontium and iron are available for most of the waters, those of dissolved rubidium, caesium, fluoride and manganese are missing for all the waters from the oil wells from North Sea.

The oil brines characterized by high amounts of halite dissolution, in which the concentrations of dissolved sodium and chloride were predominant and the concentrations of the other major species were very low, were discarded.

As for the dilute geothermal waters discharged from granite environments, thermometric relationships were investigated for the Na-Rb, Na-Cs, K-Sr, K-Fe, K-Mn and K-F systems, using molar element ratios. From figures 1 to 6, we can see that only the relationships Na-Rb and Na-Cs indicate mean square correlation coefficients higher than 0.8.
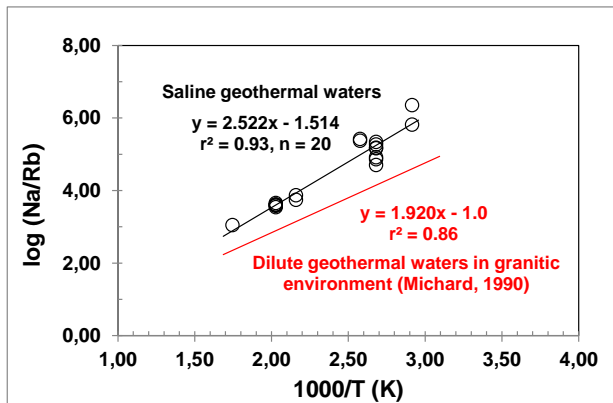


Figure 1 - Na-Rb thermometric relationships.
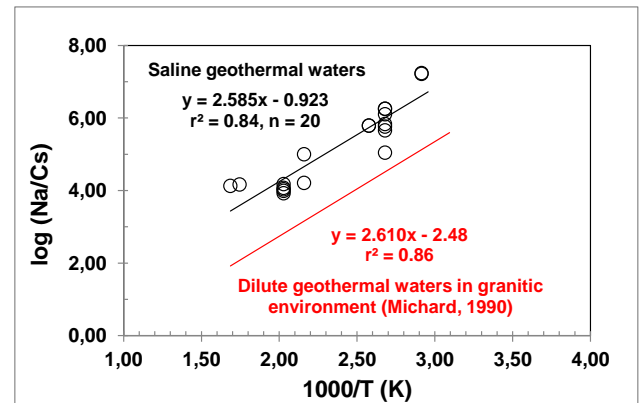


Figure 2 - Na-Cs thermometric relationships.
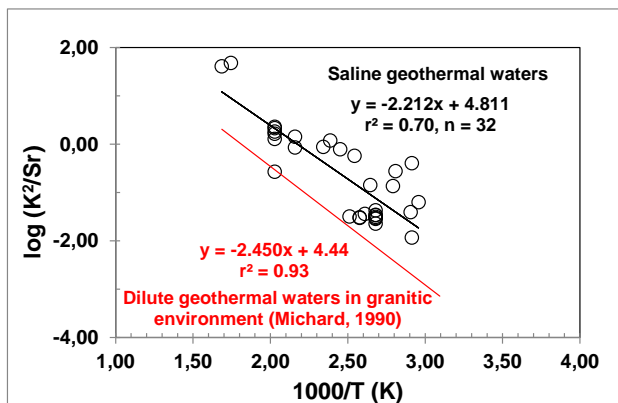


Figure 3 - K-Sr thermometric relationships.
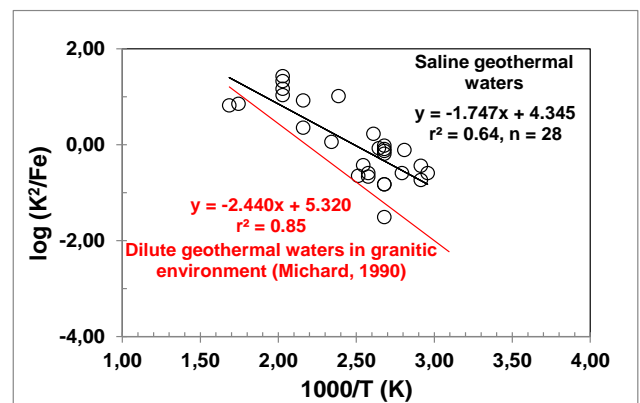


Figure 4 - K-Fe thermometric relationships.
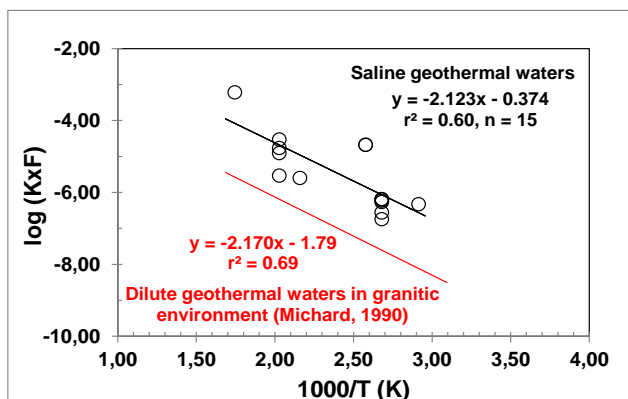


Figure 5 - K-F thermometric relationships.
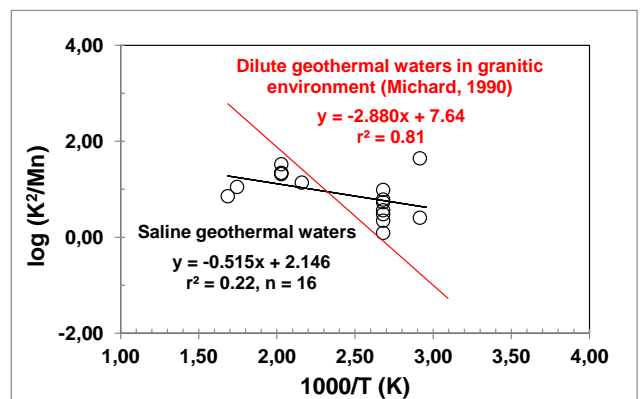


Figure 6 - K-Mn thermometric relationships.

The two corresponding thermometric equations are (with molar element ratios):

$$t \ (°C) = 2522 \ / \ [\log \ (Na/Rb) + 1.514] - 273.15 \qquad r^2 = 0.93 \qquad n = 20 \qquad (31)$$

$$t \ (°C) = 2585 \ / \ [\log \ (Na/Cs) + 0.843] - 273.15 \qquad r^2 = 0.84 \qquad n = 20 \qquad (32)$$

These two equations would have to be useful for geothermal exploration, especially for high-salinity thermal springs discharged from sedimentary basins or crystalline basements.

For the other relationships, the mean square correlation coefficients are lower than 0.7 and consequently, must be used with caution. The corresponding equations are (with molar element ratios):

$$t \ (°C) = 2212 \ / \ [4.811 - \log \ (K^2/Sr)] - 273.15 \qquad r^2 = 0.70 \qquad n = 32 \qquad (33)$$

$$t \ (°C) = 1747 \ / \ [4.345 - \log \ (K^2/Fe)] - 273.15 \qquad r^2 = 0.64 \qquad n = 28 \qquad (34)$$

$$t \ (°C) = -2123 \ / \ [\log \ (KF) + 0.374] - 273.15 \qquad r^2 = 0.60 \qquad n = 15 \qquad (35)$$

$$t \ (°C) = 515 \ / \ [2.146 - \log \ (K^2/Mn)] - 273.15 \qquad r^2 = 0.22 \qquad n = 16 \qquad (36)$$

For manganese, the thermometric relationship for only 16 waters is very poor and cannot be used.

Once again, the use of all these different thermometric relationships confirm that the concentrations of the trace elements (Li, Rb, Cs, Sr, Fe, Mn, F…) dissolved in the geothermal fluids are not only controlled by temperature, but also by other influent factors such as the fluid composition and salinity, the nature of the rock, its degree of alteration and the water-rock ratio.

For the K-Sr and K-Fe thermometric relationships, if we exclude the North Sea fluids, the mean square correlation coefficients are clearly improved ($r^2 = 0.97$ and 0.70, respectively; Figs 7 and 8) and the thermometric relationship becomes:

$$t \ (°C) = 2992 \ / \ [6.472 - \log \ (K^2/Sr)] - 273.15 \qquad r^2 = 0.97 \qquad n = 19 \qquad (37)$$

$$t \ (°C) = 1863 \ / \ [4.571 - \log \ (K^2/Fe)] - 273.15 \qquad r^2 = 0.70 \qquad n = 19 \qquad (38)$$
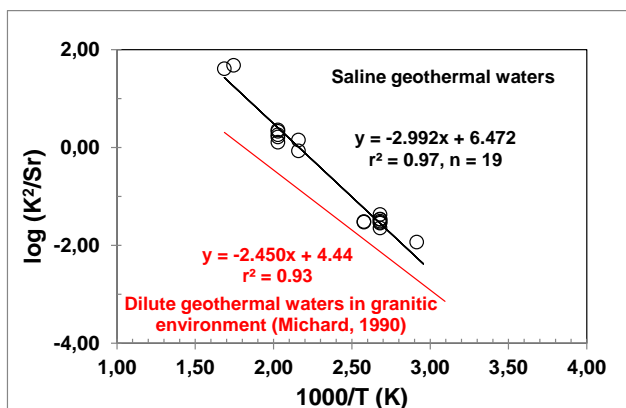


*Figure 7 - K-Sr thermometric relationships.*
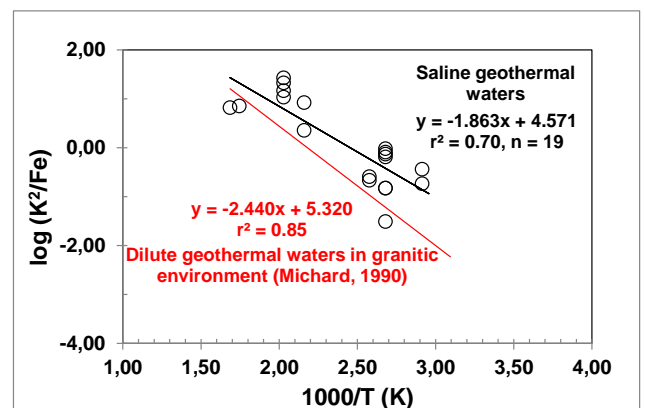


*Figure 8 - K-Fe thermometric relationships.*

All these results were presented in the Goldschmidt 2016 Conference held at Yokohama, in Japan (Sanjuan *et al.*, 2016b).

## 1.2 Tracer tests

### 1.2.1 Scope of the chemical tracer tests

Tracer testing is an efficient method to detect and characterize hydraulic connections between deep geothermal wells, to understand the migration of injected and natural fluids, and to estimate their proportions in discharged fluids, their velocities, flow rates, residence times. This method also enables to quantify fluid-rock contact surfaces, swept volumes, circulation paths and reservoir volumes. It can provide very useful information on reservoir processes. Depending upon the tracer test methodology, i.e. whether continuous tracer injection or slug injection is used and whether the test is backflow or inter-well, useful information can be obtained from the data collected during such tests after their interpretation and modelling (Sanjuan *et al.*, 2006a; Ghergut *et al.*, 2007). The tracer tests can provide information on transport properties and hydraulic connections essential for heat exchange or for fluid re-injection in geothermal reservoirs.

Following the required information, several types of modelling approach can be used to analyse the tracer Return-Curve data from a slug injection: signal processing codes such TEMPO based on a model of dispersive transfer (Sanjuan *et al.*, 2006a) or using the moment analysis method (Shook, 2005), hydraulic or hydrodynamic codes such as SHEMAT (Blumenthal *et al.*, 2007) or TOUGH2 (Pruess *et al.*, 2000), coupled hydro-mechanical codes, etc.

As the physicochemical behaviour of the tracers under given reservoir conditions (high salinity fluid, very low Redox potential, low pH, etc.) is not always well known, the use of a minimum of two tracers (or comparison with a natural tracer or laboratory experiments) is recommended.

### 1.2.2 Theoretical development of tracer tests at high temperature conditions (up to 300°C)

The requirements for using tracers adapted at high temperature conditions are:

- environmentally safe,
- thermal stability,
- conservative (non-reactant, adsorptive compounds),
- low cost (tracer and analyses),
- easily soluble,
- detectable at very low concentrations (< 5 ppb is recommended),
- absent from natural geothermal fluids and ground waters.

Until the 1990s, the main tracers used for geothermal energy were inorganic (bromide, iodide, molybdate, borate, etc.) or fluorescent compounds (fluorescein, uranine, eosin, rhodamin, sodium naphtionate, amino-G acid, etc.). A relatively complete literature review is given by Pauwels (1995). Many of these fluorescent dyes are not stable at high temperatures and some of them can be reactive. So, a lot of results obtained during the tracer tests could be qualitatively interpreted, but were difficult to quantify.

Since the 2000s, among the conservative tracers recommended in the literature for using at high temperature conditions, we can distinguish the following compounds:

*a) Liquid phase tracers*

- naphthalene (di, tri)sulfonates (nds, nts, ns) family: 1,5-, 1,6-, 2,6-, 2,7-nds, 1,3,5- and 1,3,6-nts, 1- and 2-ns (Rose *et al.*, 2001; Fig. 9). The 1,5-nds and 1,3,6-nts compounds showed modest decay (≈ 20%) upon exposure to simulated geothermal conditions for one week at 330°C. No decay was observed for either 2-ns or 2,7-nds at 330°C, indicating that these two compounds were among the most thermally stable. The thermal stability of six naphthalene sulfonic acid tracers (2,6-nds, 2,7-nds, 1,5-nds, 1,6-nds, 1-nsa and 2-nsa) was investigated by Mountain and Winick (2012) using a one-pass, continuous flow, fluid-rock interaction simulator at temperatures ranging from 270 to 390°C. Results showed that 2,6- and 2,7-nds remain stable to about 340°C while 1,5-nds begins to degrade as early 280°C. 1,6-nds shows degradation beginning at 330°C. For the nsa, the concentrations of 1-nsa increases until 330°C, after which it begins to degrade while 2-nsa concentrations increases until 380°C. It was obvious from these data that 2-nsa is the most thermally stable of the six studied sulfonic acids. The results were interpreted using three reaction mechanisms: desulfonation, isomerization and naphthalene pyrolysis ;
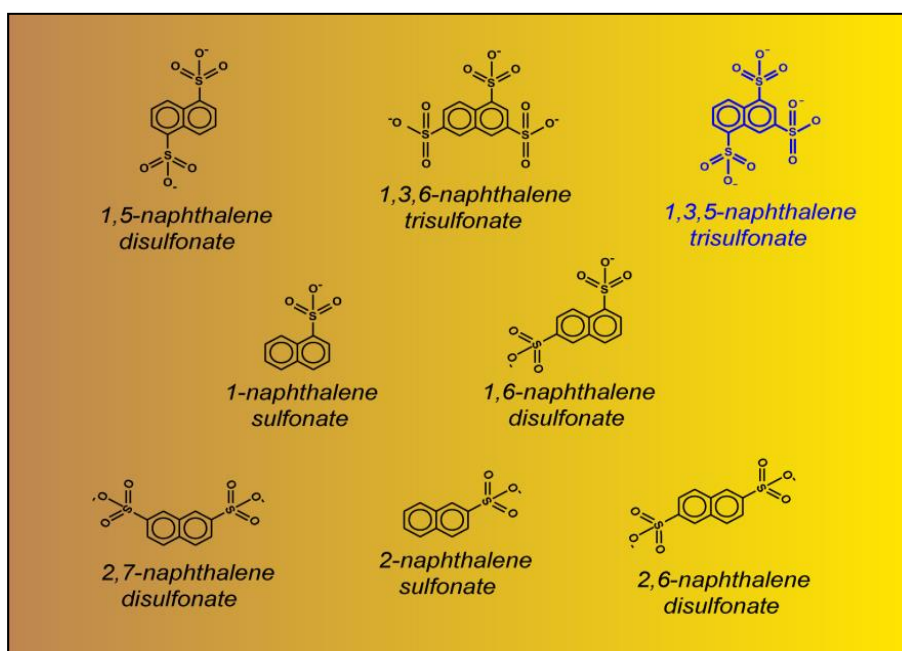


*Figure 9 - Chemical names and structures for the polyaromatic naphthalene sulfonate family compounds (Rose et al., 2001).*

- aromatic compounds such sodium benzoate or other benzoates (Adams *et al.*, 1992). Fluorobenzoic acids are water tracers widely used and preferred in oil reservoirs (J. Muller, IFE, pers. comm.);

- fluorescein up to 230-250°C because its thermal decay becomes significant above 200°C (Adams and Davis, 1991; Axelsson *et al.*, 2005; Axelsson, 2013). The other organic dyes are not recommended ;

- the gas tracer $SF_6$ is little used;

- the use of inorganic and radioactive tracers is limited because of the high natural background of the halides (Cl, Br, I…) and difficulty in obtaining permits for radioactive tracers.

b) *Vapour or two-phase tracers*

- alcohols (isopropanol, butan-2-ol, etc.), hydrofluorocarbons (volatile low molecular weight compounds R-134a ($CF_3CH_2F$) and R-23 ($CHF_3$), Adams *et al.*, 2001) and perfluorocarbons as geothermal vapour-phase tracers. Perfluorocarbons are gas tracers widely used and preferred in oil reservoirs (J. Muller, IFE, pers. comm.);
- homologous series of short-chain aliphatic alcohols as geothermal two-phase tracers: ethanol, n-propanol (Adams *et al.*, 2004; Mella *et al.*, 2006a and b).

The analytical methods usually used for each of these recommended compounds are reported below:

- naphthalene sulfonates and fluorescein: HPLC with fluorometric detection or spectro-fluorometry (for fluorescein only);
- sodium benzoate: extraction procedure coupled with HPLC with UV detection;
- $SF_6$: Fournier Transformed Infra-Red (TFIR) / Gas Chromatography with Electron-Capture Detection (ECD);
- hydrofluorocarbons, perfluorocarbons: enrichment procedure coupled with Gas Chromatography;
- ethanol, n-propanol: Gas Chromatography with a FID (Flame Ionization Detection). A new method of analysis for alcohol tracers using Solid Phase Microextraction (SPME) has reduced the limit of detection by a factor of about 30 (Mella *et al.*, 2006a).

Reactive tracers, in contrast to the inert solutes, are designed to interact with either the fluid or the rock as they are advected through a geothermal reservoir (Rose *et al.*, 2012a).

In particular, sorptive tracers sorb and desorb rapidly as they pass through the system. Their passage is thereby retarded relative to a nonreactive (or conservative) tracer. Since reversible sorption is a function of the fracture surface area, sorptive tracers can, in principle, be used to measure the fracture surface area within a geothermal reservoir, which is the area for heat transfer at the interface between the rock and the fluid. In addition to being reversibly sorptive, successful candidates must also possess all of the desirable properties of conservative-tracer candidates, including good detectability, thermal stability, affordability, nontoxicity, etc. A first experimental tracer test using Safranin T as sorbing tracer with 1,6-nds as conservative tracer simultaneously was carried out at the Soda Lake geothermal field, in USA, by Rose *et al.* (2012a) for estimating the fracture surface area along an injection-production flow path within a geothermal reservoir. This test was conducted after experimental works under laboratory conditions. During this test, both the conservative and sorbing tracers were produced, although the sorbing tracer was severely thermally degraded (effective reservoir temperature of 180°C). The tracer data were subsequently used to calibrate the flow model. In spite of the thermal instability of the Safranin T and a lack of relevant relative retardation data, this study demonstrated the first successful use of a sorbing tracer in combination with conservative tracer to calculate fracture surface area within a geothermal reservoir ever reported in the open literature (Rose *et al.*, 2012a).

Rose *et al.* (2015) showed that a thermally reactive tracer could be used in combination with a conservative tracer within a geothermal reservoir to determine the effective temperature along an injection-production pathway. The thermal decay kinetics of the UV-fluorescent optical brightener 7-amino-1,3-naphthalenedisulfonate (Amino-G) was measured under simulated geothermal conditions using a high-temperature laboratory batch reactor. This study revealed that Amino-G decays at moderate reservoir temperatures according to an Arrhenius model and that its concentration relative to that of a non-degrading tracer can therefore be used to determine the effective temperature along an injection/production pathway (Rose and Adams, 1994).

Using UPLC and high-resolution mass spectrometry, the decay product was shown to be a fluorescent, water-soluble compound (2-naphthol), possessing greater thermal stability than the parent compound. Amino-G and its daughter product thus represent a new tracer pair for use in geothermal reservoirs, suggesting that other amino-substituted or even hydroxyl-substituted naphthalene sulfonates might be used as geothermal tracers.

Nanoparticle tracers are being investigated as a potential tool to measure temperature distributions in geothermal reservoirs (Ames *et al.*, 2013; Alaskar *et al.*, 2015). If the temperature distributions could be measured more precisely, this would greatly enhance the power and accuracy of thermal breakthrough forecasting, which would in turn inform reservoir engineering and field management decisions. Works are carrying out in order to rank the informativity of various tracer candidates using modelling and in parallel, develop temperature sensitive tracers experimentally, such that they would be capable of characterizing fracture properties and temperature distribution.

## 1.2.3  Examples of appropriate tracer tests in crystalline basements

Numerous tracer tests have been conducted in high-temperature geothermal fields worldwide. Many references can be found through the web-page of the International Geothermal Association, i.e. at World Geothermal Congresses held every 5 years (Axelsson, 2013). We mention hereafter some examples among the main and most recent tests.

Naphthalene sulfonates have been or are used in numerous deep volcanic, granite and sedimentary geothermal fields such as Dixie Valley, Beowawe, Steamboat Springs, Salton Sea, Coso, Soda Lake in United States (Adams *et al.*, 1989; Rose *et al.*, 1997, 1998, 2001; 2002; 2012a), Ohaaki, Wairakei, Rotokawa, in New Zealand (Rose *et al.*, 2000; 2001; Winick *et al.*, 2015; Mountain and Winick, 2015), Los Azufres and Los Humeros in Mexico (Iglesias *et al.*, 2015), Berlin in Salvador, Las Pailas in Costa Rica (Torres-Mora and Axelsson, 2015), Hijiori in Japan (Matsunaga *et al.*, 2002), sites in Philippines and Indonesia (Rose *et al.*, 2001; Prabowo *et al.*, 2015), Copper Basin and Habanero, in Australia (Yanagisawa et al., 2009; Ayling *et al.*, 2015), Olkaria in Kenya, Laugaland and Reykjanes in Iceland (Axelsson *et al.*, 2001; Matthiasdottir *et al.*, 2015), KTB site, Bad Urach, Horstberg-Z1 and GroβSchönebeck site in Germany (Ghergut *et al.*, 2007), Soultz, Rittershoffen and Bouillante in France (Sanjuan *et al.*, 2015a, 2016c; 2013), etc.

Alcohol tracers (isopropanol, butan-2-ol, etc.) have been used as steam-phase tracers in New Zealand (Lovelock, 2001) and at the Matsukawa vapour-dominated geothermal field in Japan (Fukuda *et al.*, 2005). Halogenated alkanes and hydrofluorocarbons (R-134a and R-23) have been used as tracers in vapour-dominated systems such as The Geysers in the United States (Adams *et al.*, 2001). Ethanol and n-propanol were successfully used as two-phase tracers at the Coso site in United States (Mella *et al.*, 2006a and b).

Concerning BRGM's long experience on this topic, our most recent tracer tests have been carried out in the crystalline basement of the Soultz-sous-Forêts and Rittershoffen geothermal sites located in Alsace, in France (maximum temperature is close to 200°C; Sanjuan *et al.*, 2015a, 2016c) and in the volcanic context of high-temperature geothermal fields such as Bouillante, in Guadeloupe, in the French West Indies (Sanjuan *et al.*, 1999; 2000, 2004, 2008, 2013) and Krafla, in Iceland (Gadalia *et al.*, 2010; Asmundsson *et al.*, 2014). Temperatures are ranging from 260°C, at Bouillante, to 350°C, at Krafla.

Among all these tracer tests, the main applications in crystalline basements were selected for a more detailed description.

*a) Soultz-sous-Forêts in the Upper Rhine Graben, Alsace (France)*

After more than 25 years of scientific and technical investigations, the geothermal site of Soultz-sous-Forêts, in Alsace (France), has presently reached its stage of exploitation, *a priori* over a long-term period, and consequently, represents an unique opportunity to carry out a scientific and technical monitoring program of one the first EGS installations. Apart from GPK-1, which is more superficial (3590 m), all the other geothermal wells (GPK-2, GPK-3 and GPK-4) have been drilled at a depth of about 5000 m and temperature is close to 200°C, at bottom-hole.

During the tracer tests conducted before 2000 (Gadalia *et al.*, 1992; Vaute, 1998; Azaroual and Lassin, 2001; Aquilina *et al.*, 2004), the most relevant data were obtained from a four-month forced fluid circulation test in 1997 between the wells GPK-1 and GPK-2 (at this time, the total depth of this well was 3.9 km). During this test, a circulation loop was created between these two wells, which lie 450 m apart at depth. Hot fluid was produced from GPK-2, cooled in a surface heat exchanger, and re-injected into GPK-1 at a rate of 21 to 25 l/s. The bottom-hole temperature of GPK-2 was close to 150-160°C. During this experiment, the circulating fluid was traced using 300 kg of benzoic acid and various amounts of other tracers (fluorescein, deuterium and $SF_6$).

The test confirmed the existence of a direct hydraulic connection between the two wells. The tracers were detected in the fluid produced from GPK-2 about 3 to 6 days after their injection (Vaute, 1998; Aquilina *et al.*, 2004). Tracer maxima were observed between 6 and 10 days after their injection. Moreover, only 25 to 30% of the benzoic acid injected had been recovered at the end of the four month circulation test. The tracer-swept fracture volume and the mean residence time of this tracer were estimated to be about 16 000 $m^3$ and 36 days, respectively. Aquilina *et al.* (2004) estimated the mean linear fluid velocity to be 0.25-0.45 m/h, on the basis of the benzoic acid and deuterium data.

In the period 2000-2004, inter-well tracer tests using organic compounds such as Na-benzoate, 1,5-, 1,6-, 2,6- and 2,7-nds were conducted at the Soultz granite site at about 5 000 m depth, during hydraulic stimulation operations (Sanjuan *et al.*, 2006a and b). All these tracers were continuously injected at a controlled concentration (0.3 to 4 mg/l) into the respective well during these operations. Among the main results, these studies indicated that the tracers behaved conservatively during a long period (up to 4 years for Na-benzoate and 1,5-nds) under the harsh conditions of the Soultz reservoir. Combined with the monitoring of conservative species such as dissolved chloride, the tracer tests allowed us to estimate the fractions of native geothermal brine and injected fresh water in the fluids discharged during short-term production tests. These tests consistently indicated that only low amounts of the injected fresh water were recovered and that the proportion of native brine was relatively high in the produced fluids. The mean natural flux for the native brine was estimated at about 1-1.2 $m^3$/h.

in the framework of the FP6 European project "Soultz EGS Pilot plant (phase II), 2004-2009" and of a subcontracting for the EEIG Exploitation Minière de la Chaleur "Soutz III - EEIG, 2010-2013", BRGM has conducted several tracer tests between the different wells of the EGS pilot plant of Soultz-sous-Forêts, in parallel of the geochemical monitoring of the circulating fluid. All the tracer tests were carried out in order to better characterize the circulation of the fluids in this EGS pilot plant as well as its evolution, during the site exploitation. They had to make it possible to improve the knowledge and understanding of the fluid circulation in this EGS site. These tests also completed the results obtained in the tracer test associated with the four-month forced fluid circulation operation carried out in 1997, between the wells GPK-1 and GPK-2 (Vaute, 1998; Aquilina *et al.*, 2004), and in the previous tracer tests conducted from 2000 to 2004 (Sanjuan *et al.*, 2006a). As the EGS configuration was modified by EEIG following the obtained results and the encountered problems between 2005 and 2013, these tracer tests had to be adapted to the modified configuration in agreement with EEIG.

Between 2005 and 2013, four chemical tracer operations associated with short (2-3 months) to medium-term (5-6 months) circulation tests were conducted between the geothermal wells GPK-3 and GPK-2. The used tracers were 150 kg of fluorescein, 1.157 kg of $SF_6$ gas, 200 kg of 1,3,5-naphthalene tri-sulfonate (1,3,5-nts) and 200 kg of 1,3,6-nts. During the 2005 circulation test, fluorescein injected into GPK-3 was also monitored in the fluid discharged from GPK-4, which was the other productive well. During the 2013 circulation test, a second tracer (200 kg of fluorescein) was also injected into GPK-4 used as another injector well.

The tracer test using fluorescein accompanied a 5-month fluid circulation loop between the GPK-3 injection well and the GPK-2/GPK-4 production wells in 2005 (Sanjuan *et al.*, 2006a and b). The tracer test using 1,3,5-nts was associated to the longest fluid circulation test ever carried out at Soultz-sous-Forêts, between the two injection wells (GPK-3 and sometimes, GPK-1) and the production well GPK-2 (323 days of fluid circulation without any interruption, from November 2009 to mid-October 2010). In 2010, the fluid discharged from GPK-2 was not exclusively re-injected into GPK-3: a low amount of fluid was also re-injected into GPK-1. If the conditions of fluid re-injection into GPK-3 were similar for the tests carried out between 2005 and 2010, they were very different for the tracer test conducted in 2013 (Sanjuan *et al.*, 2015a). All these tracers behaved conservatively during a long period. The main results and conclusions obtained during these tests are reported in Sanjuan *et al.* (2006a and b; 2011), Blumenthal *et al.* (2007), Gessner *et al.* (2009), Radilla *et al.* (2011), Gentier *et al.* (2011), Sanjuan (2012), Vogt *et al.* (2012a; b), Sanjuan (2014), Held *et al.* (2014) and Sanjuan *et al.* (2015a).
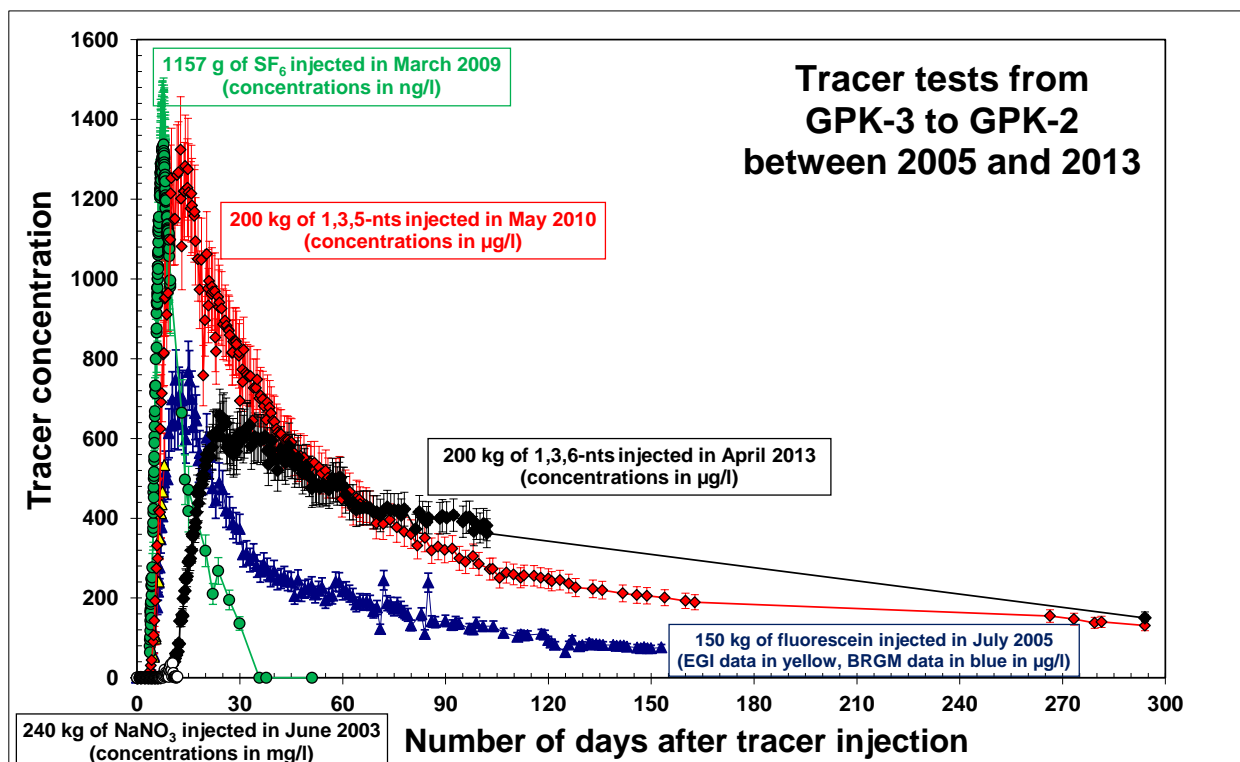


*Figure 10 - Comparison between tracer concentrations in the fluid discharged from GPK-2 during the tracer tests carried out between 2005, 2009, 2010 and 2013 (from Sanjuan et al., 2015a).*

Among the main results and conclusions (Sanjuan *et al.*, 2015a), we can notice that all the tracer tests gave evidence of fast and relatively direct hydraulic connections between GPK-3 and GPK-2 (short-scale fluid circulation loop with linear maximum velocities of about 4-8 m/h and predominant N-S fractures, Figs. 10 and 11, Tab. 4), comparable to those found from GPK-1 to GPK-2, in 1997. Except for $SF_6$ gas, the existence of other larger and slower hydraulic connections between the wells GPK-3 and GPK-2 (large-scale and quasi-infinite fluid circulation loops with predominant NE-SW and NW-SE fractures, Figs. 10 and 11, Tab. 4) was also highlighted.

| Parameter | Sanjuan *et al.* (2006a; b) Tracer test 2005 | Radilla *et al.* (2012) Tracer test 2005 | Sanjuan (2012) Tracer test 2005 | Sanjuan (2014) Tracer test 2009 | Sanjuan (2014) Tracer test 2010 | Sanjuan (2012) Tracer test 2010 | Sanjuan (2014) Tracer test 2013 |
|---|---|---|---|---|---|---|---|
| Tracer mass (kg) | 150 | 150 | 150 | 1.157 | 200 | 200 | 200 |
| Duration of the tracer test (days) | 153 | 153 | 153 | 59 | 163+27=190 | 163+27=190 | 102 |
| Mean flow-rate of GPK-3 injection (l/s) | 15.0 | 15.0 | 15.0 | 21.0 | 15.0 | 15.0 | 7.0 |
| Mean flow-rate of GPK-2 discharge (l/s) | 11.9 | 11.9 | 11.9 | 21.0 | 18.0 | 18.0 | 14.0 |
| Volume of discharged water ($m^3$) | 165500 | 165500 | 165500 | 107000 | 253086+43070=296156 | 253086+43070=296156 | 123400 |
| Time of the first tracer apparition (h) | 94 | | | 89 | 89 | | 157 |
| Linear velocity of the first tracer apparition (m/h) | 8.1 | | | 7.9 | 7.9 | | 4.3 |
| Maximum signal (µg/l) | 630-770 | | | 1.320-1.337 | 1283-1324 | | 626-658 |
| Time of the maximum signal (h) | 216-384 | | | 175-188 | 240-360 | | 528-936 |
| Linear velocity of the maximum signal (m/h) | 1.9-3.2 | | | 3.5-3.8 | 1.8-2.8 | | 0.7-1.2 |
| Mean transfer time (days) for loop 1 (short-scale loop) | 24 | 14 | 29 | | | 20 | |
| Mean transfer time (days) for loop 2 (large-scale loop) | 80 | 60 | 54 | | | 206 | |
| Mean linear fluid velocity (m/h) for loop 1 | 1.1 | | | | | | |
| Mean linear fluid velocity (m/h) for loop 2 | 0.3 | | | | | | |
| Tracer recovery (%) for loop 1 | 15.6 | 6.3 | 11.1 | | | 18.8 | |
| Tracer recovery (%) for loop 2 | 7.9 | 14.1 | 4.7 | | | 6.6 | |
| Total tracer recovery (%) | 23.5 | 20.4 | 15.8 | 2.0 | | 25.4 | 18.0 |
| Fluid volume ($m^3$) within loop 1 | 3900 | 1100 | 1676 | | | 5701 | |
| Fluid volume ($m^3$) within loop 2 | 6500 | 10900 | 8355 | | | 20942 | |

*Table 4 - Comparison of the data obtained for the tracer tests carried out by BRGM (in collaboration with GEIE) in 2005, 2009, 2010 and 2013 (from Sanjuan et al., 2015a).*
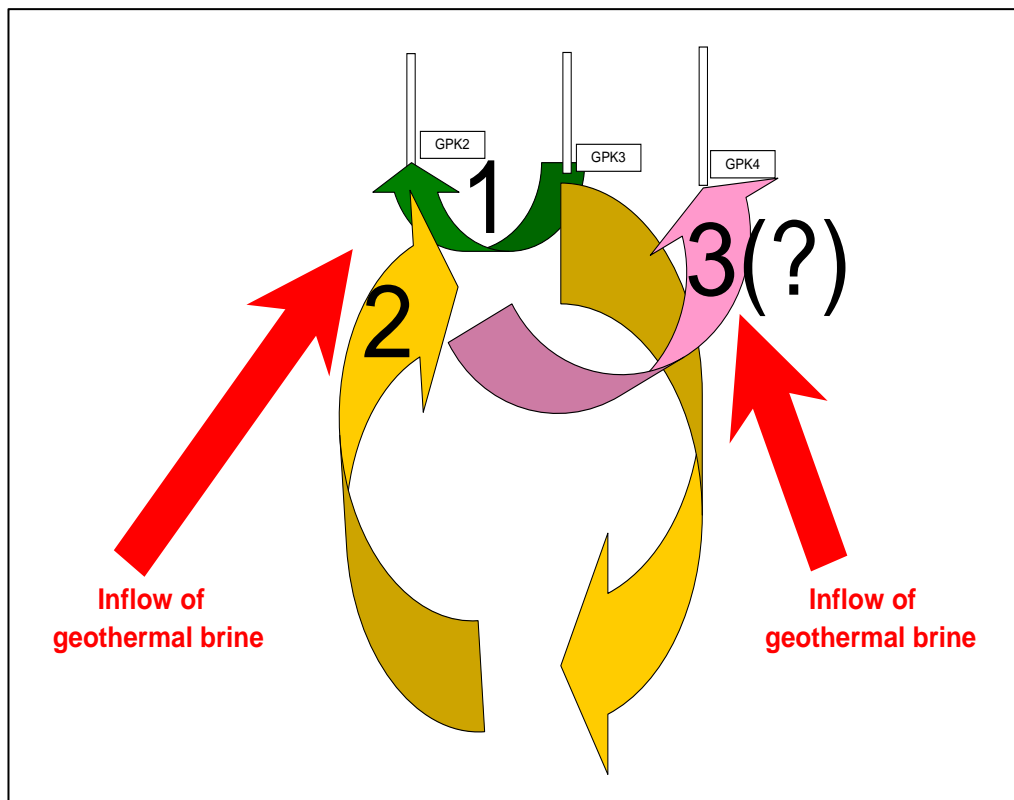


*Figure 11 - Conceptual model of fluid circulation in the Soultz EGS site: 1. Short scale loop between GPK-3 and GPK-2; 2. Large scale loop between GPK-3 and GPK-2; 3. Connection between the large scale loop and GPK-4 (from Sanjuan et al., 2006a).*

Significant contributions of native geothermal brine as well as relatively low rates of tracer recovery (< 30%) were confirmed in the fluid discharged from GPK-2. After the tracer test conducted in 2005, it was estimated that more than 750 000 $m^3$ of native reservoir brine mixed with approximately 142 000 $m^3$ of fresh water that had been injected since 2000 (Sanjuan *et al.*, 2006a). A $SF_6$ gas trapping in the complexity of the porosity of the fracture system when the flow paths lengthen could explain the absence of contribution of the large-scale circulation loop in the shape of the restitution curve of this tracer (Fig. 10) as well as its very low recovery rate (< 2%) and the absence of dissolved $SF_6$ in the geothermal fluid discharged from GPK-2. This type of tracer would mark the most direct paths with high velocity and low tortuosity.

When they exist, the discrepancies found on the shapes of the tracer restitution curves and the associated hydrodynamic characteristics depend mainly on the nature of the tracer (gas or dissolved chemical compound), the fluid reinjection conditions (injection flow-rates and pressure) used for each circulation test and flow-rates of discharged fluid. So, for example, the main factor responsible for the longer time of the first apparition of 1,3,6-nts in the GPK-2 fluid (157 hours instead of 89-94 h for the other previous tests; Fig. 10; Tab. 4) is most probably the lower flow-rate value (7 l/s) used for fluid injection into the well GPK-3, compared with those in 2005, 2009 and 2010 (≥ 15 l/s), and the lower pressure (< 3 bar). The increasing values of the tracer mass recovery rates and tracer-swept fracture volumes estimated between the 2005 and 2010 tests (from 15.8 to 25.4% for the total tracer recovery rates and from 10 031 to 26 643 $m^3$ for the total tracer-swept fracture volumes), using the same modelling methodology and taking into account the differences of discharged fluid volumes, were mainly interpreted as a possible improvement of the fluid circulation loops between GPK-3 and GPK-2, probably due to the stimulation and fluid circulation operations carried out after 2005, which induced an opening of the pre-existing connections. This improvement seems to be confirmed by the results obtained during the 2013 tracer test, but additional modelling tasks must be still performed.

Contrary to the hydraulic connections between the wells GPK-3 and GPK-2, those existing between GPK-3 and GPK-4, or between GPK-4 and GPK-2, appeared to be very poor:

- fluorescein was only detected in GPK-4 after 29 days of its injection into GPK-3 in 2005, maximum tracer concentration was about 30 µg/l and tracer recovery was lower than 2% at the end of the test;
- fluorescein injected into GPK-4 in 2013 could have been detected at very low concentrations (0.5-1 µg/l) in the fluid discharged from GPK-2, after 60-73 days of its injection;
- the linear maximum velocities for both tests were similar and close to 1 m/h.

### b) Rittershoffen in the Upper Rhine Graben, Alsace (France)

The ECOGI Company has developed a project of deep geothermal energy located in the Rittershoffen site, in Alsace, in the Upper Rhine Graben area, 50 km north of Strasbourg and 10 km east from the Soultz EGS site, in order to produce steam for the industrial drying of starch from a well doublet (injection and production wells). This site was inaugurated in June 2016. The first geothermal well, GRT-1, with a vertical depth of about 2,550 m (drilled length of about 2 580 m) was drilled in 2012, and tested and successfully stimulated in 2013. The second well, GRT-2, with a vertical depth of about 2 750 m (drilled length of about 3 196 m) and distant from GRT-1 from approximately 1.2 km at the bottom-hole, was recently completed in July 2014. The open-hole section is made of Triassic clastic sandstones and fractured crystalline basement.

On the request of the ESG Company and under ECOGI funding, a chemical tracer test using 200 kg of fluorescein and 2,7-naphthalene disulfonate (2,7-nds), respectively, associated with a short-term circulation loop between the wells GRT-1 and GRT-2, was conducted over a period of 25 days in 2014 by BRGM with the close collaboration of the GEIE "Exploitation Minière de la Chaleur (EMC)" team (Scheiber and Moeckes, 2014). During this test, about 60 000 $m^3$ of fluid were discharged from GRT-2 with a mean temperature close to 162°C and 54 000 $m^3$ of fluid were injected into GRT-1 with a mean temperature close to 40°C. Only fluorescein was analysed both on site and in laboratory.

All the results obtained during this tracer test, and their interpretation, are reported in Sanjuan *et al.* (2016c). As expected, the 2,7-nds results obtained in laboratory were the most reliable and relevant ones for data quantitative interpretation of this tracer test. The tracer detection in the GRT-2 fluid (corresponding to a volume of about 27 000 $m^3$ of fluid discharged) occurred at about 12 days after tracer injection.

The maximum signal of 2,7-nds was not reached during the production time of 25 days, after about 60 000 m$^3$ of fluid discharged from GRT-2. The concentration values of both tracers analysed in the fluid discharged from GRT-2 remained relatively low (< 15 µg/l for fluorescein and < 40 µg/l for 2,7-nds). Consequently, after 25 days of production, the recovery rates for fluorescein and 2,7-nds were very low, close to 0.06 and 0.2% in mass, respectively.

If we compare these tracing results with those obtained in the Soultz EGS site (Fig. 12), we can conclude that the hydraulic connections between GRT-1 and GRT-2 are much poorer than all those observed between the Soultz wells. Between the wells GPK-1 and GPK-2 or between GPK-3 and GPK-2, the tracer recovery rates ranged from 15 to 26% in mass. Between the wells GPK-3 and GPK-4, this parameter was estimated at about 2%. Moreover, for comparable volumes of fluid discharged from the wells GRT-2 and GPK-4, the lower tracer concentrations observed for GRT-2 indicate that the tracers injected into the Rittershoffen site have been mixed with a larger volume of native geothermal brine than in the Soultz geothermal site.
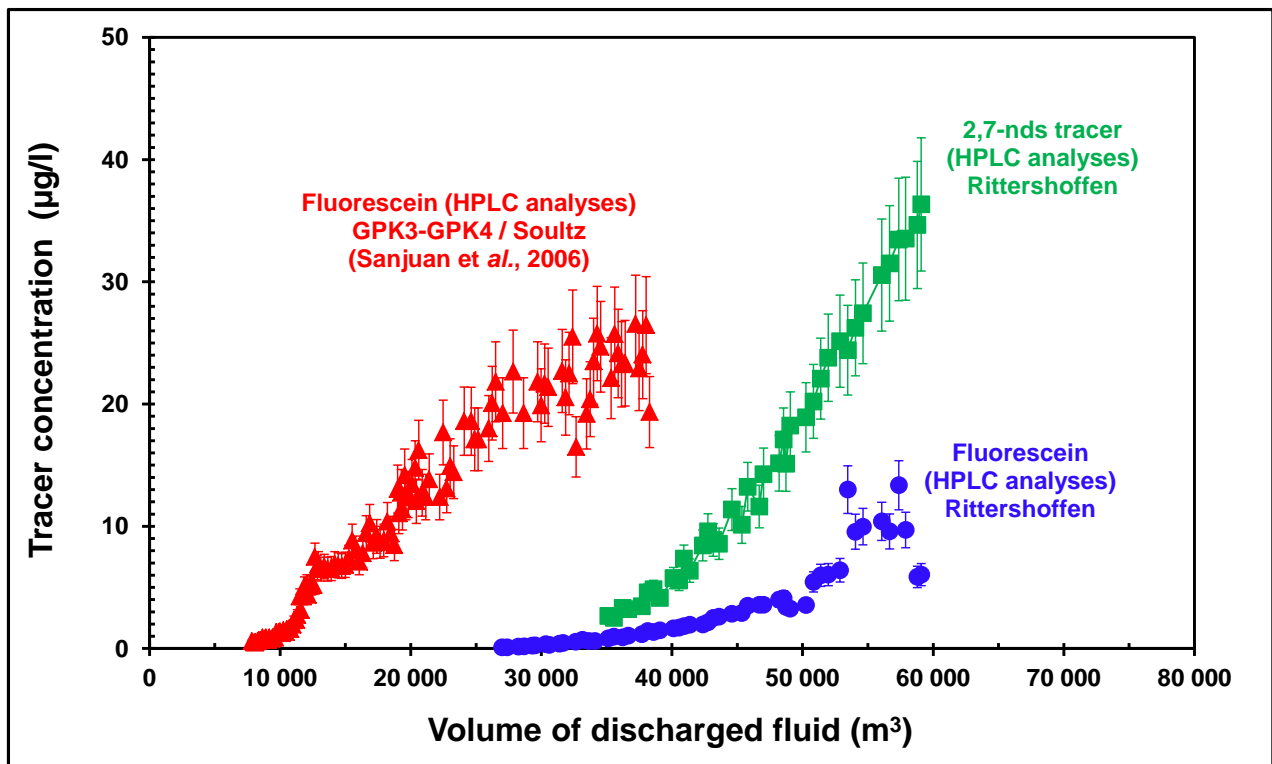


Figure 12 - Results of the ECOGI tracer test between the wells GRT-1 and GRT-2 compared with those obtained between the wells GPK-3 and GPK-4, in 2005, at Soultz-sous-Forêts (figure extracted from Sanjuan et al., 2016c).

### c) Kontinentale Tief-bohrung (KTB) site in Germany

In the deep crystalline basement of the German KTB site, a combination of short-term and long-term tracings using uranine, nds compounds and tritiated water accompanied a long-term hydraulic and seismic testing program (Ghergut et al., 2007). From tracer breakthrough curves in single-well push-pull tests, the specific area of the fluid-rock contact surface could be estimated; its change with different hydraulic regimes could be used to appreciate the effect of hydraulic stimulation. The uranine (di-natrium fluorescein) showed systematically lower recoveries than the other simultaneously injected tracers, which was mainly explained by a reaction of uranine reduction *in situ*.

*d) Habanero site in Australia*

As presented by Ayling *et al.* (2015), the Habanero Engineered Geothermal System (EGS) in central Australia has been under development since 2002, with several deep (more than 4000 m) wells drilled into the high-heat-producing granites of the Big Lake Suite to date. Multiple hydraulic stimulations have been performed to improve the existing fracture permeability in the granite. The stimulation of the newly-drilled Habanero-4 well (H-4) was completed in late 2012, and micro-seismic data indicated an increase in total stimulated reservoir area to approximately 4 km². Two well doublets have been tested, initially between Habanero-1 (H-1) and Habanero-3 (H-3), and more recently, between H-1 and H-4. Both doublets effectively operated as closed systems and excluding short-term flow tests, all production fluids were re-injected into the reservoir at depth. Two inter-well tracer tests have been conducted since 2008, to evaluate the fluid residence time in the reservoir alongside other hydraulic properties, and to provide comparative information to assess the effectiveness of the hydraulic stimulations. The closed-system and discrete nature of this engineered geothermal reservoir provides a unique opportunity to explore the relationships between the micro-seismic, rock property, production and tracer data.

The most recent inter-well tracer test occurred in June 2013, using 100 kg of 2,6-nds into H-1 to evaluate the hydraulic characteristics of the newly-created H-1/H-4 doublet (Ayling *et al.*, 2015). Sampling of the production fluids from H-4 occurred throughout the duration of the 3-month closed-circulation test. After correcting for flow hiatuses (i.e. interruptions in injection and production) and non-steady-state flow conditions, tracer breakthrough in H-4 was observed after 6 days (compared to $\approx$ 4 days for the previous H-1/H-3 doublet), with peak breakthrough occurring after 17 days. Applying moment analysis to the data indicated that approximately 56% of the tracer was returned during the circulation test (vs. approximately 70% from the 2008 H-1/H-3 tracer test). This suggests that a considerable proportion of the tracer may lie trapped in the opposite end of the reservoir from H-4 and/or may have been lost to the far field. Flow capacity - storage capacity plots derived from the H-1/H-4 tracer test indicate that the Habanero reservoir is moderately heterogeneous, with approximately half of the flow travelling *via* around 25% of the pore volume. The calculated inter-well swept pore volume was approximately 31 000 m³, which is larger than that calculated for the H-1/H-3 doublet ($\approx$ 20 000 m³). This is consistent with the inferred increase in reservoir volume following hydraulic stimulation of H-4.

## 1.2.4 Main conclusions and recommendations

Tracer testing has multiple applications in geothermal research and management (Axelsson, 2013):

- the main purpose in conventional geothermal development is to study connections between injection and production boreholes as part of reinjection research and management. The results are consequently used to predict the possible cooling of production boreholes due to long-term reinjection of colder fluid;

- in EGS system development, tracer testing has a comparable purpose even though it is rather aimed at evaluating the energy extraction efficiency and longevity of such operations through studying the nature of connections between reinjection and production boreholes.

Comprehensive interpretation of geothermal tracer data, and consequent modeling for management purposes (production well cooling predictions), has been rather limited, even though tracer tests have been used extensively. Their interpretation has mostly been qualitative rather than quantitative.

In agreement with Axelsson (2013), advances have been made in the introduction of new tracers, which both add to the multiplicity of high-sensitivity tracers available as well as being increasingly temperature tolerant. But the geothermal industry needs to follow advances in other disciplines and adopt those which are beneficial. This applies, in particular, to advances in modelling of tracer return data, which has been limited so far. The Soultz example shows the way forward.

As initiated by Rose *et al.* (2012a) and Rose and Clausen (2015), selection of reactive tracers and modelling of reactive tracer data, which can yield information on flow-channel surface areas in addition to their volumes or estimations on the temperature distribution, would have also to be developed.

## 1.2.5 Modifications of the initial tracer test program

Unfortunately, after studying the sites envisaged for tracer tests and on-site works (see chapters 2 and 3), no tracer test could be conducted in the PVGT-LT1 borehole, only borehole available in the Litomerice area, Czech Republic, and in the Thônex-1 borehole, near Geneva, in Switzerland, especially because of the very low values of fluid flow-rate existing in these boreholes. Moreover, obstacles are present in the PVGT-LT1 borehole, at a depth of 1 150 m, and in the Thônex-1 borehole, at a depth of 1 840 m, respectively.

After that GEOMEDIA was constrained to leave the IMAGE project because of a bankrupt procedure, BRGM contacted Tym Antonin from the city of Litomerice in order to try to eliminate this obstacle and to have an idea of the cost of the necessary works. These works were considered too much expansive (about 140 k€, including logging works) relative to the scientific issues and could be not sufficient.

Consequently, we decided to focus our on-site works on the development of auxiliary chemical geothermometers at low-temperatures. The task in which a tracer test had to be carried out was substituted by a thorough geochemical study about the deep fluid of the Thônex-1 and an examination of data relative to other geothermal sites in crystalline basement (see chapter 3).

# 2. Field work in the Litomerice area, in Czech Republic

After an exhaustive literature review about the use of potential auxiliary chemical geothermometers, some thermometric relationships such as Na-Li, Na-Rb, Na-Cs, K-Sr, K-Mn, K-Fe, K-F and K-W for dilute thermal waters discharged from granite reservoirs between 25 and 150°C in more than sixty areas from Europe (Michard, 1990) were identified (see chapter 1). These thermometric relationships had to be applied and validated using dilute low-temperature waters located in the Litomerice area of the Eger Graben belonging to the West European Rift System, in Northwest Bohemia, in Czech Republic.

## 2.1    Description of the site (identified boreholes)

The Litomerice area, Northwest Bohemia, in the Czech Republic, is a part of the Ohre (Eger) Graben belonging to the West European Rift system (Fig. 13). This Graben, active from Oligocene to Pleistocene and limited by set of fault structures of local and regional importance, is the most dominant structure in the Western Bohemia (Fig. 13). The precise fault position is often a subject of discussion. The principle directions of displacement zones are SW-NE (Erzgebirge) and NW-SE (Sudetic). Nevertheless, many fold and fault structures are in a W-E direction. The thickness of the sedimentary cover, which constitutes the Bohemian Cretaceous Basin (BCB), the largest sedimentary complex of the Czech Republic, typically ranges between 200 and 400 m, but in the vicinity of the city of Decin reaches up to 1 200m. Tertiary sediments and frequent small occurrences of intrusive rocks forming volcanic hills and mountains markedly affect the surface. This intra-continental Basin, formed as a seaway between the North Sea Basin and the Tethys Ocean, represents a complex hydrogeological system composed of several aquifers with very favourable hydrogeological properties. These aquifers have been exploited for more than a century, most often for water supply and geothermal purposes (Jirakova *et al.*, 2010).
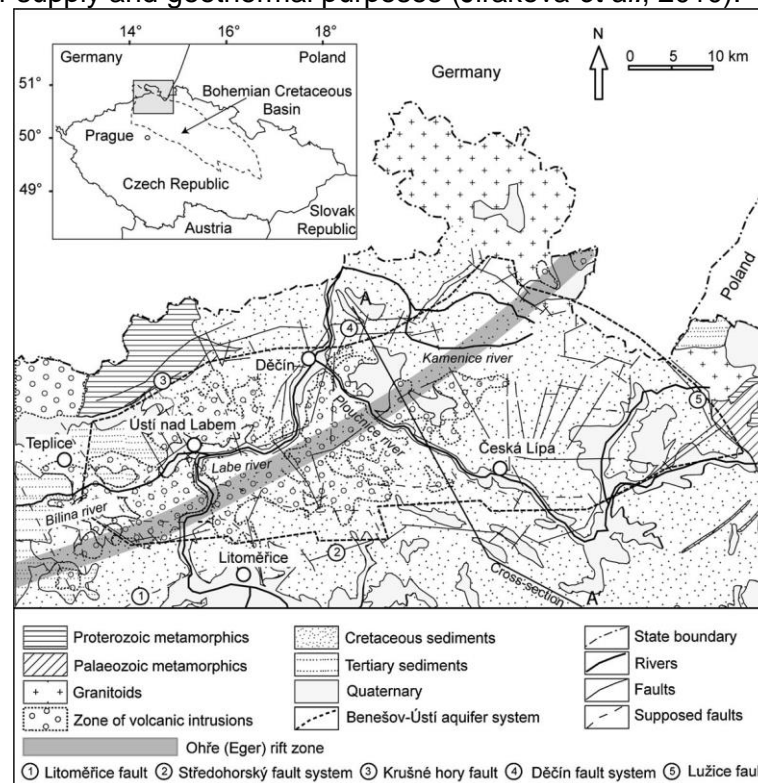


*Figure 13 - Simplified geological map with main tectonic features (from Jirakova et al., 2011). The exact location and extent of Ohre (Eger) rift is unknown so far; the grey zone represents its most probable position and extent.*

The Bohemian crystalline basement in the Litomerice area, where deep dilute fluids are circulating, was the area selected in this study for geothermometric application and tracer test development. This basement is formed by partially metamorphosed Proterozoic and Palaeozoic rocks, locally pierced by intrusive basaltic rocks and by Palaeozoic granites in the north. The occurrence of volcanic rocks is very scattered throughout the North-Western area (Jirakova *et al.*, 2011). The basement is in some places covered with Permo-Carboniferous beds of both sediments (claystones, siltstones, greywackes, arkoses, conglomerates) and volcanic rocks. During the Variscan period, the region was affected by major folding and metamorphism.

Among all the deep boreholes located in the Litomerice area in the crystalline basement (Fig. 14), only seven of them were found by GEOMEDIA (Fig. 15, 16, 17, 18, 19, 20, 21 and 22).
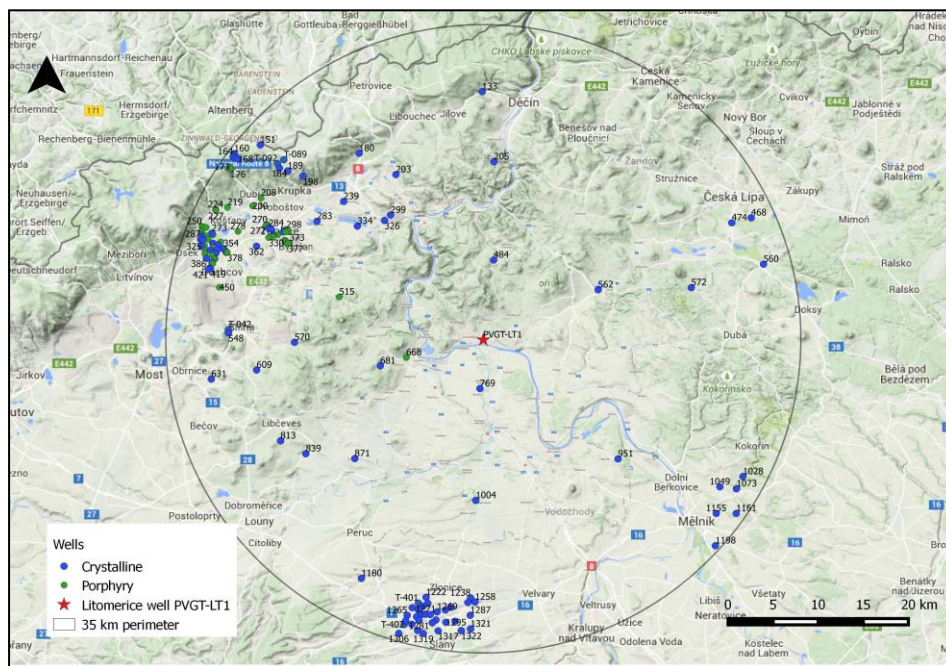


*Figure 14 - Location of the studied area and existing boreholes in the crystalline and porphyric environments.*
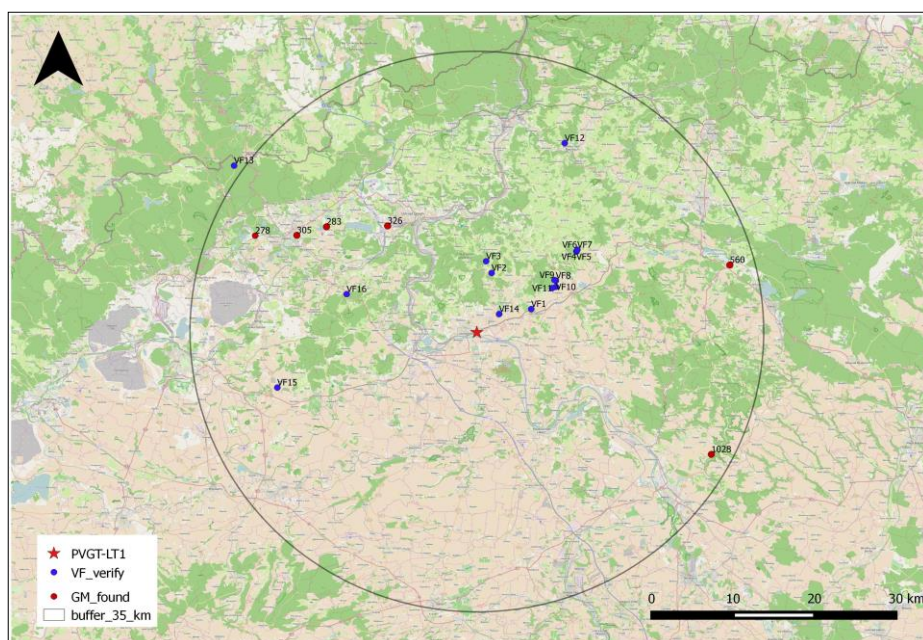


*Figure 15 - Location of the boreholes found by GEOMEDIA in the crystalline basement.*

Figure 16 - TH-31 borehole, 159 m deep, Oldrichov.



Figure 17 - TH-20 borehole, 443 m deep, Modlany.



Figure 18 - TH-10 borehole, 500 m deep, Predlice.



Figure 19 - TP-41 borehole, 546 m deep, Teplice.



Figure 20 - HV-3C borehole, 151 m deep, Jestrebi.



Figure 21 - SR-1 borehole, 1241 m deep, Stremy.

| | |
|---|---|
| | Equipment of the borehole PVGT - LT1 |

*Figure 22 - PVGT-LT1 borehole, 2 111 m deep, Litomerice.*
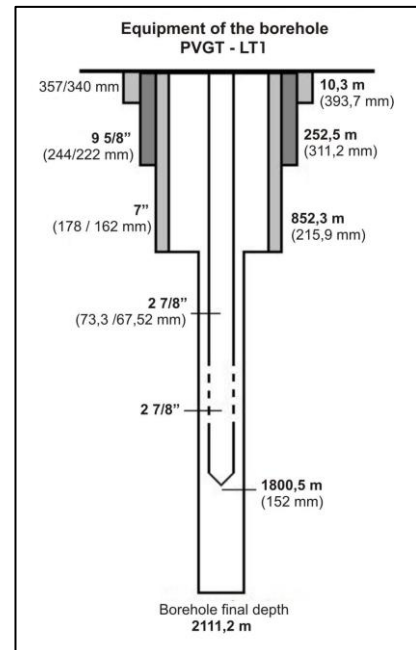
## 2.2 Fluid chemical and isotopic compositions

Only the chemical compositions associated with low-temperature waters (12-56.5°C) of 5 deep boreholes (151-2 111 m) penetrating the crystalline basement of fluids were available in the literature (Tabl. 2). Among these boreholes, only one (PVGT-LT1 borehole; Figs. 22 and 23) could be sampled by GEOMEDIA in May 2015 and by BRGM, with the help of GEOMEDIA and the Litomerice city, in November 2015 (see Appendix 1), for chemical and isotopic analyses.

This exploratory borehole was drilled in 2006-2007 in the framework of the Litomerice geothermal project and reached the metamorphic basement (gneiss) at 780 m depth (Fig. 23). Stabilised temperature measured in 1 800 m was approximately 56.5°C. Estimated temperature at a depth of 2 111 m was 63.5°C (Jirakova *et al.*, 2015).



| | | |
|---|---|---|
| 0 - 25 m | Quaternary | |
| 25 - 165 m | Cretaceous - Turonian | |
| 165 - 190 m | Cretaceous - Cenomanian | |
| 190 - 780 m | Permo-Carboniferous | 190 - 460 m Líně Fm. |
| | | 460 - 500 m Slaný Fm. |
| | | 500 - 600 m Týnec Fm. |
| | | 600 - 780 m Kladno Fm. |
| 780 - 910 m | "Teplice porphyry" | Rhyolitic ignimbrite |
| 910 - 942 m | ? | base of Permo-Carboniferous unit |
| 942 - 2050 m | Proterozoic crystalline basement | mica schist with interlayers of phyllite and actinolite-rich rock |
| 2050 - 2110 m | Proterozoic crystalline basement | phyllite |

*Figure 23 - Geology and stratigraphy of the PVGT-LT1 borehole, in the Litomerice area, Czech Republic (documents from GEOMEDIA).*

In May 2015, a water sample from this borehole was collected by GEOMEDIA and the chemical and isotopic analyses were performed in a Czech laboratory (Tabl. 2).

All the measurements carried out in this borehole by BRGM, between November 24 and 26, 2015, and the conditions of fluid sampling, are detailed and discussed in Appendix 1. In addition to the water sample which was analysed in the BRGM laboratories (Tabl. 2), two samples of dissolved gases were analysed using gas chromatography in the BRGM laboratories (Tabl. 6 in Appendix 1). No bottom-hole sample could be collected because of an unknown obstacle present at a depth of 1 150 m.

As the measured fluid flow-rate was excessively low (see Appendix 1; 20 l/h maximum and a fluid velocity at about 5 m/h), it was not possible to extract a water column longer than 2 000 m (more than 7 $m^3$ of water) from this borehole and the objective to conduct a backflow tracer test was abandoned. Only 120 m of water - less than 0.5 $m^3$ - were extracted during our intervention. Consequently, it is very difficult to know what is the degree of representativeness of the collected samples with respect to the bottom conditions of this borehole (the origin of the water should be from deeper horizons as the only perforation is between 1 600 and 1 700 m and it is open hole from 1 800 m). The continuous monitoring of the conductivity (from 890 $\mu$S.cm$^{-1}$, at the end of the 1$^{st}$ session, up to 1040 $\mu$S.cm$^{-1}$, at the end of the 5$^{th}$ session; Appendix 1) and pH (from 8.95, at the end of the 1$^{st}$ session up to 8.35, at the end of the 5$^{th}$ session) of the water discharged from the PVGT-LT1 in November 2015 suggests that the collected samples are not still fully representative of the deep fluid present at the bottom-hole.

For comparison purposes, the Pravridlo thermal spring ($T_{max}$ = 41°C), at Teplice, a city located near Litomerice (Fig. 13), was also sampled by BRGM in November 2015 (Appendix 2). Chemical and isotope analyses were performed on the water samples, in the BRGM laboratories (Tabl. 2). Several previous chemical and isotope data were also found in the literature (Tabl. 2).

The thermal waters in Teplice Spa are linked to tectonic structures within the rhyolite body (Fig. 24) of Permian-Carboniferous age, which is a part of the Altenberg Caldera, and are supposed to be recharged at the higher elevated Erzgebirge Mts ridge (Fig. 13).
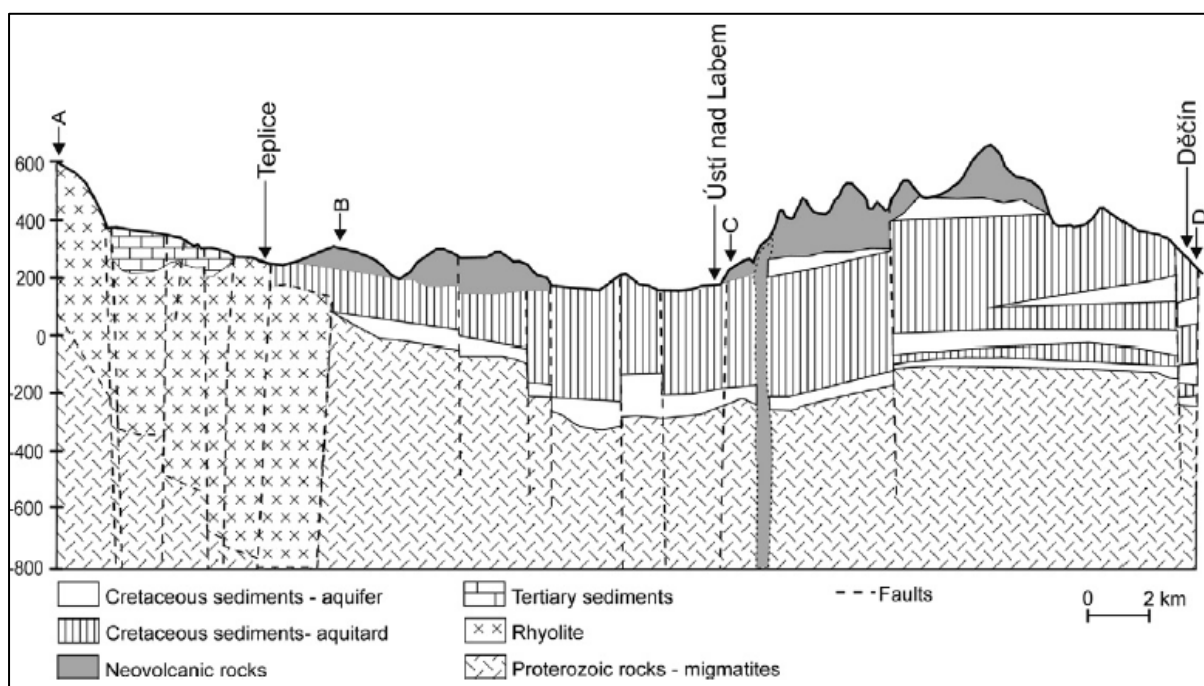


Fig. 24 - Cross section of geological units and principal aquifers (after Hazdrova et al., 1964).

During the Cenozoic rifting, the rhyolite body was tectonically disturbed by a set of faults of mostly E-W to WSW-ENE direction and covered partly by Cretaceous, and partly by Tertiary pelitic and argillous sediments. Although the rhyolite aquifer is connected to the sediments of the Most Basin, there is no evidence so far for hydraulic communication between aquifers of the BCB and rhyolite (Hazdrova et al., 1964; Dupalova et al., 2012).

All the chemical analyses for both major and trace elements in the waters collected by BRGM samples were done in its laboratories using standard water analysis techniques such as Ion Chromatography, Inductively Coupled Plasma-Atomic Emission Spectroscopy (ICP-AES), Inductively Coupled Plasma-Mass Spectrometry (ICP-MS), Flame Emission Spectrophotometry, TIC analysis and Colorimetry. The chemical analysis results have a precision better than $\pm$ 5% for major elements and $\pm$ 10% for trace elements.

The isotopic analyses of the water samples ($\delta D$ and $\delta^{18}O$ of the water, $\delta^{18}O$ and $\delta^{34}S$ of the dissolved sulphate, $\delta^{13}C$ of the carbon dioxide, plus the $\delta^7Li$, $\delta^{11}B$, and $^{87}Sr/^{86}Sr$) were also performed in the BRGM laboratories using Thermo Ionization Mass Spectrometry and Neptune Multi Collector ICP-MS. The absolute uncertainty for the $\delta D$ and $\delta^{18}O$ analyses of the water samples was $\pm$ 0.8‰ and $\pm$ 0.1‰, respectively. The absolute uncertainty for the $\delta^{18}O$ and $\delta^{34}S$ analyses of the dissolved sulphate was $\pm$ 0.1‰ and $\pm$ 0.3‰, respectively, whilst for the $\delta^{13}C$ analyses of the carbon dioxide, it was $\pm$ 0.1‰. The external reproducibility of the $\delta^7Li$ and $\delta^{11}B$ analyses was estimated at around $\pm$ 0.5‰ and $\pm$ 0.3‰, respectively, and the in-run precision of the $^{87}Sr/^{86}Sr$ ratio was generally better than $\pm$ 10 x $10^{-6}$ ($2\sigma_m$).

The isotopic analyses of $\delta^{18}O$ and $\delta^{34}S$ of the dissolved sulphates could not be done in the PVGT-LT1 sample collected in November 2015 (not sufficient volume of water sample), because of the very low analysed concentration of dissolved $SO_4$ (1 mg/l) relative to the previous analytical results (88 and 14 mg/l).

Globally, these fluids indicate different chemical compositions. The TH-31, TH-20, TH-10 and Pravridlo fluids are Na-$HCO_3$ type; the HV-3C fluid, a Na-Ca-$HCO_3$ type and the PVGT-LT1 fluid, a Na-Cl type (Tab. 2). Their TDS values range from 346 to 1386 mg/l (the highest values correspond to those of the Pravridlo thermal water). The pH values are ranging from 6.90 from 8.90.

The concentrations of dissolved Cl, Br, B, $NH_4$, Ba in the PVGT-LT1 fluid are much higher than in the Pravridlo thermal water (Tabl. 2). For F, Li, Cs and Rb, the reverse occurs.

The analyses of the water stable isotopes from the PVGT-LT1 fluid collected by GEOMEDIA and BRGM during this study indicate that its isotopic signature is pretty close to modern precipitation and infiltration values. This signature is slightly less negative than those of the Pravridlo thermal water (Tabl. 2) and other regional thermal waters (Jirakova et al., 2010; Dupalova et al., 2012), for which the values of $\delta D$ are in the range from -67.9 to -81.5‰ and those of $\delta^{18}O$ are in the range from -9.4 to -11.5‰. All the points fall on the Global Meteoric Water Line (GMWL), suggesting no significant evaporation during recharge and lack of very high temperature water-rock interaction.

Apart the $\delta^7Li$ signature which is similar, all the other isotope signatures are different between the PVGT-LT1 and Pravridlo waters (Tabl. 2). These isotopic differences, associated also with chemical discrepancies, confirm these thermal waters come from different deep reservoirs, constituted of rocks of different nature, and with varied water recharges.

| Well | Location | Country | ID | X_MAP | Y_MAP | Latitude ° | Longitude ° | Z | Depth m | Stratigraphy | Geology | Water level m | T °C |
|---|---|---|---|---|---|---|---|---|---|---|---|---|---|
| TH-31, TH 31/62 | Oldrichov | Czech Republic | 278 | -779836,60 | -975339,20 | 50,6430430 | 13,7722250 | 246,83 | 159 | Permian Spodni | Quartz | 12.7 - 159.0 | 13,0 |
| TP-41, TP 41/88 | Teplice | Czech Republic | 305 | -774819,90 | -976024,70 | 50,6434588 | 13,8438082 | 218,35 | 546 | Carbon | Granite | 494.1 - 542.0 | 44,2 |
| TH-20 | Modlany | Czech Republic | 283 | -771087,40 | -975489,00 | 50,6530443 | 13,8949501 | 194,45 | 443 | Proterozoic | Gneiss | 342.8 - 368.6 | 27,1 |
| TH-10, TH 10/61 | Predlice | Czech Republic | 326 | -763721,70 | -976443,80 | 50,6539889 | 13,9999707 | 143,72 | 500 | Proterozoic | Gneiss | 373.4 - 440.8 | 31,0 |
| HV-3C | Jestrebi | Czech Republic | 560 | -723123,00 | -987014,00 | 50,6102305 | 14,5889443 | 255,26 | 151 | Proterozoic | Phyllite | 133.8 - 145.9 | 12,0 |
| SR-1 | Stremy | Czech Republic | 1028 | -728547,20 | -1010162,80 | 50,3974582 | 14,5569988 | 211,30 | 1241 | Proterozoic | Phyllite | | 33,0 |
| PVGT-LT1 | Litomerice | Czech Republic | | | | 50,5329800 | 14,1534200 | | 2111 | Proterozoic | Gneiss | 1600 - 1800 | 56,5 |
| Pravridlo (ancient spring) | Lazne Teplice | Czech Republic | | -776056,00 | -976474,00 | | | | 217,00 | 54,3 | Palaeozoic | Rhyolite | | 49,0 |
| TP-28 | Lazne Teplice | Czech Republic | | -776068,00 | -976278,00 | | | | 217,00 | 973 | Palaeozoic | Rhyolite | 883-942 | 45,7 |
| Thônex-1 | Geneva | Switzerland | | | | 46,1928370 | 6,2027670 | 428,35 | 2530 | Upper Jurassic | Limestone | ~ 2100 | 70,0 |
| Lavey-les-Bains | Vaud | Switzerland | | | | 46,2213052 | 7,0121187 | 431,75 | 3000 ? | Hercynian | Gneiss | | 105,0 |

| Well | Location | Depth m | Stratigraphy | Geology | Water level m | T °C | pH | Eh mV | Na mg/l | K mg/l | Ca mg/l | Mg mg/l | Cl mg/l | $HCO_3$ mg/l | DOC mg/l | $SO_4$ mg/l | $NO_3$ mg/l | $SiO_2$ mg/l | TDS mg/l | $\delta D$ ‰ | $\delta^{18}O$ ‰ | $\delta^{18}O_{SO_4}$ ‰ | $\delta^{34}S$ ‰ | $\delta^{7}Li$ ‰ | $\delta^{11}B$ ‰ | $\delta^{13}C$ ‰ | $^{87}Sr/^{86}Sr$ |
|---|---|---|---|---|---|---|---|---|---|---|---|---|---|---|---|---|---|---|---|---|---|---|---|---|---|---|---|
| TH-31, TH 31/62 | Oldrichov | 159 | Permian Spodni | Quartz | 12.7 - 159.0 | 13,0 | | | 91,0 | 6,0 | 35,7 | 8,3 | 21,6 | 276 | | 65,8 | | 23,3 | 538 | | | | | | | | |
| TP-41, TP 41/88 | Teplice | 546 | Carbon | Granite | 494.1 - 542.0 | 44,2 | | | | | | | | | | | | | | | | | | | | | |
| TH-20 | Modlany | 443 | Proterozoic | Gneiss | 342.8 - 368.6 | 27,1 | | | 231 | 14,0 | 31,7 | 3,6 | 28,7 | 475 | | 173 | | 10,7 | 957 | | | | | | | | |
| TH-10, TH 10/61 | Predlice | 500 | Proterozoic | Gneiss | 373.4 - 440.8 | 31,0 | | | 234 | 17,5 | 28,9 | 3,8 | 28,0 | 445 | | 215 | | 12,6 | 760 | | | | | | | | |
| HV-3C | Jestrebi | 151 | Proterozoic | Phyllite | 133.8 - 145.9 | 12,0 | 7,30 | | 28,2 | 3,7 | 44,1 | 10,7 | 9,6 | 202 | | 50 | | 7,5 | 346 | | | | | | | | |
| SR-1 | Stremy | 1241 | Proterozoic | Phyllite | | 33,0 | | | | | | | | | | | | | | | | | | | | | |
| PVGT-LT1 (November 2007) | Litomerice | 2111 | Proterozoic | Gneiss | 1600 - 1800 | 56,5 | 8,30 | | 140 | 14,0 | 93,0 | 12,0 | 190 | 220 | | 88 | | | 718 | | | | | | | | |
| PVGT-LT1 (May 2015) | Litomerice | 2111 | Proterozoic | Gneiss | 1600 - 1800 | 53,8 | 8,91 | | 140 | 8,9 | 31,0 | 17,0 | 180 | | 17,3 | 14,0 | | | | -64,9 | -9,1 | | | | | | |
| PVGT-LT1 (November 26, 2015) | Litomerice | 2111 | Proterozoic | Gneiss | 1600 - 1800 | | 8,35 | | 164 | 9,6 | 24,5 | 5,9 | 227 | 151 | | 1,0 | < 0.5 | 1,3 | 584 | -65,7 | -8,8 | n.d. | n.d. | 0,9 | 5,88 | -8,4 | 0,710048 |
| Pravridlo (ancient spring) - Cadek *et al.* (1968) | Lazne Teplice | 54,3 | Palaeozoic | Rhyolite | ? | 41,3 | 6,90 | | 224 | 16,0 | 23,0 | 7,5 | 51,4 | 551 | | 118 | | 34,5 | 1025 | | | | | | | | |
| Pravridlo - Dupalova *et al.* (2012) | Lazne Teplice | 54,3 | Palaeozoic | Rhyolite | ? | 40,0 | 7,14 | | 229 | 10,6 | 37,2 | 5,8 | 49,8 | 528 | | 116 | 0,531 | 40,9 | 1039 | -69,0 | -9,9 | 10,4 | 1,78 | | | -5,4 | 0,718600 |
| TP-28 - Dupalova *et al.* (2012) | Lazne Teplice | 973 | Palaeozoic | Rhyolite | 883-942 | 41,0 | 7,26 | | 335 | 11,3 | 33,6 | 5,8 | 56,6 | 600 | | 275 | < 0.05 | 45,7 | 1386 | -69,0 | -9,8 | 10,5 | 1,39 | | | -6,5 | |
| Pravridlo (ancient spring, http://lazneteplice.cz) | Lazne Teplice | 54,3 | Palaeozoic | Rhyolite | ? | 35,9 | 7,29 | | 212 | 10,6 | 40,7 | 6,5 | 50,8 | 502 | | 133 | | 38,6 | 993 | | | | | | | | |
| Pravridlo (ancient spring, November 24, 2015) | Lazne Teplice | 54,3 | Palaeozoic | Rhyolite | ? | 35,9 | 7,29 | -5,4 | 217 | 8,5 | 32,2 | 4,5 | 46,4 | 481 | | 92 | < 0.5 | 43,5 | 925 | -69,5 | -9,9 | 2,8 | 3,40 | 1,2 | 9,30 | -4,5 | 0,720322 |
| Thonex-1 (17/06/2010) - Vuataz and Giroud (2010) | Geneva | 2530 | Upper Jurassic | Limestone | ~ 2100 | 70,0 | 7,92 | -5,4 | 304 | 8,6 | 52,1 | 24,1 | 440 | 411 | | 11,2 | 0 | 47,5 | 1298 | -81,0 | -10,6 | 17,6 | 87,5 | | | -2,3 | 0,707675 |
| Lavey-les-Bains (Sonney *et al.*, 2007) | Vaud | 3000 ? | Hercynian | Gneiss | | 105,0 | 7,20 | | 525 | 16,4 | 61,0 | 0,34 | 315 | 72 | | 768 | < 0.1 | 96,0 | 1854 | -98,5 | -13,4 | 8,5 | 21,9 | | | | |

| Well | Br mg/l | F mg/l | B mg/l | I mg/l | $HPO_4$ mg/l | $NH_4$ mg/l | Li mg/l | Ba mg/l | Sr mg/l | Mn mg/l | Fe mg/l | Rb µg/l | Cs µg/l | Ge µg/l | Al µg/l | Ni µg/l | Zn µg/l | Co µg/l | As µg/l | Sb µg/l | W µg/l | U µg/l | Th µg/l | Cu µg/l | Sn µg/l | Pb µg/l | Ag µg/l |
|---|---|---|---|---|---|---|---|---|---|---|---|---|---|---|---|---|---|---|---|---|---|---|---|---|---|---|---|
| TH-31, TH 31/62 | | | | | | 0,3 | 0,210 | | | 0,470 | 1,74 | | | | | | | | | | | | | | | | |
| TP-41, TP 41/88 | | | | | | | | | | | | | | | | | | | | | | | | | | | |
| TH-20 | | 7,6 | | | | | | | | | 0,24 | | | | | | | | | | | | | | | | |
| TH-10, TH 10/61 | | 6,8 | | | 0,19 | 0,3 | 0,570 | | | | 5,0 | | | | | | | | | | | | | | | | |
| HV-3C | | 0,4 | | | | 0,10 | 0,040 | | | 0,090 | 1,65 | | | | | | | | | | | | | | | | |
| SR-1 | | | | | | | | | | | | | | | | | | | | | | | | | | | |
| PVGT-LT1 (November 2007) | | < 0.5 | | | | < 0.04 | 3,1 | | | 0,130 | 0,55 | | | | | | | | | | | | | | | | |
| PVGT-LT1 (May 2015) | 1,78 | 0,38 | 0,110 | | 0,10 | 2,3 | 0,066 | 2,60 | 0,320 | 0,086 | 0,66 | | | | | | | | | | | | | | | | |
| PVGT-LT1 (November 26, 2015) | 2,09 | 0,30 | 0,060 | | < 0.05 | 3,8 | 0,078 | 2,18 | 0,386 | 0,249 | 0,81 | 35,5 | 1,23 | < 0.5 | 1,42 | 35,6 | 6,83 | 0,60 | 0,45 | 0,34 | 0,16 | 0,27 | < 0.1 | < 0.1 | < 0.05 | < 0.05 | < 0.01 |
| Pravridlo (ancient spring) - Cadek *et al.* (1968) | 0,147 | 7,8 | | | | | 0,290 | | | | | | | | | | | | | | | | | | | | |
| Pravridlo (ancient spring) - Dupalova *et al.* (2012) | | 7,2 | | | | 0,023 | 0,385 | 0,090 | 0,285 | < 0.013 | 0,022 | | | | 1,60 | | | | < 18 | | | | | | | | |
| TP-28 - Dupalova *et al.* (2012) | | 6,8 | | | | 0,104 | 0,528 | 0,083 | 0,319 | 0,016 | 0,516 | | | | 0,90 | | | | 45 | | | | | | | | |
| Pravridlo (ancient spring, http://lazneteplice.cz) | 0,157 | 5,7 | 0,066 | 0,008 | 0,024 | | 0,382 | 0,010 | 0,441 | 0,002 | 0,015 | 75,0 | 18 | | | | | | | < 0.8 | | | | 0,59 | 0,8 | | 0,43 |
| Pravridlo (ancient spring, November 24, 2015) | 0,216 | 7,3 | 0,083 | | < 0.05 | < 0.05 | 0,318 | 0,082 | 0,356 | 0,050 | < 0.02 | 72,2 | 19 | 1,64 | 1,23 | 0,52 | 8,17 | < 0.05 | 3,64 | 0,07 | 4,25 | 4,35 | < 0.1 | 22,8 | < 0.05 | 0,24 | 0,01 |
| Thonex-1 (17/06/2010) - Vuataz and Giroud (2010) | | 5,3 | | | | 4,3 | | 0,083 | | 0,110 | 0,089 | 18 | 1,50 | 5,6 | < 1 | | < 1 | | 0,33 | | 1,2 | 0,04 | | | | < 0.02 | |
| Lavey-les-Bains (Sonney *et al.*, 2007) | 3,30 | 9,3 | 3,4 | 0,4 | < 0.5 | 0,5 | 4,8 | 0,030 | 2,8 | 0,024 | 0,061 | 100 | 60 | 26 | 25 | < 10 | 12 | < 10 | < 5 | | 150 | < 0.1 | | 6 | | < 1 | |

*Table 2 - Characteristics and chemical compositions of the waters discharged from the seven deep boreholes located in the Litomerice area, in the crystalline basement, found by GEOMEDIA, as well as those of the waters from the Pravridlo-Teplice thermal spring, in Czech Republic, and from the Thônex-1 and Lavey-les-Bains geothermal boreholes, in Switzerland.*

## 2.3 Geothermometric interpretation

The concentrations of dissolved silica of the fluids discharged from the Litomerice area are very low, which suggest low deep temperatures. For three of them (TH-20, TH-10 and HV-3C), the chalcedony geothermometer gives estimations of temperatures (21, 28 and 7°C, respectively) close to those measured into the boreholes (Tabl. 3). For the TH-31 fluid, the temperature using this geothermometer is over-estimated (59°C) relative to that measured in the borehole (Tabl. 3).

| Well | Location | Depth m | Stratigraphy | Geology | Water level m | T °C | $T_{Chalc.}$ °C | $T_{Na-K}$ °C | $T_{Na-K-Ca\,(1)}$ °C | $T_{Na-K-Ca\,(2)}$ °C | $T_{Na-K-Ca-Mg}$ °C | $T_{K-Mg}$ °C | $T_{Na-Li}$ °C | $T_{Mg-Li}$ °C | $T_{Na-Rb}$ °C | $T_{Na-Cs}$ °C | $T_{K-Sr}$ °C | $T_{K-Fe}$ °C | $T_{K-Mn}$ °C | $T_{K-W}$ °C | $T_{K-F}$ °C | $T_{18O(H2O-SO4)\,(1)}$ °C | $T_{18O(H2O-SO4)\,(2)}$ °C |
|---|---|---|---|---|---|---|---|---|---|---|---|---|---|---|---|---|---|---|---|---|---|---|---|
| TH-31, TH 31/62 | Oldrichov | 159 | Permian Spodni | Quartz | 12.7 - 159.0 | 13,0 | 59 | 140 | 68 | | 64 | 57 | 135 | 60 | | | | 16 | 9 | | | | |
| TH-20 | Modlany | 443 | Proterozoic | Gneiss | 342.8 - 368.6 | 27,1 | 21 | 135 | 111 | | 112 | 86 | | | | | | 83 | | | 156 | | |
| TH-10, TH 10/61 | Predlice | 500 | Proterozoic | Gneiss | 373.4 - 440.8 | 31,0 | 28 | 148 | 123 | | 111 | 92 | 139 | 93 | | | | 33 | | | 160 | | |
| HV-3C | Jestrebi | 151 | Proterozoic | Phyllite | 133.8 - 145.9 | 12,0 | 7 | 189 | 40 | 0 | | 60 | 44 | 104 | 25 | | | 3 | 18 | | 41 | | |
| PVGT-LT1 (May 2015) | Litomerice | 2111 | Proterozoic | Gneiss | 1600 - 1800 | 56,5 | < 0 | 138 | 89 | 55 | 25 | 58 | 48 | 30 | | | 116 | 45 | 43 | | 58 | | |
| PVGT-LT1 (November 2015) | Litomerice | 2111 | Proterozoic | Gneiss | 1600 - 1800 | 56,5 | < 0 | 133 | 99 | 54 | 68 | 71 | 48 | 43 | 94 | 39 | 116 | 44 | 29 | 49 | 55 | | |
| Pravridlo (ancient spring) | Teplice | 54,3 | Palaeozoic | Rhyolite | | 41,3 | 89 | 123 | 94 | | 88 | 72 | 119 | 76 | 109 | 84 | 117 | 141 | 119 | | 136 | 81 | 57 |
| Pravridlo (November 24, 2015) | Teplice | 54,3 | Palaeozoic | Rhyolite | | 35,9 | 97 | 110 | 92 | | 94 | 72 | 106 | 76 | 107 | 84 | 111 | 129 | 50 | 96 | 137 | 148 | 116 |
| Thonex-1 (17/06/2010) - Vuataz and Giroud (2010) | Geneva | 2530 | Upper Jurassic | Limestone | ~ 2100 | 70,0 | 71 | 92 | 85 | | | 53 | 129 | 76 | 58 | 32 | 53 | 84 | 38 | 75 | 127 | 68 | 46 |
| Lavey-les-Bains (Sonney *et al.*, 2007) | Vaud | 3000 ? | Hercynian | Gneiss | | 105,0 | 108 | 98 | 111 | | 127 | 124 | 254 | 210 | 90 | 90 | 93 | 126 | 85 | 209 | 170 | 71 | 48 |

*$T_{Chalc.}$, $T_{Na-K}$, $T_{Na-Li}$, $T_{K-Sr}$, $T_{K-Fe}$, $T_{K-Mn}$, $T_{K-F}$, $T_{K-W}$: Michard (1990)*   *$T_{Na-K-Ca\,(1)}$: Fournier and Truesdell (1973)*
*$T_{Na-K-Ca\,(2)}$: Paces (1975) - Geochim. Cosmochim. Acta, 39, 541-544*   *$T_{Na-K-Ca-Mg}$: Fournier and Potter (1979)*
*$T_{K-Mg}$: Giggenbach (1988)*   *$T_{Mg-Li}$: Kharaka and Mariner (1989)*

*$T_{18O(H2O-SO4)\,(1)}$: Lloyd (1968) - J. Geophysical Research, 73, 6099-6110*
*$T_{18O(H2O-SO4)\,(2)}$: Kusakabe and Robinson (1977) - Geochim. Cosmochim. Acta, 41,1033-1040*

*Table 3 - Deep temperatures estimated using classical and auxiliary chemical geothermometers on the Litomerice waters.*

The Na-Cl fluid collected from the PVGT-LT1 borehole indicates an anomalously low $SiO_2$ content, given its temperature measured at the bottom-hole, close to 56.5°C, at a depth of 1 800 m (Tabl. 2). This low concentration could be explained by the fact that the collected samples are not still representative of the thermal water of the bottom-hole. Consequently, when applied to this fluid, the chalcedony geothermometer gives inaccurate estimated temperatures whereas the Na/K geothermometer yields overestimated temperature (Tabl. 3).

Otherwise, the Na-K-Ca (2), Na-K-Ca-Mg, K-Mg, Na-Li, Mg-Li, Na-Cs, K-Fe, K-Mn, K-W and K-F geothermometers give estimations of deep temperature (39-71°C, or 55 ± 20°C) close to that measured at the bottom-hole (Tabl. 3), and suggest that the elemental ratios of the collected fluid samples could be close to those of the water present at the bottom-hole.

The chemical analyses of the dissolved gases sampled in the PVGT-LT1 borehole show that $CH_4$ (78%) and $N_2$ (19%) are the predominant gases ($CO_2$ is present at about 0.2%; Appendix 1), and are in agreement with the low temperature measured at the bottom-hole and estimated using the auxiliary chemical geothermometers.

If this water is in chemical equilibrium with few minerals, we can consider that a chemical steady-state between water and felsic rocks is attained (Paces, 1975; see the concordant temperature estimated using the corresponding Na-K-Ca relationship proposed by this author in table 3).

For the other fluids of the Litomerice area, apart TH-20, only the temperatures estimated using the auxiliary K-Fe geothermometer (33, 3 and 16°C, respectively) are close to those measured (Tabl. 3). For the TH-31 and HV-3C fluids, the temperatures estimated using the auxiliary K-Mn geothermometer are also in agreement with those measured (Tabl. 3). Due to the quasi-absence of chemical equilibrium reactions at low temperatures, only the classical chalcedony and the K-Mn and K-Fe auxiliary geothermometers yield correct estimations of deep temperature for these waters.

For the Pravridlo thermal water, located at Teplice, apart the K-Fe and K-F thermometric relationships, the other auxiliary geothermometers give concordant temperature values ranging from 76 to 119°C, which are in agreement with those estimated (72-123°C) using the chalcedony, Na-K, Na-K-Ca, Na-K-Ca-Mg and K-Mg classical geothermometers (Tabl. 3). In contrast to the Litomerice water, overall chemical equilibrium between this thermal water and reservoir minerals seems to be reached at a temperature close to 100 ± 25°C.

Among the two isotope thermometric relationships ($\delta^{18}O_{H2O}$-$\delta^{18}O_{SO4}$), the concordant temperature is given by the first one, for the first Pravridlo water sample, and by the second one, for the water sample collected by BRGM, in November 2015. If the $\delta^{18}O_{H2O}$ values between the two water samples are similar, the $\delta^{18}O_{SO4}$ values are very different (Tabl. 3). It is probable that these last values are controlled by different processes in each of the water samples.

The figure 25 illustrates the geothermometric results.
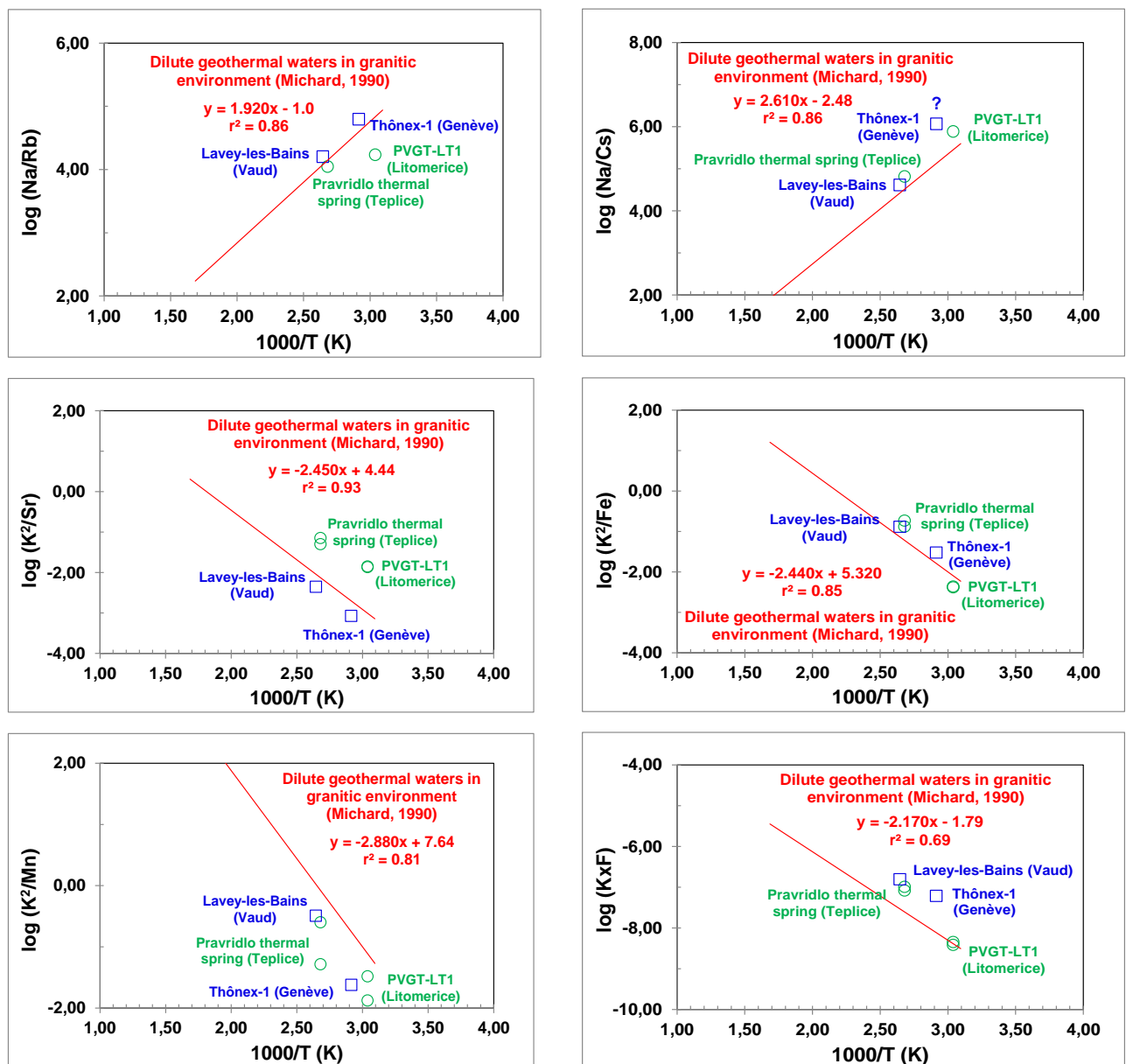


Fig. 25 - Applications of the auxiliary geothermometers defined by Michard (1990) to the Litomerice PVGT-LT1 and Pravridlo thermal waters, in the Czech Republic, as well as the Thônex-1 and Lavey-Les-Bains thermal waters, in Switzerland.

## 2.4 Main conclusions

A part of the results obtained in this study was summarized in an abstract and a poster presented during the Mid-Term Conference held in Pisa, Italy, on October 12-13, 2015 (Sanjuan *et al.*, 2015b).

At temperatures ≤ 50°C, the poor concordance between the temperatures estimated using chemical geothermometers and the measured values in 4 deep boreholes penetrating the crystalline basement, in the Litomerice area, is due to the low values of this parameter, which do not allow the deep waters to reach chemical equilibria with the surroundings rocks. At these low values of temperature, only the chalcedony geothermometer and the auxiliary K-Fe and K-Mn geothermometers, defined by Michard (1990), seem to be able to give relatively good estimations of temperatures.

At temperatures > 50°C, the auxiliary geothermometers such as Na-Li, Mg-Li, Na-Cs, K-Mn and K-W give concordant temperature values for the Litomerice PVGT-LT1 water (55 ± 20°C) and for the Pravridlo thermal water, at Teplice (100 ± 25°C). However, some auxiliary geothermometers such as Na-Rb and K-Sr give discordant temperature values for the Litomerice PVGT-LT1 water and concordant values for the Pravridlo thermal water (Tabl. 2). Similarly, other auxiliary geothermometers such as K-Fe and K-F give concordant temperature values for the Litomerice PVGT-LT1 water and discordant values for the Pravridlo thermal water (Tabl. 2).

In contrast to the PVGT-LT1 water, overall chemical equilibrium between the Pravridlo thermal water and reservoir minerals seems to be reached at a temperature close to 100 ± 25°C.

# 3. Field work relative to the Thonex-1 borehole, in Switzerland

After that the GEOMEDIA Company was constrained to leave the IMAGE project and in order to complete the geothermometric data obtained for low-temperature dilute waters located in the Litomerice and Teplice thermal areas of the Eger Graben, in Czech Republic, for testing the auxiliary chemical geothermometers such as Na-Li, Na-Rb, Na-Cs, K-Sr, K-Mn, K-Fe, K-F and K-W, determined by Michard (1990), we had the opportunity to engage a collaboration with new partners from Switzerland (SIG and University of Geneva). It was decided with them to carry out works on the old Thônex-1 geothermal exploration borehole, which is located in the Geneva canton (Fig. 26).

## 3.1    Description of the site

The Thônex-1 geothermal exploration borehole was drilled in 1993, at Thônex, near Geneva, in the Geneva canton (Fig. 26). It was deviated from a depth of 700 m, with an angle of 25°, and reached a vertical depth of 2 530 m for a drilled length of  2 690 m (Vuataz and Giroud, 2010).

The Thônex-1 borehole has penetrated the Tertiary Molasse, the Cretaceous units and the Upper Jurassic of the Geneva basin (Fig. 26). In 2010, a seismic survey has allowed validating the depth of the deep formations, especially that of the crystalline basement in the Thônex area, as well as the presence, the position and the internal structure of a major regional fault (Arve fault), located near Thônex and oriented NW-SE, and of other faults down to the Permo-Carboniferous formation. The crystalline basement is estimated to be deeper than 5 600 m.
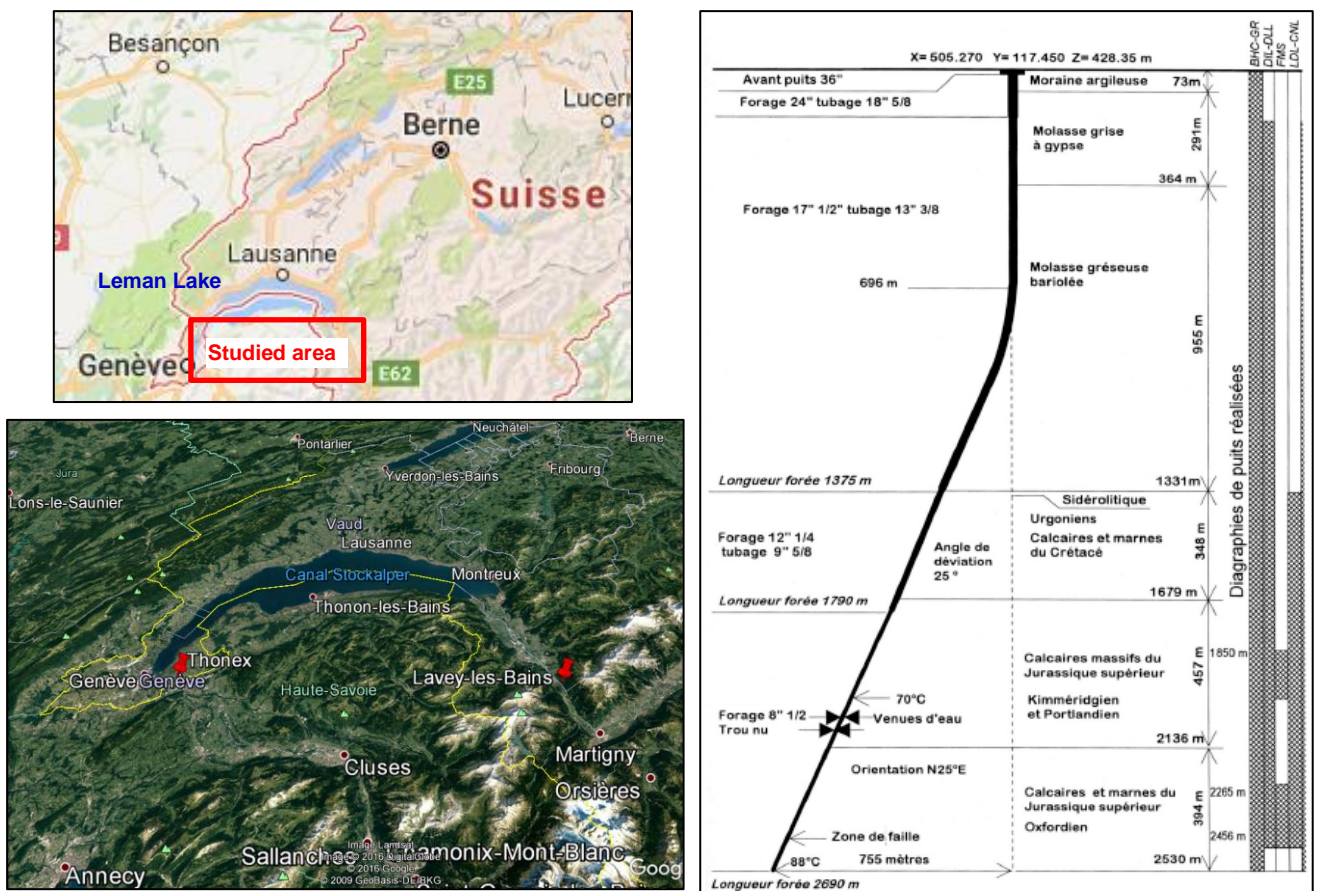


*Fig. 26 - Lift: Map of the location of the Thônex-1 and Lavey-les-Bains boreholes, in the Geneva and Vaud cantons respectively, in Switzerland (extracted from the BDFGeotherm database of the geothermal fluids, in Switzerland, associated with a Google Earth map; Sonney and Vuataz, 2007). Right: Geometry and characteristics of the Thônex-1 geothermal borehole (after Jenny et al., 1995).*

The two geothermal targets were the Urgonian limestone from the Lower Cretaceous and the reef limestone from Upper Jurassic. In order to obtain economically interesting fluid flow-rates, it was necessary to intersect karstic and/or fractured formations. Unfortunately, after the acidification of the first target (Cretaceous), the productivity of this borehole remained very low. In the formations of the second target (Jurassic), three permeable levels were detected, but the results of the production tests, after massive HCl stimulation operations, were disappointing.

According to Vuataz and Giroud (2010), the duration of the longer production test carried out using air-lift was about 55 hours. The initial fluid flow-rate was 35 $m^3$/h and progressively decreased down to 20 $m^3$/h, then 11 $m^3$/h. The volume of discharged fluid, at the end of this production test, was 794 $m^3$ (Tabl. 4), which represents about 5 times the total volume of the borehole (147 $m^3$). The calculated productivity index was lower than 0.42 $m^3$/h/bar and the artesian flow-rate remained very low (< 1 $m^3$/h).

Later, the Geology-Geophysics Bureau of Geneva carried out a production test using the artesian flow-rate (free flowing) during 37 days, from May 20 to June 27, 1996. A progressive decrease of the flow-rate from 9 to 0.3 $m^3$/h was observed. In 1996, the Thônex-1 borehole was opened during more than 1 year (up to August 11, 1997), and several measurements were performed showing a decrease of the flow-rate down to 0.17 $m^3$/h. Globally, a total volume of 2 158 $m^3$ was discharged from the limestone reservoir. The very low flow-rate value measured from this borehole does not allow carrying out any tracer tests.

In 2009, an introspection of the borehole has shown the good state of preservation of the tubing (down to 1 790 m). Below the tubing, the part in bare rock is clogged at a depth of 1 840 m/ground (limestone blocks), preventing any fluid sampling at the bottom-hole. The temperature measured at this depth was about 67°C.

In the framework of valorisation works of the Thônex-1 borehole, several options were evaluated in 2010: installation of a geothermal probe at high depth, stimulation of the existing borehole or deepening of this borehole down to the crystalline basement. In case of installation of a deep geothermal probe or deepening of the borehole, or definitive closure of this borehole, the access to the deep fluid would not be possible.

Consequently, it was decided to carry out a geochemical study of this fluid, based on a fluid sampling from the well-head and corresponding chemical and isotope analyses, after a period of artesian production of 6 months and a significant total volume of discharged fluid (about 780 $m^3$; Tabl. 4). The CREGE geothermal Laboratory was mandated to carry out a complete collection of the deep fluid for chemical and isotope analyses, in order to determine its main characteristics, its origins and its behaviour in the geothermal reservoir (Vuataz and Giroud, 2010).

| Production test | Duration | Volume of discharged fluid ($m^3$) | Measurement date | Fluid conductivity (µS/cm) | Cl (mg/l) |
|---|---|---|---|---|---|
| 18/09/93 - 19/09/93 | 2 days | 340 | - | | |
| 29/09/93 - 01/10/93 | 3 days | 795 | 01/10/93 | 6260 | 3300 |
| 26/11/93 - 29/03/94 | 4 months | 300 to 500 | 29/03/94 | 5670 | 2500 |
| 20/05/96 - 11/08/97 | 14 months | 2158 | 05/11/97 | 2500 | 667 |
| Jan. to June 2010 | 6 months | about 780 | 14/06/2010 | 1954 | 431 |

*Table 4 - Characteristics of the production tests carried out in the Thônex-1 borehole (from Vuataz and Giroud, 2010), before this study.*

## 3.2 Fluid chemical and isotopic compositions

### 3.2.1 Existing data

Several more or less complete analyses have been performed in the geothermal fluid collected from the limestone formations from the Upper Jurassic, between the end of the Thônex-1 drilling and the production tests, in 1993, then in 1996 and in 1997 (Sonney and Vuataz, 2007; Vuataz and Giroud, 2010). The analytical results indicated anomalously high TDS values, resulting from the residues of the HCl acid used for the chemical stimulation in 1993. In particular, high Cl concentrations were observed (Tabl. 4). During all the production tests, the concentrations of the main dissolved chemical species decreased. Up to 2010, despite large volumes of fluid discharged from the borehole, no water sample could be considered as representative of the deep natural geothermal fluid. All the analyses indicated high concentrations for most of the chemical species (Vuataz and Giroud, 2010). Some tentative to reconstruct the chemical composition of the deep fluid and its origins was attempted by Jenny *et al.* (1995) and Murat (1999).

In 2010, during a period of artesian production of 6 months (Tabl. 4), 4 water samples were collected and analysed by the SIG laboratory, between May and June 2010. The analyses indicated stable Cl concentration values (418-465 mg/l), which were the lowest analysed ones. Consequently, it was decided to perform a complete collection of fluid samples for chemical and isotope analyses on June 17, 2010, and the corresponding on-site measurements. The detailed chemical and isotope analyses are presented in Vuataz and Giroud (2010). They are also reported in table 2. Most of the trace species (F, Sr, Li, Rb, Cs, Fe, Mn, W) and isotopes ($^{18}$O of the dissolved sulphate) which are interesting for our study were analysed.

Some of the main conclusions of Vuataz and Giroud (2010) about the characteristics of this fluid were:

- this Na-Cl fluid which has a relatively low TDS value (about 1 466 mg/) and a pH value close to 7.92 seems to be representative of the deep limestone reservoir;
- according to the $\delta^{18}$O and $\delta$D values, the mean altitude of the recharge area would be ranging from 800 to 1200 m, in the first Jura range, under climatic conditions colder than today;
- the tritium and $^{14}$C data indicate that the sampled fluid is an old water with a residence time in the order of 10 000 to 15 000 years and has not been mixed with more recent waters. These estimations can be compatible with the water recharge areas;
- the $\delta^{13}$C value shows a signature lower than that of the limestone formation from the Upper Jurassic, and could be the result of a $CO_2$ degassing and corresponding carbonate precipitation, during the ascent of the fluid in the borehole;
- the analyses of $^{34}$S in the dissolved sulphates and sulphides indicate very high and atypical values for thermal waters. These values are probably due to the oxidation of rock sulphides during the underground transit.

The geothermometric data obtained in their study will be commented in section 3.3.

In order to complete the geothermometric interpretation for low-temperature dilute waters in Switzerland, a detailed study about the chemical and isotope composition of the deep geothermal water which could be discharged from the Lavey-les-Bains borehole, located in the Vaud canton (Fig. 26; Sonney *et al.*, 2007), and penetrating the crystalline basement (gneiss), was included in our study. This composition of the deep fluid, which was reconstructed by the authors from the existing geochemical data and chemical modelling simulations using PHREEQC (Sonney and Vuataz, 2007; Sonney *et al.*, 2007), is reported in table 2.

## 3.2.2 Data obtained during this study

In order to confirm and to be sure that the chemical and isotope composition determined in 2010 for the Thônex-1 geothermal water was representative of the deep reservoir (Vuataz and Giroud, 2010), it was proposed to do a new complete collection of samples for chemical and isotope analyses, from the well-head of the Thônex-1 borehole, after a significant volume of discharged fluid.

A first fluid sampling and corresponding on-site measurements, before the fluid discharge, was conducted by BRGM in collaboration with SIG on July 27, 2016, in order to be able to follow the evolution of the chemical composition of the water discharged from the Thônex-1 borehole. The on-site measurements are reported in table 5.

| Parameter | T °C | Conductivity µS/cm | pH | Eh mV | O$_2$ % |
|-----------|------|--------------------|----|-------|--------|
| 27/07/2016 | 21.3 | 1974 | 7.27 | -276 | 3.1 |

*Table 5 - On-site measurements performed on the water discharged from the Thônex-1 borehole at the beginning of this discharge in July 2016.*

The conductivity value (Tabl. 5) compared with that measured in 2010 (Tabl. 4) indicates the TDS values of the two water samples are close and suggests the chemical compositions are similar. The pH value is lower than that measured in 2010 (7.92; Tabl. 2). The content of dissolved O$_2$ indicates a slight contribution of atmospheric O$_2$ which would have to disappear at the end of the fluid discharge.

BRGM and SIG decided to carry out a new complete collection of fluid samples for chemical and isotope analyses, and the corresponding on-site measurements (T, conductivity, pH, Redox potential, dissolved oxygen, alkalinity, etc.) on October 25, 2016, after estimations of volumes of fluid discharged from the Thônex-1 borehole ranging from 221 m$^3$ (138 m$^3$ + 83 m$^3$) to 570 m$^3$ (432 m$^3$ + 138 m$^3$; Tabl. 6), which represents about from 2 to 4 times the entire volume of the borehole (147 m$^3$). These estimations of discharged volumes were done because the artesian fluid flow-rate highly decreased from 0.30 l/s to 0.12 l/s, after a week of fluid production (SIG personal communication). If possible, samples of dissolved and incondensable gases will be also collected for chemical (major species) and isotope analyses ($\delta^{13}$C value).

| Dates | 25/07 -> 19/08/2016 | 19/08 -> 07/10/2016 | 07/10 -> 15/10/2016 |
|-------|---------------------|---------------------|---------------------|
| Number of days | 25 | 49 | 8 |
| Volume (m$^3$) of discharged water with a max. observed flow-rate: 0.3 l/s | 648 | closed well | 207 |
| Volume (m$^3$) of discharged water with a mean observed flow-rate: 0.2 l/s? | 432 | closed well | 138 |
| Volume (m$^3$) of discharged water with a min. observed flow-rate: 0.12 l/s | 259 | closed well | 83 |

*Table 6 - Estimations of the volumes (m$^3$) of fluid discharged from the Thônex-1 borehole in 2010, following the considered fluid flow-rates (after F. Martin, SIG; personal communication).*

The chemical and isotopes analyses which will be performed on these fluid samples are:

- the major species such as Na, K, Ca, Mg, Cl, $SO_4$, $HCO_3$, DOC, $NO_3$, $SiO_2$;
- the trace species such as F, B, I, Br, $PO_4$, $NH_4$, Ba, Sr, Li, Cs, Rb, Ge, Fe, Mn, As, Al, W, Ni, Co, Cr, Cu, Pb and Zn;
- the stable isotopes of the water ($\delta D$ and $\delta^{18}O$ values);
- the $\delta^{18}O$ and $\delta^{34}S$ values of the dissolved sulphates;
- the $\delta^7Li$ and $\delta^{11}B$ values;
- the isotopic $^{87}Sr/^{86}Sr$ ratio.

The methods used for these analyses and the corresponding uncertainties are already mentioned in section 2.2.

The analytical results which will be obtained in the next months will be presented in the WP8 framework.

## 3.3 Geothermometric interpretation

According to Vuataz and Giroud (2010), the classical geothermometers (Na-K, Na-K-Ca, K-Mg, chalcedony, $\delta^{18}O_{H2O}$-$SO4$, etc.) applied to the chemical composition of the Thônex-1 deep water indicate a relative concordance of the estimated temperatures between 60 and 85°C, with the measured temperatures in the borehole and confirm the chemical equilibrium of the fluid with a fractured system at a depth of 2 000-2 500 m. They consider that a temperature close to 75 ± 5°C can be selected using these geothermometers, which corresponds to the temperature measured in the production areas of the Thônex-1 borehole, from the Upper Jurassic (Fig. 26). Apparently, the geothermal fluid does not quickly come (not in equilibrium state) from deeper levels than those known in the borehole.

If we apply the auxiliary geothermometers to this water (Tabl. 3; Fig. 25), we can see that the Na-Li and K-F geothermometers give over-estimated temperature values (129 and 127°C, respectively), and the Na-Cs and K-Mn geothermometers yield under-estimated values (32 and 38°C, respectively). All the other auxiliary geothermometers (Mg-Li, Na-Rb, K-Sr, K-Fe and K-W) give temperature values ranging from 53 to 84°C (Tabl. 3), in agreement with the measured temperature and those estimated using the classical geothermometers. From the temperature values estimated using the auxiliary geothermometers, a temperature close to 70 ± 20°C can be selected.

Most of the geothermometers applied to the reconstructed chemical composition of the Lavey-les-Bains geothermal water (Tabl. 2) give concordant temperature values ranging from 85 to 127°C (Tabl. 3). From all these estimated values, the selected temperature value is 105 ± 25°C. As for the Thônex-1 water, the Na-Li and K-F geothermometers give over-estimated temperature values (254 and 170°C, respectively). In contrast, the Mg-Li and K-W geothermometers also yield over-estimated temperature values (210 and 209 °C) whereas the Na-Cs gives a concordant value (90°C).

## 3.4 Main conclusions

Even if we wait for additional chemical and isotope analyses of the Thônex-1 water, which must be performed in the next months on the water samples collected on October 25, 2016, in order to confirm and to be sure that this water is representative of the deep reservoir, some results and conclusions can be drawn.

The application of the auxiliary geothermometers on the chemical composition of this water determined in 2010 indicates that a part of them (Na-Rb, Mg-Li, K-Sr, K-Fe and K-W geothermometers) gives concordant temperature values (70 ± 20°C) in agreement with the measured temperature and those estimated using classical chemical and isotope geothermometers (75 ± 5°C; Vuataz and Giroud, 2010).

For the reconstructed chemical composition of the Lavey-les-Bains geothermal water, similar results are obtained using most of the geothermometers, which indicated a deep temperature close to 105 ± 25°C.

For both waters, the Na-Li and K-F geothermometers yield over-estimated temperature values.

These results, in addition to those obtained in Czech Republic, show the auxiliary geothermometers determined by Michard (1990) give, sometimes, discordant temperature values for low-temperature waters, but they remain very useful tools, when a significant part of them gives concordant temperature values.

# 4. Conclusions and recommendations

In the framework of the IMAGE project, the main objective of the task 7.3 was to develop auxiliary chemical geothermometers and tracer tests adapted to environments of crystalline basements and sedimentary basins in order to consolidate the temperature estimation of the geothermal reservoir from surface exploration and better know the fluid circulation in this type of reservoir, respectively.

The first literature review about the existing geothermometers for environments of crystalline basements and sedimentary basins has shown that several auxiliary chemical geothermometers existed in addition to the classical geothermometers Na-K, silica, Na-K-Ca, K-Mg, $\delta^{18}O_{H2O-SO4}$, etc.

For dilute geothermal waters discharged from granite environments, between 25 and 150°C, thermometric relationships such as Na-Li, Na-Rb, Na-Cs, K-Sr, K-Fe, K-Mn, K-F and K-W, determined by Michard (1990), are available and can be used.

For saline geothermal waters discharged from crystalline basements and sedimentary basins at temperatures ranging from 25 to 320°C, only Na-Li and Mg-Li thermometric relationships are proposed in the literature. In the framework of this project, three new thermometric relationships, Na-Rb, Na-Cs and K-Sr, were determined from literature data about 20 deep saline waters, especially those discharged from wells located in geothermal areas and oil fields of the Rhine Graben, and in the geothermal area of Salton Sea, at temperatures ranging from 70 to 320°C (Sanjuan *et al.*, 2016b). Other less reliable thermometric relationships (K-Fe, K-Mn, K-F) were also found. The three new thermometric relationships are:

$$t\,(°C) = 2522 / [\log (Na/Rb) + 1.514] - 273.15 \qquad r^2 = 0.93 \qquad n = 20$$

$$t\,(°C) = 2585 / [\log (Na/Cs) + 0.843] - 273.15 \qquad r^2 = 0.84 \qquad n = 20$$

$$t\,(°C) = 2992 / [6.472 - \log (K^2/Sr)] - 273.15 \qquad r^2 = 0.97 \qquad n = 19$$

The second literature review was associated with the development of tracing tests in environments of crystalline basement and has benefited from the long BRGM experience in the Soultz geothermal site. After a review of the tracers recommended in the literature following the fixed objectives, examples of applications in different crystalline sites were given. The most recent inter-well tracer tests conducted in June 2013 at the Habanero EGS site, central Australia, and in 2014, in the Rittershoffen site, Alsace, near Soultz-sous-Forêts, in a granite environment, were also integrated in this review.

Unfortunately, after on-site works, no tracer test could be conducted in the PVGT-LT1 borehole, only borehole available in the Litomerice area, Czech Republic, and in the Thônex-1 borehole, near Geneva, in Switzerland, especially because of the very low fluid flow-rate existing in these boreholes. Consequently, we decided to focus our on-site works on the development of auxiliary chemical geothermometers at low-temperatures.

After the literature review, the chemical compositions of deep dilute fluids discharged from existing boreholes drilled up down the crystalline basement, in the Litomerice area, in Czech Republic, were collected and exploited. Only the chemical compositions of fluids from five deep boreholes were found and among these boreholes, only one (PVGT-LT1 borehole) could be sampled by GEOMEDIA in May 2015 and by BRGM, with the help of GEOMEDIA and the Litomerice city, in October 2015. Another fluid sample was collected by BRGM from the Pravridlo thermal spring, at Teplice, a city located near Litomerice. These two water samples were analysed in the BRGM laboratories. A part of the results obtained in this study was summarized in an abstract and a

poster presented during the Mid-Term Conference held in Pisa, Italy, on October 12-13, 2015 (Sanjuan *et al.*, 2015b).

At temperatures ≤ 50°C, the poor concordance between the temperatures estimated using chemical geothermometers and the measured values in 4 deep boreholes penetrating the crystalline basement, in the Litomerice area, is due to the low values of this parameter, which do not allow the deep waters to reach chemical equilibria with the surroundings rocks. At these low values of temperature, only the chalcedony geothermometer and the auxiliary K-Fe and K-Mn geothermometers, defined by Michard (1990), seem to be able to give relatively good estimations of temperatures.

At temperatures > 50°C, the auxiliary chemical geothermometers such as Na-Li, Mg-Li, Na-Cs, K-Mn and K-W give concordant temperature values for the Litomerice PVGT-LT1 water (55 ± 20°C) and for the Pravridlo thermal water, at Teplice (100 ± 25°C). However, some auxiliary geothermometers such as Na-Rb and K-Sr give discordant temperature values for the Litomerice PVGT-LT1 water and concordant values for the Pravridlo thermal water (Tabl. 2). Similarly, other auxiliary geothermometers such as K-Fe and K-F give concordant temperature values for the Litomerice PVGT-LT1 water and discordant values for the Pravridlo thermal water (Tabl. 2).

Note that the chemical composition of the PVGT-LT1 fluid is not probably fully representative of that of the fluid present at the bottom-hole because of the very low fluid flow-rate measured in the borehole, which does not allow discharging large volumes of fluid. In contrast to this water, overall chemical equilibrium between the Pravridlo thermal water and reservoir minerals seems to be reached at a temperature close to 100 ± 25°C.

Even if we wait for additional chemical and isotope analyses of the Thônex-1 water, which must be performed in the next months on the water samples collected on October 25, 2016, in order to confirm and to be sure that this water is representative of the deep reservoir, some results and conclusions can be drawn from the existing chemical and isotope data.

The application of the auxiliary geothermometers determined by Michard (1990) on the chemical composition of this water determined in 2010 indicates that a part of them (Na-Rb, K-Sr, K-Fe and K-W geothermometers) gives concordant temperature values (70 ± 20°C) in agreement with the measured temperature and those estimated using classical chemical and isotope geothermometers (75 ± 5°C; Vuataz and Giroud, 2010).

For the reconstructed chemical composition of the Lavey-les-Bains geothermal water (Sonney *et al.*, 2007), similar results are obtained using most of the geothermometers, which indicated a deep temperature close to 105 ± 25°C.

For both waters, the Na-Li and K-F geothermometers yield over-estimated temperature values.

These results, in addition to those obtained in Czech Republic, show the auxiliary geothermometers determined by Michard (1990) give, sometimes, discordant temperature values for low-temperature waters, but they remain very useful tools, when a significant part of them gives concordant temperature values. These tools must be always used together and in the framework of a global geochemical data interpretation because if it is not the case, they may induce important errors in the estimations of the reservoir temperatures in geothermal exploration.

A scientific paper that summarizes and exploits all the developments obtained with the auxiliary chemical geothermometers during this study in order to improve the geochemical methods for geothermal exploration is envisaged in 2017 within the WP8 framework.

# 5. References

## *Auxiliary Chemical geothermometers*

Alaux-Négrel G. (1991) - Etude de l'évolution des eaux profondes en milieu granitiques et assimilés. Comportement des éléments en trace. *Thesis, University of Paris 7*, 218 p.

Alaux-Négrel G., Beaucaire C., Michard G., Toulhoat P., Ouzounian G. (1993) - Trace-metal behaviour in natural granitic waters. *Journal of Contaminant Hydrology*, 13, 309-325.

Arnorsson S. (1983) - Chemical equilibria in Icelandic geothermal systems. Implications for chemical geothermometry investigations. *Geothermics*, 12, 2-3, 119-128.

Arnorsson S. (2000) - The quartz and Na/K geothermometers. I. New thermodynamic calibration. Proceedings World Geothermal Congress 2000, Kyushu - Tohoku, Japan, May 28 - June 10, 2000, 929-934.

Cadek J., Hazdrova M., Kacura G., Krasny J., Malkovsky M. (1968) - Hydrogeology of the thermal waters at Teplice and Usti nad Labem. Sb. Geol. Ved. Geol. HIG, 6, 7-208.

Dupalova T., Sracek O., Vencelides Z., Zak K. (2012) - The origin of thermal waters in the northeastern part of the Eger Rift, Czech Republic. *Applied Geochemistry*, 27, 689-702.

Fouillac Ch. and Michard G. (1981) Sodium/lithium ratio in water applied to geothermometry of geothermal reservoirs. *Geothermics*, 10, 55-70.

Fournier R.O. (1979) - A revised equation for the Na/K geothermometer. *Geoth. Res. Council Trans.*, **3**, 221-224.

Fournier R.O. and Truesdell A.H. (1973) - An empirical Na-K-Ca geothermometer for natural waters. *Geochimica et Cosmochimica Acta*, 37, 1255-1275.

Fournier R.O. and Potter R.W. (1979) - Magnesium correction to the Na-K-Ca chemical geothermometer. *Geochimica et Cosmochimica Acta*, 43, 1543-1550.

Giggenbach W.F. (1988) - Geothermal solute equilibria. Derivation of Na-K-Mg-Ca geoindicators. *Geochimica et Cosmochimica Acta*, 52, 2749-2765.

Hazdrova M., Kacura G., Krasny J. (1964) - Solution of protection zones of the Teplice Spa. Part II: Hydrogeology. *MS Geofond Praha*.

Jenny J., Burri J.-P., Muralt R., Pugin A., Schegg R., Ungemach P., Vuataz F.-D. and Wernli R. (1995) - Le forage géothermique de Thônex (canton de Genève) : Aspects stratigraphiques, tectoniques, diagénétiques, géophysiques et hydrogéologiques. *Eclogae geol. Helv.*, 88/2, 365-396.

Muralt R. (1999) - Processus hydrogéologiques e t hydrochimiques dans les circulations profondes des calcaires du Malm de l'arc jurassien (zones de Delémont, Yverdon-les-Bains, Moiry, Genève et Aix-les-Bains). *Matériaux pour la Géologie de la Suisse, série Géotechnique*, 82, 236 p.

Jirakova H., Huneau F., Hrkal Z., Celle-Jeanton H., Le Coustumer Ph. (2010) - Carbon isotopes to constrain the origin and circulation pattern of groundwater in the north-western part of the Bohemian Cretaceous Basin (Czech Republic). *Applied Geochemistry*, 25, 1265-1279.

Jirakova H., Prochazka M., Dedecek P., Kobr M., Hrkal Z., Huneau F., Le Coustumer Ph. (2011) - Geothermal assessment of the deep aquifers of the northwestern part of the Bohemian Cretaceous Basin, Czech Republic. *Geothermics*, 40, 112-124.

Jirakova H., Stibitz M., Frydrych V., Durajova M. (2015) - Geothermal country update for the Czech Republic. *Proceedings World Geothermal Congress 2015, Melbourne, Australia, 19-25 April 2015*, 7 p.

Kharaka Y.K., Lico M.S. and Law L.M. (1982) - Chemical geothermometers applied to formation waters, Gulf of Mexico and California Basins (abstract). *Am. Ass. Petrol. Geol. Bull.*, 66, 588.

Kharaka Y.K., Mariner R.H. (1989) - Chemical geothermometers and their application to formation waters from sedimentary basins. *In: Naeser N.D. and McCulloch T.H. (Eds), Thermal history of sedimentary basins: methods and case histories. Springer-Verlag, New York*, 99-117.

Kusakabe M., Robinson B.W. (1977) - Oxygen and sulfur isotope equilibria in the $BaSO_4$-$HSO_4^-$-$H_2O$ system from 110 to 350 °C and applications. *Geochim. Cosmochim. Acta*, 41, 1033-1040.

Lloyd R.M. (1968) - Oxygen isotope behaviour in the sulphate-water system. *Journal of Geophysical Research*, 73, 6099-6110.

McKibben M.A., Williams A.E., Elders W.A., Eldridge C.S. (1987) - Saline brines and metallogenesis in a modern sediment-filled rift: the Salton Sea geothermal system, California, USA. *Applied Geochemistry*, 2, 563-578.

Michard G. (1979) - Géothermomètres chimiques. *Bull. BRGM, Section III*, 2, 183-189.

Michard G. (1990) - Behaviour of major elements and some trace elements (Li, Rb, Cs, Fe, Mn, W, F) in deep hot waters from granitic areas. *Chemical Geol*ogy, 89, 117-134.

Mizutani Y., Rafter T.A. (1969) - Oxygen isotopic composition of sulphates. 3. Oxygen isotopic fractionation in the bisulphate ion-water system. *New Zealand J. of Sci.*, 12, 54-59.

Myslil V., Karous M., Paces T., Posmourny K., Rukavickova L., Frydrych V., Gregor P., Hanych I. (2012) - Geothermal project for the Litomerice heating plant. *GEOTERN rep*ort, 140 p.

Nicholson K. (1993) - Geothermal fluids. Chemistry and Exploration Techniques. *Springer-Verlag Berlin, Heidelberg*, 260 p.

Pauwels H., Fouillac C., Fouillac A.-M. (1993) - Chemistry and isotopes of deep geothermal saline fluids in the Upper Rhine Graben: Origin of compounds and water-rock interactions. *Geochimica et Cosmochimica Acta*, 57, 2737-2749.

Sanjuan B., Millot R. (2009) - Bibliographical review about Na/Li geothermometry and lithium isotopes applied to worldwide geothermal waters. *BRGM/RP-57346-FR final report*, 58 p.

Sanjuan B., Millot R., Dezayes Ch., Brach M. (2010) - Main characteristics of the deep geothermal brine (5 km) at Soultz-sous-Forêts (France) determined using geochemical and tracer test data. *CR. Geoscience*, 342, 546-559.

Sanjuan B., Millot R., Asmundsson R., Brach M., Giroud N. (2014) - Use of two new Na/Li geothermometric relationships for geothermal fluids in volcanic environments. *Chemical Geology*, 389, 60-81.

Sanjuan B., Millot R., Dezayes Ch., Jirakova H., Frydrych V. (2015b) - Development and use of auxiliary chemical geothermometers applied to low-temperature fluids collected from the crystalline basement in the Litomerice area, Czech Republic. Abstract and poster presented during the Mid-Term Conference, Pisa, Italy, October 12-13, 2015.

Sanjuan B., Millot R., Innocent Ch., Dezayes Ch., Scheiber J., Brach M. (2016a) - Main geochemical characteristics of geothermal brines collected from the granite basement in the Upper Rhine Graben and constraints on their deep temperature and circulation. *Chemical Geology,* 428, 27-47.

Sanjuan B., Millot R., Dezayes Ch. (2016b) - Three new auxiliary chemical geothermometers for hot brines from geothermal reservoirs. *Abstract and oral presentation in the Goldschmidt 2016 Conference, Yokohama, Japan, June 26 - July 1, 2016*.

Serra H., Sanjuan B. (2004) - Synthèse bibliographique des géothermomètres chimiques. BRGM/RP-52430-FR report, 80 p.

Sonney R., Vuataz F.-D. (2007) - BDFGeotherm. Base de données des fluides géothermiques de la Suisse. Notice explicative, Office fédéral de l'Energie OFEN, CREGE, Centre de Recherche en géothermie de Neuchâtel, 47 p.

Sonney P., Portier S., Vuataz F.-D. (2007) - Estimation de la composition chimique de l'eau thermale en profondeur à Lavey-les-Bains (Vaud). *Rapport CREGE, Centre de Recherche en géothermie, UNINE, Université de Neuchâtel, Projet AGEPP : Alpine Geothermal Power Production*, 42 p.

Verma P.S., Santoyo E. (1997) - New improved equations for Na/K, Na/Li and $SiO_2$ geothermometers by outlier detection and rejection. *Journal of Volcanology and Geothermal Research*, 79, 9-23.

Vuataz F.-D., Giroud N. (2010) - Caractéristiques géochimiques du fluide profond du forage géothermique Thônex-1, Genève. *Rapport CREGE, UNINE, Université de Neuchâtel*, 29 p.

Warren E.A. and Smalley P.C. (1994) - North Sea formation waters Atlas. *Geological Society Memoir 15, Geological Society Publishing House, Bath,* 208 p.

Weinlich F.H., Bräuer K., Kämpf H., Strauch G., Tesar J., Weise M. (1999) - An active subcontinental mantle volatile systems in the western Eger rift, Central Europe: fGas flux, isotopic (He, C, and N) and compositional fingerprints. *Geochim. & Cosmochim. Acta*, 63, n°21, 3653-3671.

Werner H.H. (1970) - Contribution to the mineral extraction from supersaturated geothermal brines, Salton Sea area, California. *U.N. Symposium on the Development and Utilization of Geothermal Resources, Pisa 1970,* vol. 2, Part 2, 1651-1655.

White D.E (1970) - Geochemistry applied to the discovery, evaluation, and exploitation of geothermal energy resources. *Geothermics, Special Issue 2 on U.N. Symposium on the development and utilization of geothermal resources, Pisa, Italy*, vol. 1, section V, 58-80.

Williams A.E. and McKibben M.A. (1989) - A brine interface in the Salton Sea geothermal system, California: fluid geochemical and isotopic characteristics. *Geochimica et Cosmochimica Acta*, 53, 1905-1920.

Ziegler K., Coleman M.L., Howarth R.J. (2001) - Palaeohydrodynamics of fluids in the Brent group (Oseberg field, Norwegian North Sea) from chemical and isotopic compositions of formation waters. *Applied Geochemistry*, 16, 609-632.

## *Tracer tests*

Adams M.C, Benoit W.R., Bodvarsson G.S., Moore J.N. (1989) - The Dixie Valley, Nevada tracer test. *Trans. Geothermal Resource Council*, 13, 215-220.

Adams M.C, Davis J. (1991) - Kinetics of fluorescein decay and its application as a geothermal tracer. *Geothermics*, 20 (1/2), 53-66.

Adams M.C., Moore J.N., Lazlo G.F. and Jong-Hong A. (1992) - Thermal stabilities of aromatic acids as geothermal tracers. *Geothermics*, vol. 21, n°3, 323-339.

Adams M.C., Yamada Y., Yagi M., Kondo T. and Wada T. (2000) - Stability of Methanol, Propanol, and $SF_6$ as High-Temperature Tracers. *World Geothermal Congress*, 3015-3019.

Adams M.C., Beall J.J., Enedy S.L., Hirtz P.N., Kilbourn P., Koenig B.A., Kunzman R. and Bill Smith J.L. (2001) - Hydrofluorocarbons as geothermal vapor-phase tracers. *Geothermics, 30*, 747-775.

Adams M.C., Yamada Y., Yagi M., Kasteler C., Kilbourn P. and Dahdah N. (2004) - Alcohols as Two-Phase Tracers. *Proceedings 29th Workshop on Geothermal Reservoir Engineering, Stanford University, California, January 26-28, 2004, SGP-TR-175.*

Alaskar M., Ames M., Liu C., Li K., Horne R. (2015) - Nanotracers for fracture characterization in conventional geothermal and EGS reservoirs. *Proceedings World Geothermal Congress, Melbourne, Australia, 19-25 April 2015*, 23 p.

Ames M., Li K., Horne R. (2013) - The utility of threshold reactive tracers for characterizing temperature distributions in geothermal reservoirs. *Mathematical Geosciences, Special Issue*.

Aquilina L., De Dreuzy J.-R., Bour O., Davy Ph. (2004) - Porosity and fluid velocities in the upper continental crust (2 to 4 km) inferred from injection tests at the Soultz-sous-Forêts geothermal site. *Geochimica et Cosmochimica Acta*, 68, 2405-2415.

Ásmundsson R., Pezard Ph., Sanjuan B., Henninges J., Deltombe J.-L., Halladay N., Lebert F., Gadalia A., Millot R., Gibert B., Violay M., Reinsch Th., Naisse J.-M., Massiot C., Azaïs P., Mainprice D., Karytsas C., Johnston C. (2014) - High temperature instruments and methods developed for supercritical geothermal reservoir characterization and exploitation - the HiTI project. *Geothermics,* 49, 90-98.

Axelsson G., Flovenz O.G., Hauksdottir S., Hjartarson A., Liu J. (2001) - Analysis of tracer data, and injection-induced cooling, in the Laugaland geothermal field, N-Iceland. *Geothermics*, 30, 697-725.

Axelsson G., Björnsson G., Montalvo F. (2005) - Quantitative interpretation of tracer test data. *Proceedings World Geothermal Congress, Antalya, Turkey, 24-29 April 2005*, 12 p.

Axelsson (2013) - Tracer tests in geothermal resource management. *EPJ Web of Conferences, 50, DOI: 10.1051/epjconf/20135002001*, 8 p.

Ayling B.F., Hogarth R.A., Rose P.E. (2015) - Tracer testing at the Habanero EGS site, central Australia. *Geothermics, in press*.

Azaroual M., Lassin A. (2001) - Historique du traçage chimique dans le reservoir géothermique Roches Chaudes Sèches de Soultz-sous-Forêts (Alsace, France). *BRGM/RP-50883-FR final report*, 68 p.

Blumenthal M., Kühn M., Pape H., Rath V. and Clauser Ch. (2007) - Hydraulic model of the deep reservoir quantifying the multi-well tracer test. *EHDRA Scientific Conference, 28-29 June 2007, Soultz-sous-Forêts*, 5 p.

Fukuda D., Asanuma M., Hishi Y. and Kotanaka K. (2005) - Alcohol tracer testing at the Matsukawa vapour-dominated geothermal field, Northeast Japan. *Proceedings 30th Workshop on Geothermal Reservoir Engineering, Stanford University, California, January 31-February 2, 2005, SGP-TR-176.*

Gadalia A., Pauwels H., Brach M., Wilkins C., and Welsh D. (1992) - Using various tracers during single well geothermal hot dry rock experiments, Soultz-sous-Forêts, Alsace, France. *In Tracer Hydrogeology (edited by Werner H.)*, 329-333.

Gadalia A., Braibant G., Touzelet S., Sanjuan B. (2010) - Tracing tests using organic compounds in a very high temperature geothermal field, Krafla (Iceland). *BRGM/RP-57661-FR final report*, 102 p.

Gentier S., Rachez X., Peter M., Blaisonneau A., Sanjuan B. (2011) - Transport and flow modelling of the deep geothermal exchanger between wells at Soultz-sous-Forêts (France). *Proceedings of the Geothermal Research Council (GRC) Annual Meeting, San Diego, USA, October 2011*, 12 p.

Gessner, K., Kühn, M., Rath, V., Kosack, C., Blumenthal, M., and Clauser, C. (2009) - Coupled process models as a tool for analyzing hydrothermal systems. *Surv Geophys.*, 30, 133-162.

Ghergut I., Sauter M., Behrens H., Licha T., McDermott C.I., Herfort M., Rose P., Zimmermann G., Orzol J., Jung R., Huenges E., Kolditz O., Lodemann M., Fisher S., Wittig U., Güthoff F. and Kühr M. (2007) - Tracer tests evaluating hydraulic stimulation at deep geothermal reservoirs in Germany. *Proceedings 32nd Workshop on Geothermal Reservoir Engineering, Stanford University, California, January 22-24, 2007, SGP-TR-183.*

Held S., Genter A., Kohl Th., Kölbel Th., Sausse J., Schoenball M. (2014) - Economic evaluation of geothermal reservoir performance through modeling the complexity of the operating EGS in Soultz-sous-Forêts. *Geothermics*, 51, 270-280.

Iglesias E.R., Flores-Armenta M., Torres R.J., Ramirez-Montes M., Reyes-Picaso N., Cruz-Grajales I. (2015) - Tracer testing at Los Humeros, Mexico, high-enthalpy geothermal field. *Proceedings World Geothermal Congress 2015, Melbourne, Australia, 19-25 April 2015*, 7 p.

Lovelock B.G. (2001) - Steam flow measurement using alcohol tracers. *Geothermics,* 30, 6, 641-654.

Matsunaga I. *et al.* (2002) - Reservoir monitoring by tracer testing during a long-term circulation test at the Hijiori HDR site. *Proceedings 27th Workshop on Geothermal Reservoir Engineering, Stanford University, Stanford, California, USA*, 101.

Matthiasdottir K.V., Albertsson A., Sigurdsson O., Fridleifsson G.O. (2015) - Tracer tests at Reykjanes geothermal field, Iceland. *Proceedings World Geothermal Congress 2015, Melbourne, Australia, 19-25 April 2015*, 6 p.

Mella M.J., Rose P.E., Adams M.C., Dahdah N.F., McCulloch J., Buck C. (2006a) - The use of n-Propanol at the Site of the Coso Engineered Geothermal System. *Proceedings 31st Workshop*

on *Geothermal Reservoir Engineering, Stanford University, California, January 30-February 1, 2006, SGP-TR-179.*

Mella M.J., Rose P.E., McCulloch J., Buck C. (2006b) - A tracer test using Ethanol as a two-phase tracer and 2-Naphthalene Sulfonate as a liquid-phase tracer at the Coso geothermal field. *GRC Transactions, 30*, 919-921.

Mountain B.W., Winick J.A. (2012) - The thermal stability of the naphthalene sulfonic and naphthalene disulfonic acids under geothermal conditions: Experimental results and a field-based example. *New Zealand Geothermal Workshop 2012, Proceedings, 19-21 November 2012, Auckland, New Zealand.*

Pauwels H. (1995) - Evaluation de traceurs artificiels pour l'étude du transport de solutés dans les eaux souterraines. *BRGM/RP-38323-FR final report*, 90 p.

Prabowo T., Yuniar D.M., Suryanto S., Silaban M. (2015) - Tracer test implementation and analysis in order to evaluate reinjection effects in Lahendong field. *Proceedings World Geothermal Congress 2015, Melbourne, Australia, 19-25 April 2015*, 7 p.

Pruess K., O'Sullivan M.J. and Kennedy B.M. (2000) - Modelling of phase-partitioning tracers in fractured reservoirs. *Proceedings 25$^{th}$ Workshop on Geothermal Reservoir Engineering, Stanford University, Stanford, California, January 24-26, 2000, SGP-TR-165.*

Radilla G., Sausse J., Sanjuan B., Fourar M. (2012) - Interpreting tracer tests in the enhanced geothermal system (EGS) of Soultz-sous-Forêts. *Geothermics, 44,* 43-51.

Rose P.E. and Adams M.C. (1994) - The application of rhodamine WT as a geothermal tracer. *Geothermal Resource Council Transactions*, 18, 237-240.

Rose P.E., Apperson K.D., Faulder D.D. (1997) - Fluid volume and flow constraints for a hydrothermal system at Beowawe, Nevada. *Presented at the SPE Annual Technical Conference and Exhibition, San Antonio, Texas, 5-8 October 1997, SPE-38762-MS.*

Rose P.E., Benoit W.R., Adams M.C. (1998) - Tracer testing at Dixie Valley, Nevada, using pyrene tetrasulfonate, amino-G, and fluorescein. *Geothermal Resource Council Transactions*, 22, 583-587.

Rose P.E., Benoit D., Lee S. G., Tandia B., Kilbourn P. (2000) - Testing the naphthalene sulfonates as geothermal tracers at Dixie Valley, Ohaaki and Awibengkok. *Proceedings 25$^{th}$ Workshop on Geoothermal Reservoir Engineering, Stanford University, Stanford, California, USA, January 24-26, 2000, SGP-TR-165*, 7 p.

Rose P.E., Benoit W. R. and Kilbourn P.M. (2001) - The application of the poly-aromatic sulfonates as tracers in geothermal reservoirs. *Geothermics, 30*, 617-640.

Rose P.E., Johnson S.D., Kilbourn P., Kasteler Ch. (2002) - Tracer testing at Dixie Valley, Nevada, using 1-naphthalene sulfonate and 2,6-naphthalene disulfonate. *Proceeding 27$^{th}$ Workshop on Geothermal Reservoir Engineering, Stanford University, Stanford, California, USA, January 28-30, 2002, SGP-TR-171*, 6 p.

Rose P.E., Leecaster K., Clausen S., Sanjuan R., Ames M., Reimus P., Williams M., Vermeul V., Benoit D. (2012a) - A tracer test at the Soda Lake, Nevada, geothermal field using a sorbing tracer. *In Proceedings, 37$^{th}$ Workshop on Geothermal Reservoir Engineering, Stanford University, Stanford, CA, SGP-TR-194.*

Rose P.E., McCulloch J., Buck C., Mella M., Rambani M. (2012b) - The use of butanols as tracers at the Coso geothermal field. *GCR Trans.*, 36, 1377-1382.

Rose P.E., Clausen S. (2015) - The use of Amino-G as a thermally reactive tracer for geothermal applications. *Proceedings World Geothermal Congress 2015, Melbourne, Australia, 19-25 April 2015*, 5 p.

Sanjuan B., Lasne E., Brach M. and Vaute L. (1999) - Bouillante geothermal field (Guadeloupe): II. Geochemical monitoring during the stimulation operation. Critical evaluation of chemical and isotopic data. *Rapport BRGM-CFG R40646*, 99 p.

Sanjuan B., Lasne E. and Brach M. (2000) - Bouillante geothermal field (Guadeloupe, West Indies): Geochemical monitoring during a thermal stimulation operation. *Proceedings, 25th Workshop on Geothermal Reservoir Engineering, Stanford University, California, January 24-26*, 215-222.

Sanjuan B., Le Nindre Y.M., Menjoz A., Sbai A., Brach M., Lasne E. (2004) - Travaux de recherche liés au développement du champ géothermique de Bouillante (Guadeloupe). *BRGM/RP-53136-FR final report*, 166 p.

Sanjuan B., Pinault J.-L., Rose P., Gérard A., Brach M., Braibant G., Crouzet C., Foucher J.-C., Gautier A., Touzelet S. (2006a) - Tracer testing of the geothermal heat exchanger at Soultz-sous-Forêts (France) between 2000 and 2005. *Geothermics, 35, n°5-6*, 622-653.

Sanjuan B., Pinault J.-L., Rose P., Gérard A., Brach, M. , Braibant G., Crouzet C., Foucher J.-C., Gautier A., Touzelet S. (2006b) - Geochemical fluid characteristics and main achievements about tracer tests at Soultz-sous-Forêts (France). *BRGM/RP-54776-FR report*, 64 p.

Sanjuan B., Lopez S., Guillou-Frottier L., Le Nindre Y.-M., Menjoz A. (2008) - Travaux de recherche liés au projet GHEDOM-ADEME (2006-2008). *BRGM/RP-56432-FR final report*, 214 p.

Sanjuan B., Brach M., Béchu E., Jean-Prost V., Bruzac S., Sontot O. (2011) - On-site Soultz-sous-Forêts (France) research works carried out between March 2010 and February 2011: Geochemical monitoring and tracing operations. *Soultz geothermal Conference, October 5-6, 2011, Soultz-sous-Forêts, France*.

Sanjuan R. (2012) - Etude et suivi physico-chimique des fluides de la centrale géothermique de Soultz-sous-Forêts. Quantification des émissions de gaz, budget $CO_2$. Amélioration technique des outils de monitoring, *Rapport final de stage de fin d'études Ingénieur ENSIACET, Génie chimique, option Eco-Energies*, 74 p.

Sanjuan B., Bouchot V., Mathieu F., Jousset Ph., Delatre M., De Michele M., Millot R., Innocent Ch. (2013) - Travaux de recherche sur le champ géothermique haute température de Bouillante, en Guadeloupe (2009-2012). *BRGM/RP-61715-FR final report*.

Sanjuan B. (2014) - Soultz EGS pilot plant exploitation - Phase III: Scientific program about on-site operations of geochemical monitoring and tracing (2010-2013). *Final BRGM/RP-63352-FR report,* 122 p.

Sanjuan B., Brach M., Genter A., Sanjuan R., Scheiber J., Touzelet S. (2015a) - Tracer testing of the EGS site at Soultz-sous-Forêts (Alsace, France) between 2005 and 2013. *In Proceedings World Geothermal Congress 2015, Melbourne, Australia, 19-25 April 2015*, 12 p.

Sanjuan B., Scheiber J., Gal F., Touzelet S., Genter A., Villadangos G. (2016c) - Inter-well chemical tracer testing at the Rittershoffen geothermal site (Alsace, France). *European Geothermal Congress 2016 (EGC2016), Strasbourg, France, 19-24 Sept 2016*, 7 p.

Shook (2005) - A systematic method for tracer test analysis: an example using Beowawe tracer data. *Proceedings 30th Workshop on Geothermal Reservoir Engineering, Stanford University, Stanford, California, January 31-February 2, 2005, SGP-TR-176.*

Torres-Mora Y., Axelsson G. (2015) - Chemical tracer test in Las Pailas geothermal field, Costa Rica. *In Proceedings World Geothermal Congress 2015, Melbourne, Australia, 19-25 April 2015*, 7 p.

Vaute L. (1998) - Tests de traçage réalisés sur le site géothermique de Soultz-sous-Forêts (juillet-novembre 1997). *BRGM report n° 40230*, 39 p.

Vogt C., Kosack C., Marquart G. (2012a) - Stochastic inversion of the tracer experiment of the enhanced geothermal system demonstration reservoir in Soultz-sous-Forêts. Revealing pathways and estimating permeability distribution. *Geothermics*, 42, 1-12.

Vogt C., Marquart G., Kosack C., Wolf A., Clauser C. (2012b) - Estimating the permeability distribution and its uncertainty at the EGS demonstration reservoir Soultz-sous-Forêts using the ensemble Kalman filter. *Water Resource Research*, 48, W08517, doi:10.1029/2011WR011673.

Winick J., Siega F., Addison S., Richardson I., Mountain B., Barry B. (2015) - Coupled Iodine-125 and 2NSA reservoir tracer testing at the Rotokowa geothermal field, New Zealand. *Proceedings World Geothermal Congress 2015, Melbourne, Australia, 19-25 April 2015*, 10 p.

Yanagisawa N., Matsunaga I., Rose P., Wyborn D. (2009) - HDR reservoir evaluation by tracer test with circulation condition. *Proceedings World Geothermal Congress 2010, Bali, Indonesia,* 10 p.

***Note the existence of Geothermics Special Issue (2001): Tracer applications in geothermal systems, vol. 30, n°6, 571-775.***

# Appendix 1. On-site BRGM investigations and fluid sampling in the Litomerice PVGT-LT1 borehole (November 2015)

# 1. Context

PVGT-LT1 borehole has been opened Tuesday the 24th of November mid-day, with the assistance of Mr. Vaclav Frydrych (GEOMEDIA) and a representative of the city of Litomerice. Discussions about next works on this site were undertaken with Mr. Frydrych and also, in the following days, with Mr. Antonin Tym, from the city of Limerice, who is engaged in the IMAGE project from the beginning, and assured that the city of Litomerice shall continue to support the IMAGE activities as much as possible, despite the fact that it cannot provide the scientific work. It was decided that a new adapted scientific program would be proposed after examination of the results obtained during these works.

Borehole wellhead is 80 cm above ground level. During the opening, gas overpressure has been noticed. Once opened, water gently flows indicating that the borehole is naturally artesian. The presence of gas bubbles was also noticed in the water column (Fig. 1). Table summarizes the physico-chemical parameters of the water as measured directly in the water column once the borehole has been opened. These values may represent values of water that has interacted with the borehole completion and may thus not directly reflect real parameters of the water further at depth.



*Figure 1 - PVGT-LT1 borehole at opening on the 24th of November (GPS WGS84 location: 50°32'4.44"N – 14°9'13.6"E).*

| Date & Time | Water temperature (°C) | Electrical conductivity ($\mu S.cm^{-1}$) | Dissolved oxygen (ppm) | Dissolved oxygen (% of sat.) | pH | ORP (mV, corrected) |
|---|---|---|---|---|---|---|
| 11/24/15 13:40 | 10.4 | 885 | 0.35 | 3 | 8.92 | -170 |

*Table 1 - Physico-chemical parameters measured in the water column of PVGT-LT1 borehole at the time of opening.*

## 2. Pumping procedure

Once opened, a submersible pump (MP1 from Grundfos) has been lowered down to 40 m depth below surface in PVGT-LT1 borehole. Exhaust has been set in the pool located near the borehole, as shown in figure 2. Taking into account the diameter on the inner tubing, the volume of water is about 3.6 liters per meter of tubing. By setting the pump at 40 m depth, this suggests that a volume of approx. 145 liters is located above the pump.



*Figure 2 - Overview of the field operations; left: multi-parameter probe and pool for discharge of pumped water; middle: borehole and pumping system; right: material for physico-chemical monitoring and material for sampling water.*

### a) Pumping on the 24 November

Pumping has begun at 15:15, the speed regulator of the pump being set at its maximum in order to produce a significant flow of water since hundreds of meters are required to be pumped prior to getting water that is more representative of downhole conditions. According to manufacturer's specifications, theoretical pumping rate in these conditions (40 m of water column, water table level near the ground surface level) is close to 1 800 l/h. After 5 minutes of pumping the physico-chemical parameters were measured (Tabl. 2). At 15:22, water flow at surface was interrupted. The pump has been switched off and the water table level was monitored, indicating that the water table was drawdown to less than 40 m and the pump consequently un-watered. During pumping, the water table has to be monitored, but in the present case, the drawdown was so quick that the operators had no time to check the level during the first minutes of the pumping as they were busy with the physico-chemical data acquisitions.

The time needed to empty the 40 m of tubing is 6 to 7 minutes. This is coherent with the estimate that can be made from theoretical pumping rate (1 800 l/h) and the volume of water pumped (145 l): expected time of purge in that case will be of 5 minutes. Here, the duration is longer as the lowering of the water table induces a decrease of the pumping rate. Indeed, the strength needed to extract water depends from the water table level depth, and is higher as the water table is deeper. After a few minutes (15:22 to 15:28), the pumping was started again, but at lower rate in order to take into account previous findings. Nonetheless, the power needed to get water back at the surface is around 60% of the maximum power of the pump in the present conditions. During this phase, new measurements were made (Tabl. 2). The pumping lasted 4 minutes, new unwatering of the pump has been stated at 15:32. As a consequence, pumping operations were stopped.

| Date & Time | Water temperature (°C) | Electrical conductivity ($\mu$S.cm$^{-1}$) | Dissolved oxygen (ppm) | Dissolved oxygen (% of sat.) | pH | ORP (mV, corrected) |
|---|---|---|---|---|---|---|
| **11/24/15 15:20** | 11 | 895 | 1.18 | - | 8.90 | +20 |
| **11/24/15 15:30** | 11 | 887 | 5.46 | - | 8.82 | +200 |

*Table 2 - Physico-chemical parameters measured in the water flow during pumping of PVGT-LT1 borehole - 24 November.*

### b) Pumping on the 25 November

After 18 hours without pumping, and considering that the borehole was closed during the night, the water level did not recover its equilibrium height. A rise from -18.7 m (reference: top of the wellhead) to -4.4 m has been stated, corresponding to a rise of +80 cm per hour. When the borehole is closed, the rise of the water level may be reduced as a result of the presence of gas accumulating at the top of the casing. Pumping has begun at 09:20, at the lowest rate that allowed water to be drawn to the surface.

Physico-chemical parameters were again measured (Tabl. 3). After 5 minutes of pumping, water table level was lowered down to 25.50 m below wellhead thus indicating a decrease of 1 m in 22 seconds or a rate of -4.5 cm per second. An intermediate record of physico-chemical parameters was done at 09:26 and a last one at 09:32 (end of pumping; Tabl. 3).

| Date & Time | Water temperature (°C) | Electrical conductivity ($\mu$S.cm$^{-1}$) | Dissolved oxygen (ppm) | Dissolved oxygen (% of sat.) | pH | ORP (mV, corrected) |
|---|---|---|---|---|---|---|
| **11/25/15 09:20** | 9.3 | 979 | 0.34 | - | 9.00 | +130 |
| **11/25/15 09:26** | - | 980 | 0.15 | - | 8.42 | +100 |
| **11/25/15 09:32** | - | 986 | 0.12 | - | 8.65 | +70 |
| **11/25/15 16:30** | 10.4 | 1007 | 9.5 | - | 8.90 | +180 |
| **11/25/15 16:38** | 11.3 | 1004 | 4.6 | - | 8.83 | +120 |

*Table 3 - Physico-chemical parameters measured in the water flow during pumping of PVGT-LT1 borehole - 25 November.*

In order to allow water to rise again upward in the borehole, investigations were stopped until the end of the day; spare-time was allocated to sampling at Teplice thermal springs (see dedicated section).

A new pumping phase was done during the afternoon at PVGT-LT1 borehole. The borehole was left opened during the day, with plastic capping on the top allowing gas migration. The consequence is a far higher recovery rate, evaluated at +32 m of water column in 6 hours (+5.3 m per hour, compared to +0.8 m per hour when the borehole is closed). Nevertheless, the situation may be more complicated, as the rise of the water level may not be linear over the entire column relying on how the dissolved gases degas. Pumping was initiated at 16:30 and stopped at 16:38 (Tabl. 3); in between the drawdown has been evaluated to 1 m in 20 seconds, close to that measured during the morning's investigations.

### c) Pumping on the 26 November

The last pumping operations have been performed on the 26th of November. At 08:50, the water table level did not reach its maximum value and was measured at -30 cm below top of wellhead. As a consequence, the rise of the water table can be evaluated at + 2.4m per hour. This value is lesser than the one calculated for the previous night (November 24 to 25) but remains far above the rate calculated when the borehole is closed. This difference is to our opinion linked to the dynamics of the rise of a mix of water and gas inside the tubing. The water level rises as a consequence of the own productivity of the aquifer – that is very low in the present case – and the overpressure brought by the gas phase. The pressure of gas has to be higher and higher when the water column is longer; then the rate of water table rise decreases as the water table is closest to the ground surface. This is especially true when the water level has to elevate above the ground level up to +80 cm. This is exactly what was stated on the 26th of November: at 09:13, the level was at -14 cm below top of wellhead: the rise is only + 40 cm per hour at surface. Overflow occurred at 09:42 and some small gas bubbles were noticed at that time (Fig. 3). A synthesis of the different recovery rates of the water level in the borehole is presented in table 4.

| Date & Time | Status of the borehole | Initial level | Final level | Duration | Recovery rate |
|---|---|---|---|---|---|
| 11/24/15 PM to 11/25/15 AM | Closed | -18.7 m | -4.4 m | 18 h | + 0.8 m/h |
| 11/25/15 AM to 11/25/15 PM | Opened | -40 m | -8 m | 6 h | + 5.3 m/h |
| 11/25/15 PM to 11/26/15 AM | Opened | -40 m | -0.3 m | 17 h | + 2.4 m/h |
| 11/26/15 AM | Opened | -0.3 m | -0.14 m | 23 min | + 0.4 m/h |
| 11/26/15 AM | Opened | -0.14 m | 0 (top of casing) | 31 min | + 0.3 m/h |
| 11/26/15 AM | Opened | -24.1 m | -21.91m | 24 min | + 5.5 m/h |

*Table 4 - Summary of the recovery rates of the water level in the borehole.*

Pumping was initiated at 10:00 and stopped at 10:08; parameters are reported in table 5. Samples were taken and classically conditioned (Sanjuan *et al.*, 2016a) for subsequent chemical analyses at lab during this pumping phase (concentrations in major and trace elements; isotope ratio determinations of $^7Li$, $^{18}O$ and $^2H$ of water, $^{18}O$ of sulphates, $^{87}Sr/^{86}Sr$, $^{11}B$ and $^{13}C$ of total dissolved inorganic carbon). The rate of pumping was evaluated at 1 litre in 11 seconds at 10:05 (pumping rate of c.a. 330 l/h) – this value is only informative as the pumping rate always decreases during time as a consequence of the perpetual drawdown of the water table level. The alkalinity (expressed as the $HCO_3$ content) has been determined few days after water collection and is close to 151 mg/l (2.47 meq/l), lower than the value reported in 2007 (220 mg/l) for $HCO_3$.

| Date & Time | Water temperature (°C) | Electrical conductivity ($\mu S.cm^{-1}$) | Dissolved oxygen (ppm) | Dissolved oxygen (% of sat.) | pH | ORP (mV, corrected) |
|---|---|---|---|---|---|---|
| 11/26/15 10:02 | 11.1 | 1043 | 3.7 | - | 9.00 | +130 |
| 11/26/15 10:08 | - | 1062 | 1.9 | - | 8.42 | -20 |

*Table 5 - Physico-chemical parameters measured in the water flow during pumping of PVGT-LT1 borehole – November 25.*
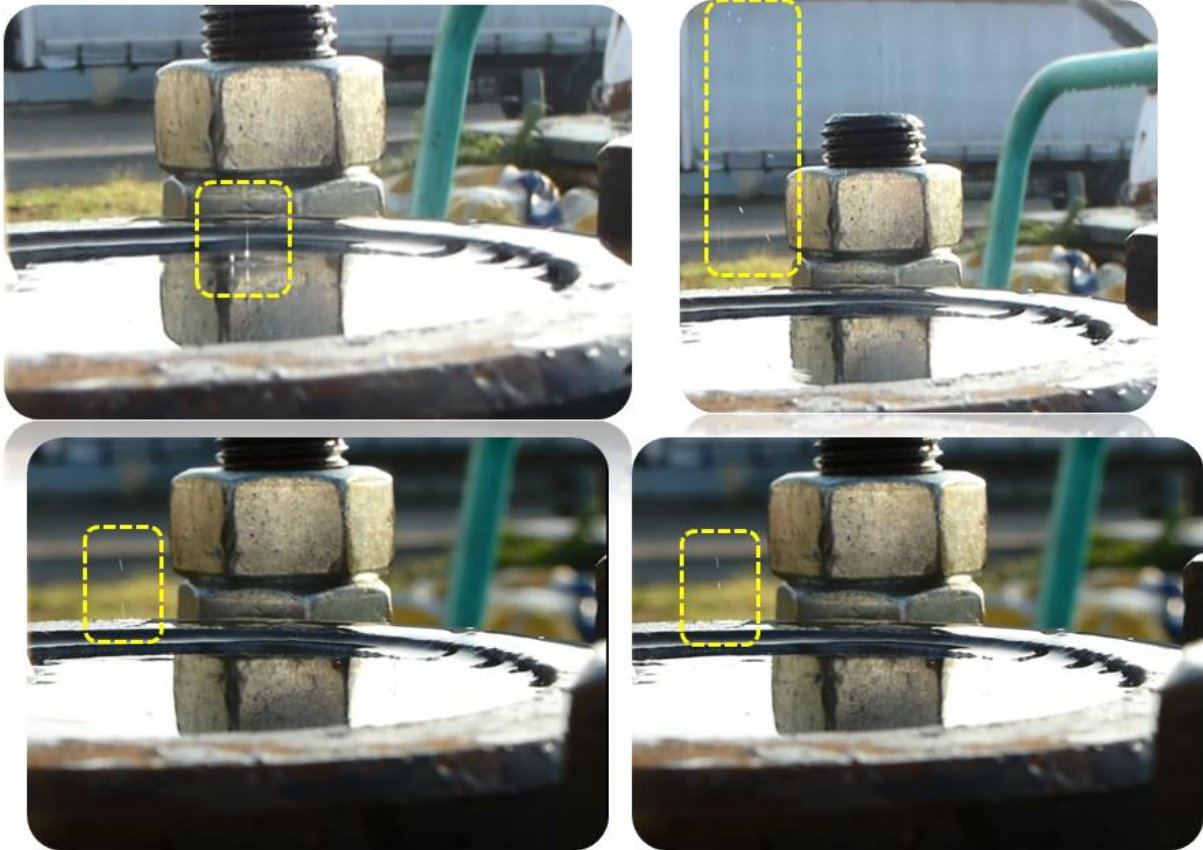
*Figure 3 - Small gas bubbles escaping at the surface of the water.*

## 3. Monitoring during pumping

Physico-chemical parameters were not only monitored from time to time and were also acquired under continuous mode during the pumping using Idronaut probe (Fig. 4). Five sessions of pumping were performed between the 24 and the 26 November; a synthesis of these acquisitions is presented in figures 5 to 9.



*Figure 4 - Close view of the Idronaut probe used for continuous physico-chemical monitoring during pumping; portable multi-meters for spot data acquisitions are also visible (bottom part of the image).*

From this series of figures, the following conclusions can be made:

- *All parameters:* there is a delay before stable conditions are reached during the pumping process, especially considering external weather conditions (near freezing point). For figures 7 and 8, this is especially true as some water was remaining inside the plastic reservoir used to set the Idronaut probe thus leading to anomalously low temperatures at the beginning of the monitoring;

- *Temperature:* maximum temperature reached at the surface during pumping is close to 11.8°C at the end of each pumping session. This is far below the bottom temperature, the cooling being attributed to thermal re-equilibration of the water inside the tubing. This is also less than the value reported in May 2015, but this can be attributed to external forcing, as the atmosphere temperature in May is warmer than in November. As the flow is very low, there is no way to reach significantly higher temperatures only referring to pumping. The only approach that would be meaningful is sampling at depth, but this is not technically feasible since the inner tubing of the borehole is collapsed at c.a. 1 150 m depth (screens are located 450 m below this depth);

- *Dissolved oxygen:* this parameter is interesting to consider as groundwater from depth shall not be rich in oxygen – ideally the value must be equal to zero. The five pumping sessions show a gradual decrease of the dissolved oxygen concentration, from c.a. 70% of saturation (Fig. 5) down to c.a. 10% of saturation (Fig. 9). This suggests that the first tens of water discharged at the surface have evolved during time and have being subject to processes either producing oxygen or to contamination by air. By displacing to the surface waters that have less evolved, the pumping allows to gradually decrease the concentration of oxygen in water but not to down to zero. This parameter thus suggests that 2 minutes of pumping are required to get water less enriched in oxygen at the surface. The values measured in November are congruent with the value reported in May 2015 (0.55 mg/l in November and 0.21 mg/l in May);

- *Electrical conductivity:* considering the information on temperature and dissolved oxygen, the water may be more "representative" by the end of each pumping session. As a consequence, the progressive renewal of the water can be imaged by the increasing conductivities found during the monitoring, from 890 $\mu$S.cm$^{-1}$ at the end of 1$^{st}$ session (Fig. 5) up to 1040 $\mu$S.cm$^{-1}$, at the end of the 5$^{th}$ session (Fig. 9). The conductivities measured during the firsts 2 minutes of pumping may exhibit higher conductivities but they have not to be considered as they reflect non-equilibrium conditions. Values of electrical conductivity cannot be compared to previous measurements as these are expressed in mS.cm$^{-1}$ (respectively 117 mS.cm$^{-1}$ in November 2007 and 575 mS.cm$^{-1}$ in May 2015) and did not seem to represent realistic values when compared to chemical analyses;

- *pH:* as the temperature evolves during the pumping, the pH values evolve with time, especially at the beginning of the pumping. Once again, values to consider are those recorded when the temperature of the water reaches stability. There is a decrease of the pH value during time, as the pumping draws deeper water to the surface. On the 24 November, the pH was close to 8.95 and falls down to 8.35 on the 26 November. Both values are in agreement with previous measurements (respectively 8.3 in November 2007 and 8.91 in May 2015). Note that water at surface may present iridescence and that the pH value may be influenced by the presence of oil and/or grease residues;

- *Redox potential (ORP):* this parameter is related to the dissolved oxygen concentration. As a consequence, its value may decrease when the dissolved oxygen concentration decreases. Second, this parameter can be highly variable and is quite difficult to measure. Nonetheless, except the values monitored the 24 November afternoon (Fig. 6), ORP values are in agreement with low oxidizing conditions (potential close to +80 mV);

- *Chlorine content:* this parameter is shown only for informative purpose. The sensor was not calibrated to give chlorine concentrations in the present conditions (values are dependent from temperature and from fluid salinity). As a consequence values are reported as raw data. The measurements are quite stable in between the different acquisitions, only showing a slight depletion from +136 mV (Fig. 5) to +124 mV (Fig. 9). This suggests that chlorine concentration remains stable in the water column, such behaviour being understandable as chlorine is often referred to as a conservative element.

Last, there is a very good agreement between the values measured continuously and the data measured punctually.
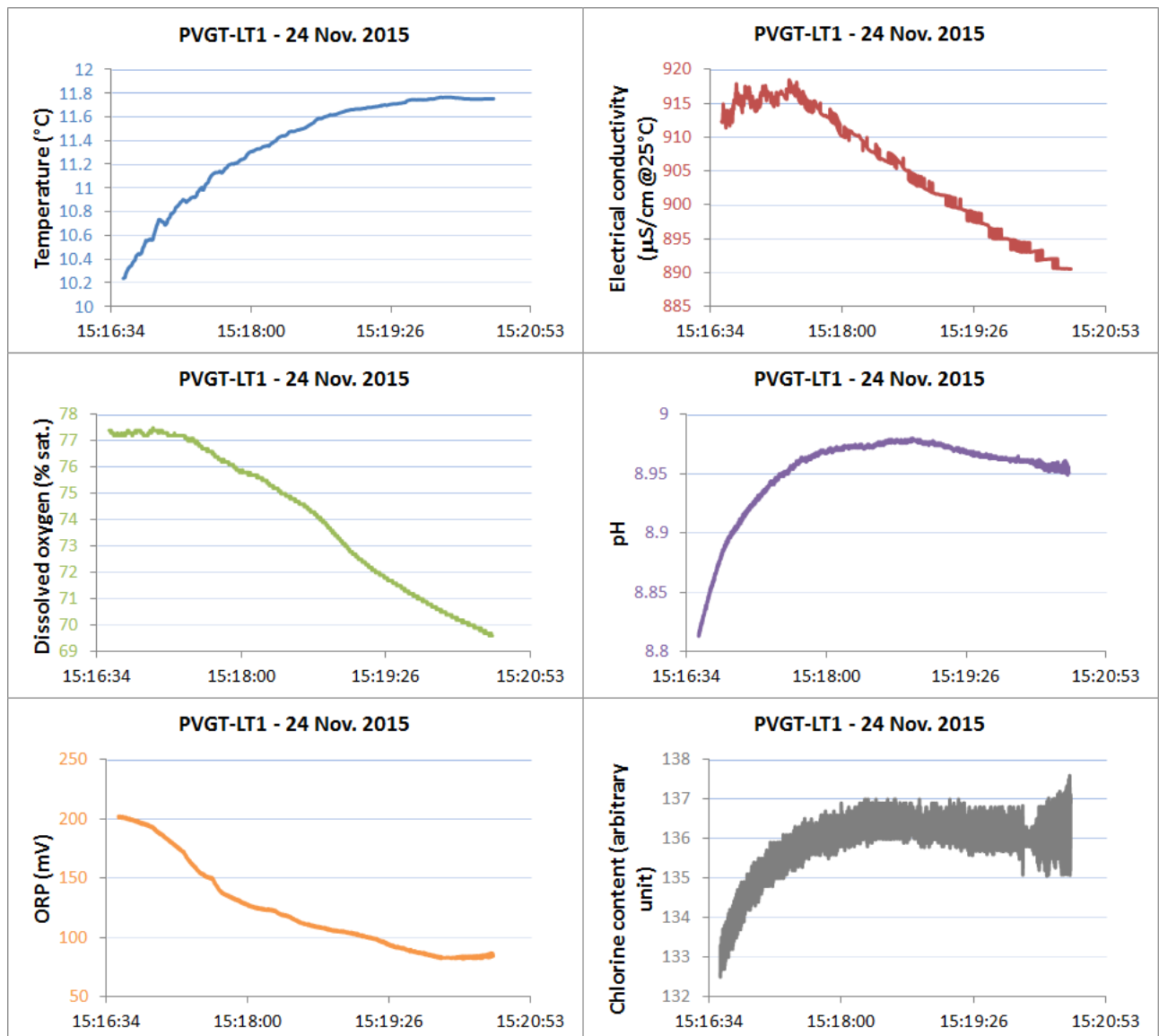


*Figure 5 - Monitoring of the water discharged on the 24 November – 1$^{st}$ pumping session.*
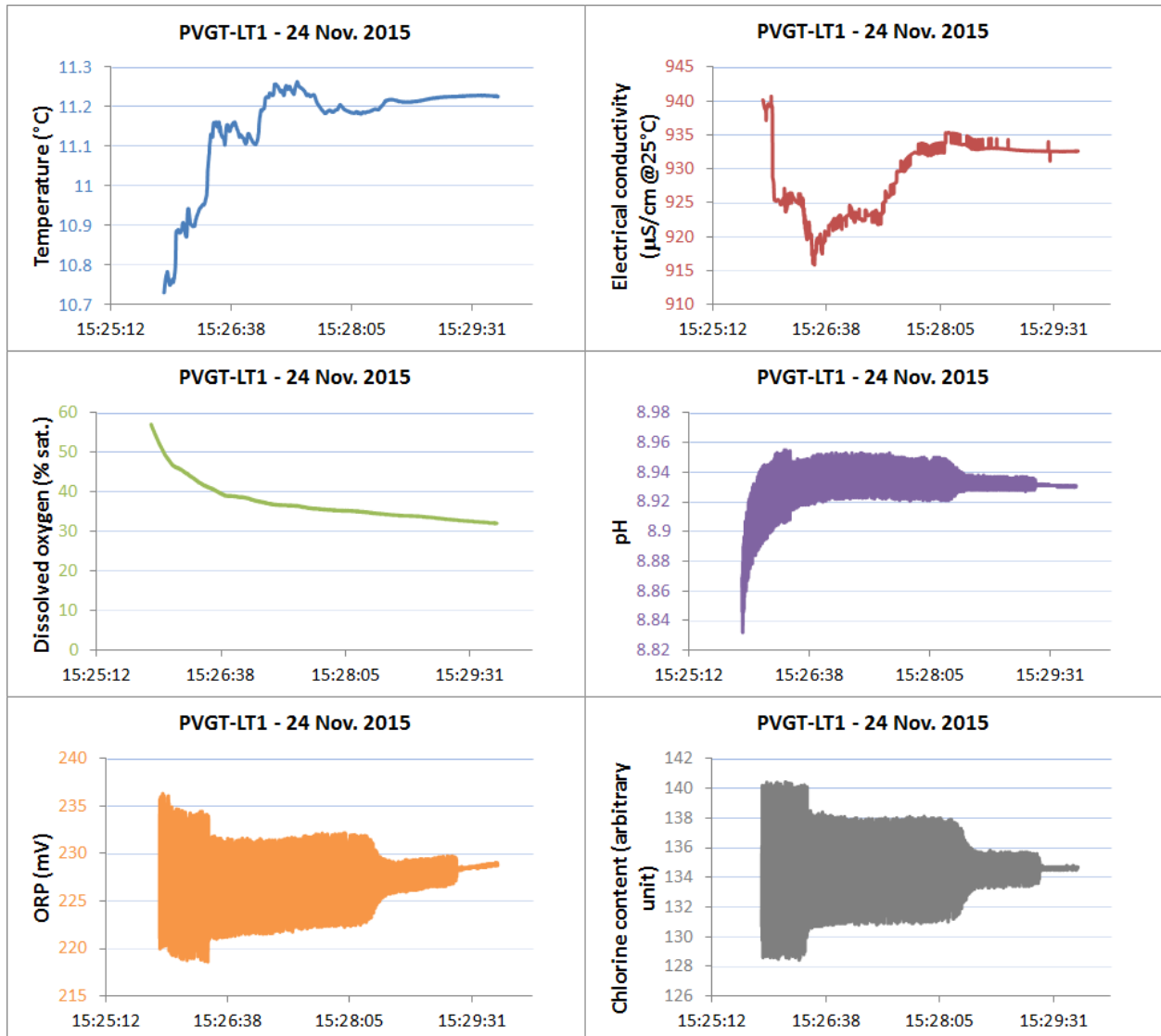
*Figure 6 - Monitoring of the water discharged on the 24 November – 2nd pumping session.*
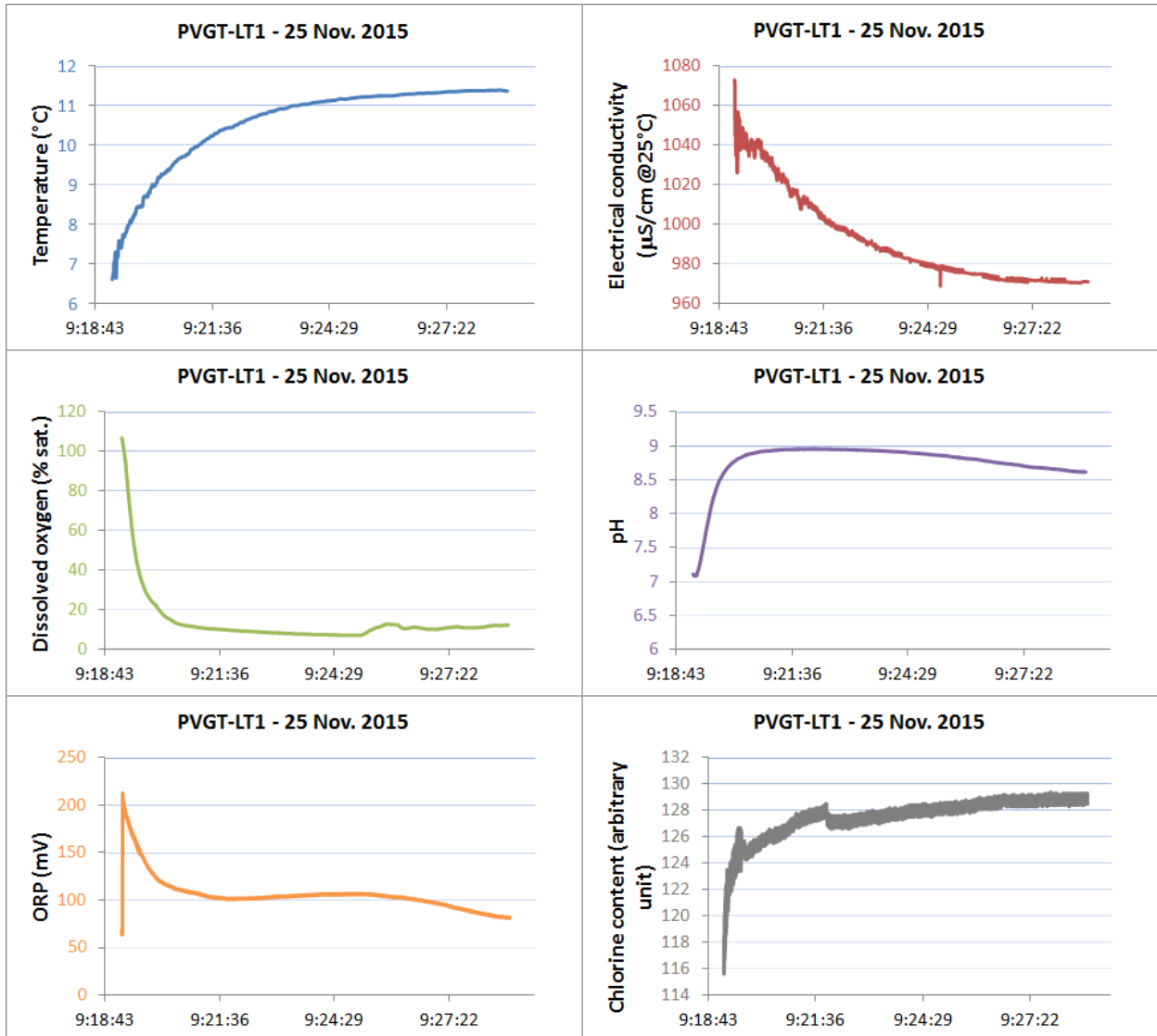
*Figure 7 - Monitoring of the water discharged on the 25 November – 3$^{rd}$ pumping session.*
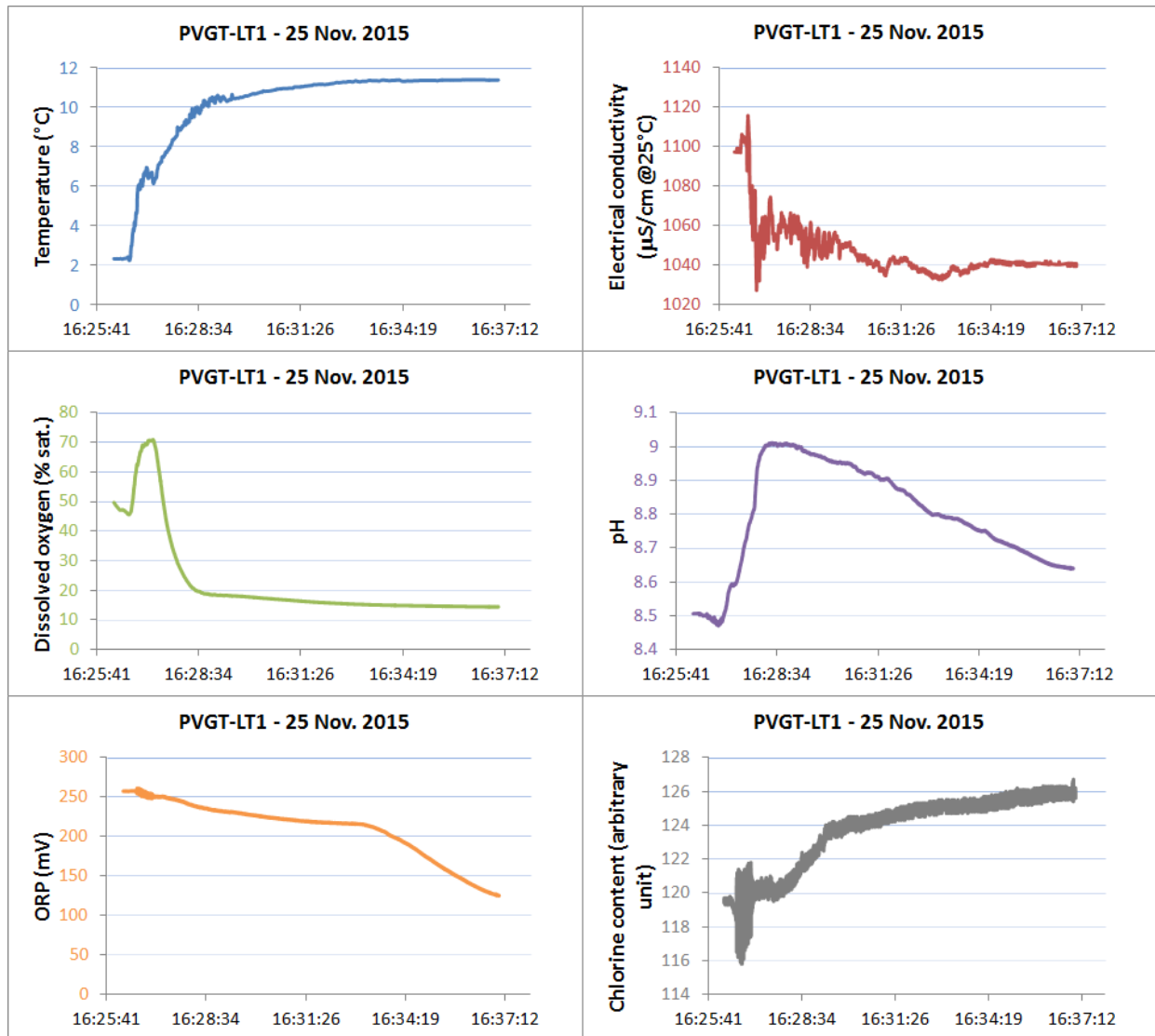
*Figure 8 - Monitoring of the water discharged on the 25 November – 4th pumping session.*
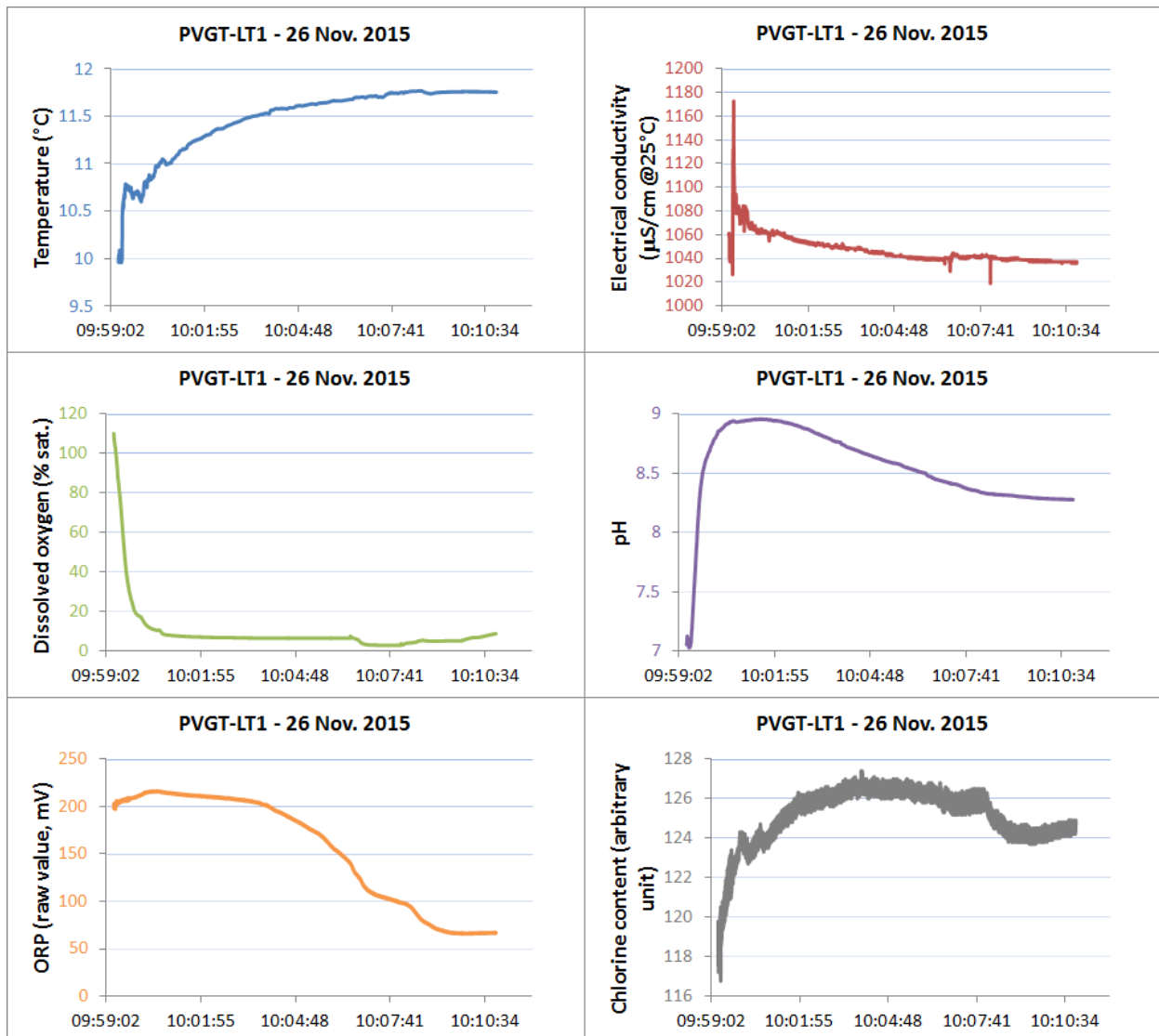
*Figure 9 - Monitoring of the water discharged on the 26 November – 5th pumping session.*

## 4. Gas phase

As gas bubbles were noticed at the opening of the borehole (Fig. 1), after pumping when the water level reaches the top of the wellhead (Fig. 3) and during pumping (Fig. 10), two samples were collected in appropriate containers under vacuum (Fig. 11). One sample was collected directly at the surface, by lowering one end of the glass bulb in the water and by opening the cock to allow water and gas penetrating in the bulb thanks to the vacuum existing inside the bulb. The second sample was collected during pumping, directly at the mouth of the pipe discharging water (Fig. 10).

*Figure 10 - Degassing of the water during a pumping session.*



*Figure 11 - Glass bulb under vacuum prior its use for collection of dissolved gases.*

Results of the lab analyses using gas chromatography are shown in table 6. The sample collected directly in the flow line is c.a. ten times depleted in oxygen compared to the sample collected at borehole wellhead. This is congruent with statements previously made when considering the dissolved oxygen concentration at the beginning and at the end of pumping phases. As nitrogen is also more abundant in the sample collected at surface (and argon too), this $O_2$ and $N_2$ enrichment may be attributed to contamination by atmospheric air. The relative abundances of $N_2$ and $O_2$ in air (c.a. 78% and 21% vol. respectively) lead to a ratio of $N_2/O_2$ close to 4. Here the ratios are close to 12 for the sample collected at surface and close to 74 for the sample collected in the flow line. This last ratio is clearly disconnected from atmospheric ratio, but the second may be influenced by air intrusion. Nevertheless there in no proportionality in this eventual air contamination, as the rise in oxygen concentration is far greater (+930%) than suggested by the rise in nitrogen concentration (+150%). This potential air contamination is also not in agreement with the $CO_2$ concentrations in the two samples: if some air has to be present in the surface sample, then the concentration in $CO_2$ has not to be strongly enriched ($CO_2$ concentration in atmosphere is close to 0.04% only).

As a consequence, the sample collected in the flow line has to be considered as more representative of in-situ conditions than the surface sample – even if the strong depletion in $CO_2$ is not explained in this sample. A trial to measure carbon isotope ratios will be done in January, in order to determine what can be the origin of this gas, but results are not guaranteed as gas pressure in the glass bulb are very low (only a tenth of the atmospheric pressure). The gas phase is very rich in methane and traces of other alkanes are also found. There is also a strong enrichment in helium (hundreds of ppm).

| Gas phase (% vol.) | Sample collected at surface | Sample collected in the flow line |
|---|---|---|
| $CO_2$ | 5.75 | 0.18 |
| Ar | 0.50 | 0.42 |
| $O_2$ | 2.41 | 0.26 |
| $N_2$ | 28.2 | 19.3 |
| He | 0.15 | 0.094 |
| $H_2$ | 0.017 | < 0.005 |
| $H_2S$ | < 0.005 | < 0.005 |
| $CH_4$ | 61.9 | 78.2 |
| $C_2H_6$ | 0.26 | 0.41 |
| $C_3H_8$ | 0.022 | 0.050 |
| $C_4H_{10}$ | < 0.0004 | 0.0053 |
| *Sum* | *98.9* | *99.1* |
| *Pressure inside the glass bulb (mbar)* | *99* | *130* |

*Table 6 - Gas analyses performed on dissolved gas samples – results for the exsolved gas phase.*

Referring to existing data in the Litomeriče area (Myslil *et al.*, 2012), the following points have to be mentioned:

- near the surface, upper cretaceous formations (from 15 to 190 m depth), of Ca-$HCO_3$ type, may be characterized by traces of $CO_2$;

- Permo-Carboniferous sediments (from 190 to 780 m depth in PVGT-LT1 borehole) are known to house pressurized aquifers with low transmissivity and virtually no flow (stagnant waters). These saline waters range from Ca-($HCO_3$)-$SO_4$ to Na-Cl types and can be saturated in $CO_2$, $H_2S$ or $CH_4$ depending of the nature of the sediments at the considered depth;

- in the crystalline basement (from 910 m to bottom), some levels may be water-saturated too. Water can be of Ca-SO$_4$ type, less saline than Permo-Carboniferous waters and may be slightly oversaturated in CO$_2$ or H$_2$S;

- further in depth, graphite beds have been recognized by gamma-ray and resistivity investigations, in the 1792-1835 m interval and the 1993-2017 m interval;

- the presence of CO$_2$ and helium of mantle origin is reported in lien with the Ohre (Eger) Graben structure (Weinlich *et al.*, 1999; Jirakova *et al.*, 2010).

Gas phases quantified during this survey are by order of importance CH$_4$, CO$_2$ and He, and no H$_2$S has been detected. Based on the above mentioned literature data, it seems that CH$_4$ may preferentially be originated from the Permo-Carboniferous sediments rather than from the crystalline basement. The origin of helium and CO$_2$ may be more debatable, especially for the low soluble and highly mobile helium gas, so that deeper origin may be advocated for these phases.

# Appendix 2. BRGM investigations about the Pravridlo - Teplice thermal spring (November 2015)

As ignimbrites are mentioned in the PVGT-LT1 geological section, between 780 and 910 m depth, it was decided to sample, at Tepliče, thermal springs located in this city being known to have interacted with such geological formations. Numerous springs are emplaced in this area (Fig. 1). Among them, the historical spring of Pravřidlo has been found to be easy to sample as it flows in a public area (Figures 2 and 3).



*Figure 1 - Thermal springs existing at Tepliče.*



*Figure 2 - Pravřidlo spring (GPS WGS84 location: 50°38'15.87"N – 13°49'37.68"E). Left: location of the sampling point; right: location of the spring itself, protected by the pyramidal cap. Onto this protection is written: this is the location of the Pravridlo (Ancient spring) – a 51 m deep spring shaft, which thermal water has been drawn from since 1879. This world famous, natural, curative spring has been restoring people to health since long ago.*

*Figure 3 - Pravřidlo spring – detailed view.*

The sample has thus been done at the mouth of a copper tube, flow rate being close to 0.5 l per minute at the sampling point. Field parameters are reported in table 1. As for Litomeriče PVGT-LT1 water, samples have been collected for subsequent laboratory analyses of concentrations in major and trace elements as well as isotope ratio determinations of $^7Li$, $^{18}O$ and $^2H$ of water, $^{18}O$ of sulfates, $^{87}Sr/^{86}Sr$, $^{11}B$ and $^{13}C$ of total dissolved inorganic carbon.

The alkalinity has been measured at 7.89 meq/l (corresponding to 481 mg/l expressed as the $HCO_3$ concentration). This value is close to the value reported in database (502 mg/l; http://www.lazneteplice.cz/en/lecebna-specializace/thermal-water/).

| Date & Time | Water temperature (°C) | Electrical conductivity ($\mu S.cm^{-1}$) | Dissolved oxygen (ppm) | Dissolved oxygen (% of sat.) | pH | ORP (mV, corrected) |
|---|---|---|---|---|---|---|
| **11/25/15 13:30** | 35.9 | 1160 | 3.30 | 49.7 | 7.29 | +330 |

*Table 1 - Physico-chemical parameters measured at Pravřidlo spring.*